



Benjamin Jauk, BSc.

Influence of arbitrary resistivity distribution of ground on the surface potential of earthing systems

MASTER'S THESIS

to achieve the university degree of

Diplom-Ingenieur

Master's degree programme: Electrical Engineering

submitted to

Graz University of Technology

Supervisor

Ass.Prof Dipl.-Ing. Dr.techn. Katrin Friedl

Institute of Electrical Power Systems

Graz, February 2020

AFFIDAVIT

I declare that I have authored this thesis independently, that I have not used other than the declared sources/resources, and that I have explicitly indicated all material which has been quoted either literally or by content from the sources used. The text document uploaded to TUGRAZonline is identical to the present master's thesis.

Date

Signature

*Thinking is the hardest work there is,
which is probably the reason why so few engage in it.*
~ Henry Ford ~

Contents

1. Summary	3
1.1. Object	3
1.2. Method	3
1.3. Result	3
1.4. Conclusion	4
1.5. Outlook	4
2. Introduction	5
2.1. Motivation	5
2.2. The problem	6
2.3. Questions and Goal	6
3. Measurement	7
3.1. Theory	7
3.1.1. Soil resistivity distribution	11
3.1.2. Measurement methods	11
3.1.3. Wenner Array	12
3.1.4. Dipole-Dipole Array	13
3.1.5. Profiling	14
3.1.6. 3D model	16
3.2. Method	17
3.2.1. General	17
3.2.2. Weather Condition	20
3.2.3. Measurement	20
3.2.4. Apparent Resistivity Plot	22
3.3. Results	22
3.3.1. Median Depths	22
3.3.2. Measurement results	23
4. Inverse Modelling	27
4.1. Theory	27
4.2. Method	29
4.3. Results	30
5. Simulation	35
5.1. Theory	35
5.1.1. Finite Difference Method	35

5.1.2. Finite Element Method	38
5.1.3. Earthing system	40
5.2. Method	41
5.3. Results	44
6. Conclusion	51
6.1. Discussion	51
6.2. Outlook	52
Appendices	I
A. Figures	I
B. Tables	V
C. Parameters	XXIX

List of Figures

2.1. Main steps of this mater's thesis	5
3.1. Infinite half space with point current source	9
3.2. Different soil models	10
3.3. Wenner Array	12
3.4. Dipole-Dipole Array	13
3.5. Selected electrodes with obtained data points (Wenner method)	15
3.6. Measured Site [6]	18
3.7. Photos from site	19
3.8. Weather Archive for the site [7]	20
3.9. Electrodes Arrangement	21
3.10. 3D Pseudosection	23
3.11. Apparent resistivity Line 0 - Wenner vs. Dipole-Dipole Array	25
4.1. 3D Inversesection	30
4.2. 3D Inversion Model	31
4.3. Apparent vs. Inverse Modelling resistivity of Line 0	33
5.1. Common FDM (Finite Difference Method) grid patterns [9]	36
5.2. FDM molecules [9]	36
5.3. FDM mesh in 2D [9]	37
5.4. Common finite elements [9]	39
5.5. Example surface potential profile (left: without potential grading, right: with potential grading) [11]	40
5.6. Calculated vs. Simulated Line Surface Potential Distribution	44
5.7. Different Surface Potential Distributions on the line between the electrodes	45
5.8. Relative error between simulated and calculated surface potential distribution	46
5.9. Error of the models in comparison to the inversion model related to the EPR (Earth Potential Rise)	47
5.10. 3D surface potential distribution of Resistivity blocks model	48
5.11. FEM (Finite Element Method) simulation model	49
A.1. Apparent Resistivities Line 0-5	II
A.2. Apparent resistivity Line 5 - Wenner vs. Dipole-Dipole Array	III

List of Tables

3.1. Different Wenner configurations	12
3.2. Calculated Median Depths of investigation	22
4.1. Changed Forward modelling Parameters for 3D inversion	29
4.2. Changed Forward modelling Parameters for 2D inversion	29
5.1. Minimum, Maximum, Average of all apparent resistivities	42
5.2. Layers with average of apparent resistivities	42
5.3. Average of all inversion model resistivities	42
5.4. Layers with average of inversion model resistivities	43
B.1. Measured values Wenner Pseudo-3D	V
B.2. Measured values Dipole-Dipole Line0	XIII
B.3. Measured values Dipole-Dipole Line5	XVI
B.4. Center coordinates of inversion model resistivity	XIX

Abbreviations

EPR	Earth Potential Rise
ERT	Electrical Resistance Tomography
FDM	Finite Difference Method
FEM	Finite Element Method
GPS	Global Positioning System
IP	Induced Polarization
Lvl	Depth Level
PDE	Partial Differential Equation
SP	Self Potential (Spontaneous polarization)
VES	Vertical Electrical Sounding

Nomenclature

a	Equidistant spacing of the electrodes in m
\vec{B}	Magnetic Flux Intensity in T
\mathbf{C}_i	Roughness Filter Matrix in direction i
\vec{D}	Electric Flux Density in $\frac{\text{C}}{\text{m}^2}$
$\vec{\nabla}$	Del $\left(\frac{\partial}{\partial x}, \frac{\partial}{\partial y}, \frac{\partial}{\partial z}\right)$
\vec{E}	Electric Field Intensity in $\frac{\text{V}}{\text{m}}$
E_{U_s}	Error related on earthing voltage in p.u.
E	Error function
\mathbf{F}	Filter Matrix
\vec{f}	Model response vector
$f_i(x)$	Convenient set of known functions
\vec{H}	Magnetic Field Intensity in $\frac{\text{A}}{\text{m}}$
#	Number
I_C	Injected current intensity between electrodes C1 and C2 in A
\vec{J}	Electric Current Density in $\frac{\text{A}}{\text{m}^2}$
\mathbf{J}	Jacobian Matrix
k	Geometric factor of the array in m
L	Total array length in m
m	Maximum number of datapoint rows
n_e	Number of electrodes per line
$\frac{\partial}{\partial t}$	Partial Derivative over the time
\vec{q}	Model parameter vector
r	Radial distance in m
r_{C1}	Distance to C_1 in m
r_{C1P1}	Distance between C_1 and P_1 in m

r_{C1P2}	Distance between C_1 and P_2 in m
r_{C2}	Distance to C_2 in m
r_{C2P1}	Distance between C_2 and P_1 in m
r_{C2P2}	Distance between C_2 and P_2 in m
U_S	Step voltage
U_P	Potential difference between electrodes P1 and P2 in V
W	Energy loss in J
x_{C1}	Position of Current electrode C1 in x direction in m
x_{C2}	Position of Current electrode C2 in x direction in m
x_{P1}	Position of Potential electrode P1 in x direction in m
x_{P2}	Position of Potential electrode P2 in x direction in m
\vec{y}	Measured data vector
z	Position of point in z direction in m
z_e	Median depth of investigation in m

Greek Letters

α_i	Relative weighting factor in direction i
Δ	Finite change of the variable
$\vec{\Gamma}$	Surface vector
λ	Damping factor
φ_{surf}	Electric Potential on the surface in V
φ_i	Unknown coefficients on each element
Φ	Potential
φ	Electric Scalar Potential in V
ρ	Resistivity in Ωm
ρ_a	Apparent Resistivity in Ωm
ρ_c	Charge density in C
σ	Standard deviation in %

1. Summary

1.1. Object

The aim of this thesis is to give an overview of how the measured soil resistivity of a test area can be used to get a good approximation of the real distribution of soil resistivity in a model. This approximation is the reference model to compare different, simplified models in their behaviour of the surface potential distribution. The effect of this simplification on the error is shown to avoid dimensioning errors of earthing systems.

This work contributes to the question either detailed ground investigation is needed or not.

The following questions and goals are defined:

- How can one derive the "real" resistivity from the apparent resistivity?
- How can the soil model be implemented for a numerical simulation process?
- How does the arbitrary resistivity distribution influence the surface potential?
- What is the influence if the soil model will be simplified (e.g. homogeneous, layered)?

1.2. Method

For the measurement a soil measurement unit with an automatic measuring routine is used. The electrodes were in Wenner- α configuration. The measurement is a Pseudo-3D measurement, meaning the area is investigated line by line.

The reference model is found by solving the inverse problem with an inversion software. This found model is then imported into a finite element method software, where the surface potential distribution of a simple earthing system, consisting of two half spherical shaped electrodes, is evaluated. The model is placed in vacuum, so the excitation current can only flow through the model.

In the whole thesis the static current field is used for calculation.

1.3. Result

A homogenised model where only the apparent resistivity values are used, shows the biggest error. Using a layered model with the average apparent resistivities shows a better approximation. The best approximation is achieved by using a layered model with

the average inversion model resistivities (reference model).

Due to the change of the resistivity in the inversion model along the investigated line, it can be seen that the zero crossing of the surface potential is not in the middle of the electrodes, but slightly before. Therefore the step and touch voltages would be affected due to this horizontal distribution of the resistivity.

1.4. Conclusion

For good dimensioning of the earthing system, a detailed ground investigation and inversion process to find a good approximation of the real soil resistivity distribution is necessary. The better the soil measurement, the better is the inversion process, the better is the final soil model. A quick estimation can be easily made with the apparent resistivity.

1.5. Outlook

Due to different soils at different places, no general statement can be achieved by this thesis. To be able to analyse the influence more precisely, several different models would have to be established.

To get better data for the inversion process, the measurement should be made, using a true 3D measurement.

Maybe this type of measurement can be used to find and evaluate the condition of an earthing system.

This thesis shows only the influence on the surface potential. More interesting will be the step voltage. The calculation of the step voltage along a line can be easily made, but maybe there is a way to plot the step voltage somehow in a Difference Plot for the whole surface.

The investigated earthing system consists only of two half spherical shaped electrodes, more complex earthing systems shall be investigated.

The next steps would be taking the soil ionization effect into account, because this effect show a significant reduction of the occurring surface potential, as in [1] shown.

Use the quasi-static magnetic field to find the influence of the soil impedances, where also magnetic couplings occur, because power systems normally do not work with static currents.

2. Introduction

2.1. Motivation

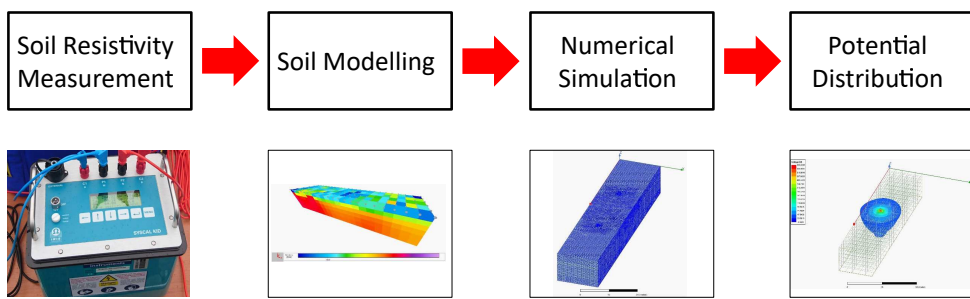


Figure 2.1.: Main steps of this master's thesis

Earthing systems play an important role in peoples' safety and equipment protection. To ensure a properly grounding the soil resistivity is a significant parameter in dimensioning such earthing systems. The resistivity has to be measured to find its value. So, the motivation of this master's thesis is to make an ERT (Electrical Resistance Tomography) with a new measurement equipment. The measurement is mainly used for geophysical surveys which include groundwater investigations, dike detection, orebody search, etc. In electrical engineering a common approach is to make a few soil resistivity measurements and assume homogeneous resistivity distribution. In some cases a few horizontal or vertical layers of different soil resistivities are modelled. But in this work, the basic idea is to make a soil resistivity survey and use the arbitrary soil resistivity distribution for evaluating the behaviour of the surface potential distribution in contrast to homogeneous and layered resistivity. With an ERT only the apparent resistivities can be measured. To find the "real" resistivity (representing the best approximation) of the ground, an inversion modelling process has to be performed. This step is proceed by an inversion software, with reproducible parameters. The solution is the soil resistivity model, with discrete blocks of its inversion model resistivity values, which would cause the same measurement results as the real soil. Due to the different resistivities, analytical methods for evaluating the surface potential are too complex for solving, so a numerical method is used in solving this problem. It is clear that the found resistivity model is unique and only valid for its investigation area. So to give a statement on a specific place, the measurement has to be taken on sight.

The main steps in this master's thesis are summarized in figure 2.1.

2.2. The problem

If homogeneous soil is assumed, there are two possible scenarios:

1. If a measured point gives a low resistivity value and the whole area around has a higher resistivity value, the earthing system will be too small and the occurring surface potential reaches values which can be harmful to humans or animals.
2. If the measured point has a high resistivity value in comparison to its surrounding, the earthing system will be much greater than needed, which will be good on the view of safety, but will end up with higher costs.

This work contributes to the question either detailed ground investigation is needed or not.

2.3. Questions and Goal

The following questions and goals are defined:

- How can one derive the "real" resistivity from the apparent resistivity?
- How can the soil model be implemented for a numerical simulation process?
- How does the arbitrary resistivity distribution influence the surface potential?
- What is the influence if the soil model will be simplified (e.g. homogeneous, layered)?

3. Measurement

3.1. Theory

Assuming infinite space with constant resistivity (homogeneous space) the static current field can be calculated by starting with Maxwell's set of equations [2]:

$$\vec{\nabla} \times \vec{H} = \vec{J} + \frac{\partial \vec{D}}{\partial t} \quad (3.1)$$

$$\vec{\nabla} \times \vec{E} = -\frac{\partial \vec{B}}{\partial t} \quad (3.2)$$

$$\vec{\nabla} \cdot \vec{B} = 0 \quad (3.3)$$

$$\vec{\nabla} \cdot \vec{D} = \rho_c \quad (3.4)$$

Where:

$$\vec{\nabla} = \text{Del} \left(\frac{\partial}{\partial x}, \frac{\partial}{\partial y}, \frac{\partial}{\partial z} \right)$$

$$\vec{H} \quad \text{Magnetic Field Intensity in } \frac{\text{A}}{\text{m}}$$

$$\vec{J} \quad \text{Electric Current Density in } \frac{\text{A}}{\text{m}^2}$$

$$\vec{D} \quad \text{Electric Flux Density in } \frac{\text{C}}{\text{m}^2}$$

$$\frac{\partial}{\partial t} \quad \text{Partial Derivative over the time}$$

$$\vec{E} \quad \text{Electric Field Intensity in } \frac{\text{V}}{\text{m}}$$

$$\vec{B} \quad \text{Magnetic Flux Intensity in T}$$

$$\rho_c \quad \text{Charge density in C}$$

For static fields the partial derivative over the time is zero, and applying the divergence on (3.1). The set of equations for the static current field is:

$$\vec{\nabla} \cdot \vec{J} = 0 \quad (3.5)$$

$$\vec{\nabla} \times \vec{E} = 0 \quad (3.6)$$

$$(3.7)$$

Substitute with:

$$\vec{E} = -\vec{\nabla} \varphi \quad (3.8)$$

$$\vec{J} = \gamma \vec{E} = \frac{1}{\rho} \vec{E} \quad (3.9)$$

Where:

ρ Resistivity in Ωm

The final PDE (Partial Differential Equation) is:

$$\vec{\nabla} \cdot \left(\frac{1}{\rho} \vec{\nabla} \varphi \right) = 0 \quad (3.10)$$

For further investigations it will be assumed that a excitation current will enter the problem region through a sphere. Where the supply line is isolated, so the supplying current is equal to the current which flows out through the surface. Integrating over the surface, excluding the excitation:

$$I = \int_{\Gamma} \vec{J} \cdot d\vec{\Gamma} = \frac{J}{4\pi r^2} \quad (3.11)$$

Where:

r Radial distance in m

$\vec{\Gamma}$ Surface vector

The solution for φ (Electric Scalar Potential in V) in infinite space would then be:

$$\varphi(r) = \frac{\rho I}{4\pi r} \quad (3.12)$$

Adding a second electrode (source C_1 and sink C_2):

$$\varphi(r) = \frac{\rho I}{4\pi} \left(\frac{1}{r_{C1}} - \frac{1}{r_{C2}} \right) \quad (3.13)$$

Where:

r_{C1} Distance to C_1 in m

r_{C2} Distance to C_2 in m

In case of soil resistivity surveys we can assume two infinite half spaces as illustrated in figure 3.1. It is clear, that the current can only flow in the halfspace with constant resistivity, so the current in the lower space will get doubled and the solution for the φ changes to:

$$\varphi(r) = \frac{\rho I}{2\pi r} \quad (3.14)$$

Respectively for two electrodes:

$$\varphi(r) = \frac{\rho I}{2\pi} \left(\frac{1}{r_{C1}} - \frac{1}{r_{C2}} \right) \quad (3.15)$$

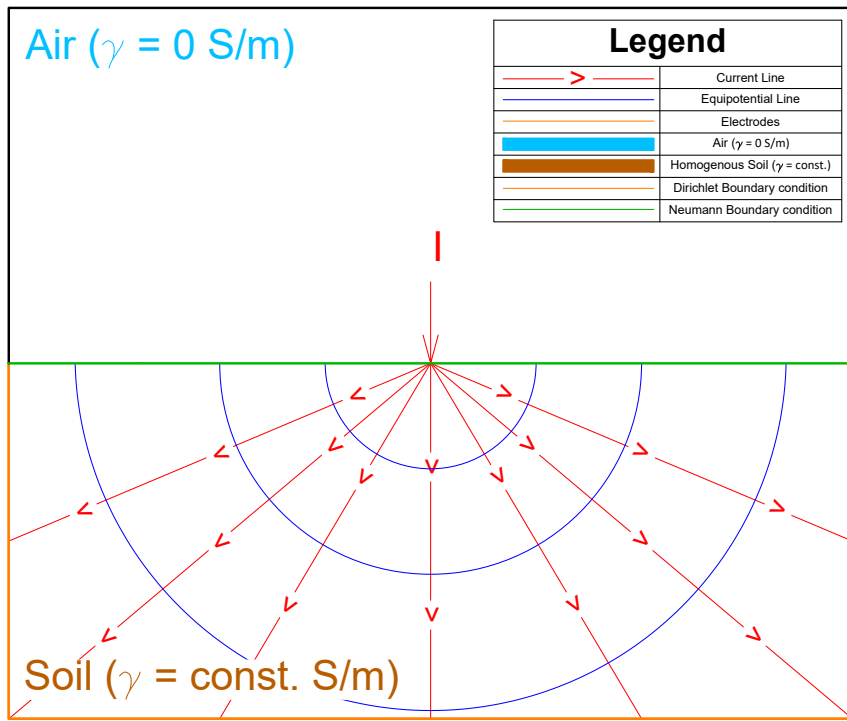


Figure 3.1.: Infinite half space with point current source

In ERT four electrodes arrays are used and the potential difference between the potential electrodes gets [3]:

$$U_P = \frac{\rho_a I_C}{2\pi} \left(\frac{1}{r_{C1P1}} - \frac{1}{r_{C2P1}} - \frac{1}{r_{C1P2}} + \frac{1}{r_{C2P2}} \right) \quad (3.16)$$

Where:

- U_P Potential difference between electrodes P1 and P2 in V
- ρ_a Apparent Resistivity in Ωm
- I_C Injected current intensity between electrodes C1 and C2 in A
- r_{C1P1} Distance between C_1 and P_1 in m
- r_{C2P1} Distance between C_2 and P_1 in m
- r_{C1P2} Distance between C_1 and P_2 in m
- r_{C2P2} Distance between C_2 and P_2 in m

Which can be rewritten for the apparent resistivity [3]:

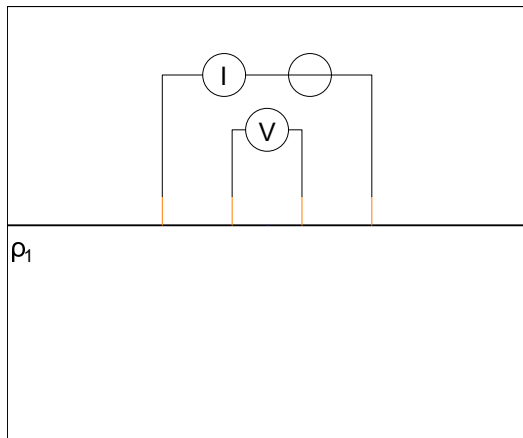
$$\rho_a = k \frac{U_P}{I_C} \quad (3.17)$$

with:

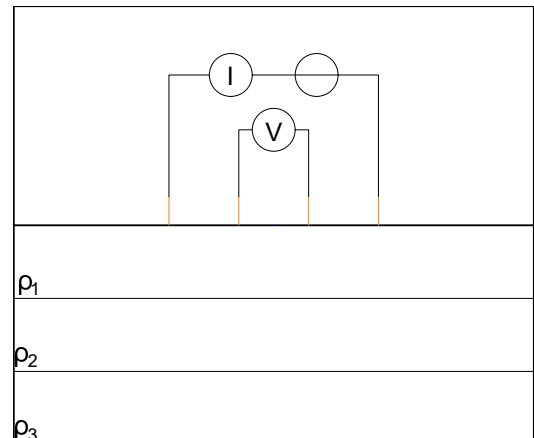
$$k = \frac{2\pi}{\left(\frac{1}{r_{C1P1}} - \frac{1}{r_{C2P1}} - \frac{1}{r_{C1P2}} + \frac{1}{r_{C2P2}} \right)} \quad (3.18)$$

Where:

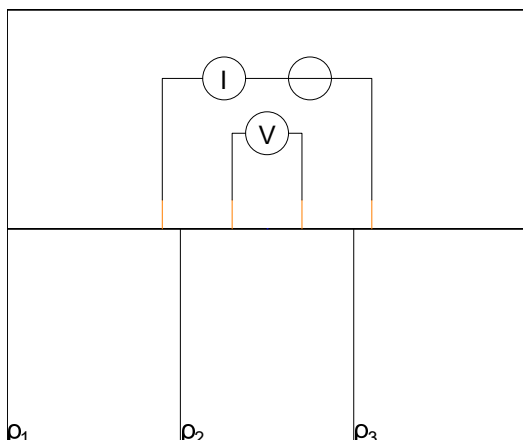
k Geometric factor of the array in m



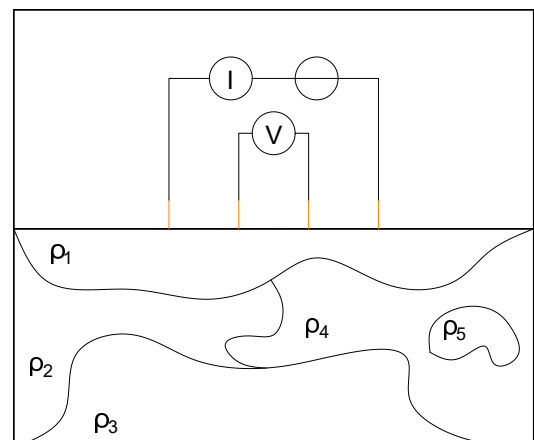
(a) homogeneous soil model



(b) horizontal layered model



(c) vertical layered model



(d) arbitrary layered model

Figure 3.2.: Different soil models

3.1.1. Soil resistivity distribution

There are different ways to model soil resistivity:

- homogeneous soil distribution (figure 3.2a)
- heterogeneous soil distribution
 - horizontal layers (figure 3.2b)
 - vertical layers (figure 3.2c)
 - arbitrary shaped layers (figure 3.2d)

To analyse those models, analytical or numerical methods can be used. Analytical methods (e.g. method of images) are quite limited to homogeneous, horizontal or vertical layered soil, due to the fact that for arbitrary soil distribution a change in resistivity can occur in three dimensions (x, y, z), which would end up in a huge computing time, so the common approach is to solve this in a numerical manner.

3.1.2. Measurement methods

For soil resistivity measurements a four electrodes array is used. Two electrodes for current injection, two electrodes are used for voltage measurement. The following electrode arrays are commonly used in field surveys [3], [4]:

- Wenner Array (α, β, γ)
- Schlumberger Array
- Dipole-Dipole Array
- Pole-Dipole Array
- Pole-Pole Array

For the measurements in this thesis, only the Wenner- α and the Dipole-Dipole Array are used. The schematic of both are represented in figures 3.3 and 3.4 respectively, where C_i are the current electrodes and P_i are the potential electrodes. Detailed information of the used arrays can be found in the following subsections.

3.1.3. Wenner Array

The Wenner array (normal configuration is α) is a four electrode array with equidistant spacing a (figure 3.3). According to [3] the array shows up with good noise immunity and is very sensitive to vertical changes in the ground layers. Meaning this method is useful for detection of horizontal layers, but poor in finding small vertical structures (e.g. vertical earthing rods). [3]

By analysing the sensitivity function of this array, as in [3], the good horizontal detection capabilities can be explained with the nearly horizontal sensitivity lines under the electrodes.

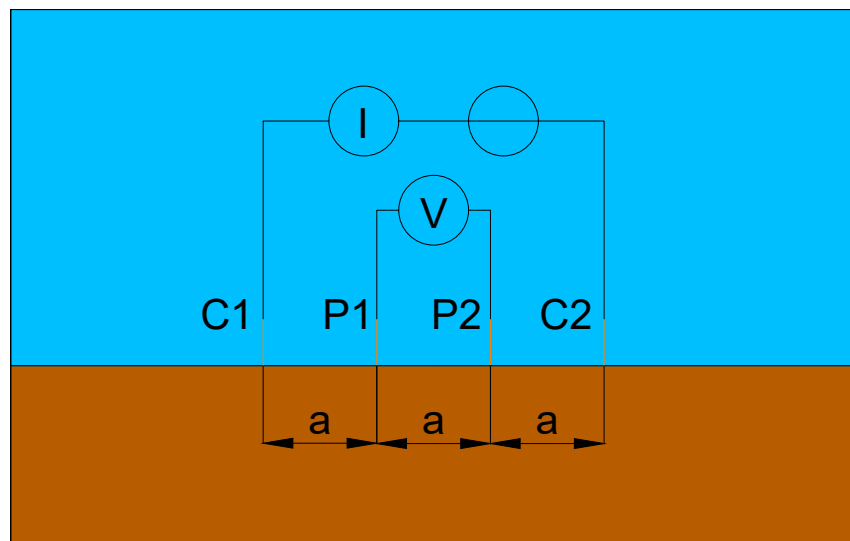


Figure 3.3.: Wenner Array

The other possible Wenner Array configurations are schematically shown in the following table (electrode position from left to right):

Table 3.1.: Different Wenner configurations

Configuration	Electrodes			
α	C1	P1	P2	C2
β	C2	C1	P1	P2
γ	C1	P1	C2	P2

The geometric factor for the Wenner- α array can be calculated by using equation (3.18)

$$k = \frac{2\pi}{\left(\frac{1}{a} - \frac{1}{2a} - \frac{1}{2a} + \frac{1}{a}\right)} = 2a\pi \quad (3.19)$$

3.1.4. Dipole-Dipole Array

The Dipole-Dipole array is also a four electrode array. The array is build as seen in figure 3.4. The spacing between the dipoles itself (distance between C1-C2 and between P1-P2) is represented by a , where the distance between the both dipoles is represented by $n \cdot a$ and will be changed in the switching process for profiling. This array is good for vertical layer detection and has a better horizontal data coverage than the Wenner array. [3] The better horizontal coverage of the Dipole-Dipole array can be seen in the Pseudosection plots (e.g. figure 3.11).

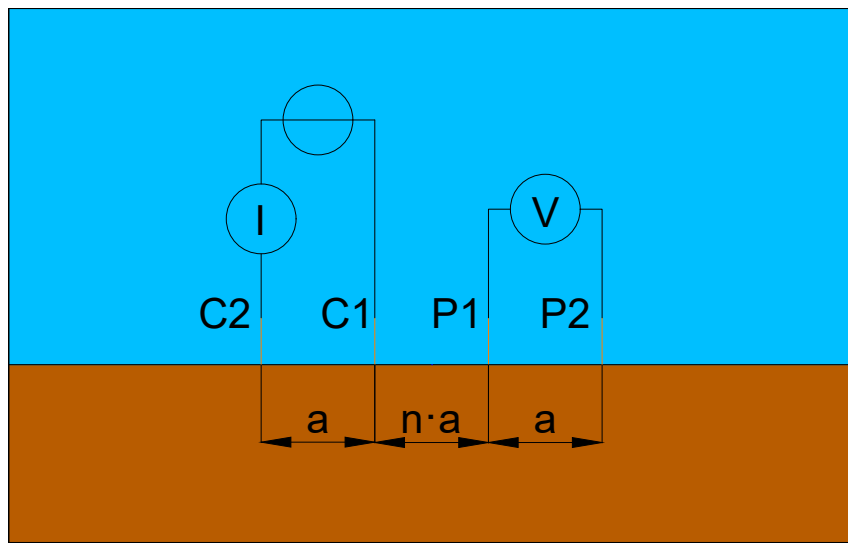


Figure 3.4.: Dipole-Dipole Array

3.1.5. Profiling

To investigate soil resistivity two approaches are possible:

1. VES (Vertical Electrical Sounding)
2. Profiling

The difference between both is, that in VES the center of the measurement remains on the same location and the electrodes distances are increased to get in deeper layers (mainly used for deep vertical soundings of a point). Where in profiling the electrode array is moved from a starting point on a line. [5]

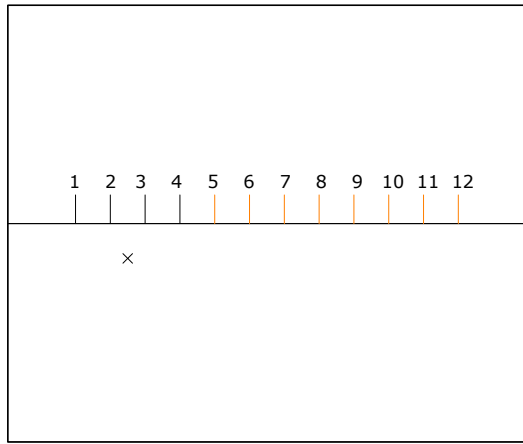
Each measurement produces a data point in the middle of the four electrodes. To get the data points deeper in the soil, the distance between the electrodes is changed to greater values. This is done by switching of the measurement unit [5].

Switching Process, exemplarily for the Wenner Array:

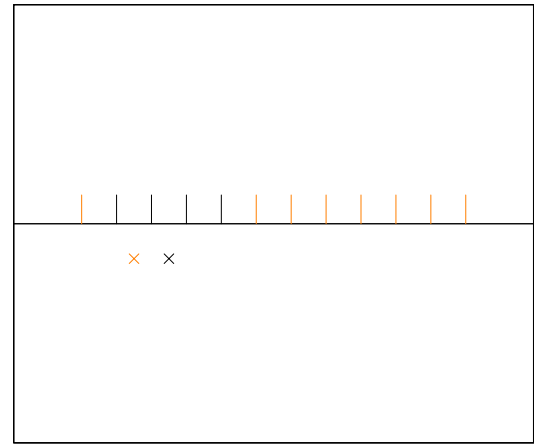
- 1st row (spacing: a):
 - 1. {1, 2, 3, 4}
 - 2. {2, 3, 4, 5}
 - ...
 - k. {k, (k + 1), (k + 2), (k + 3)}
 - (n_e - 3): {(n_e - 3), (n_e - 2), (n_e - 1), n_e}
- 2nd row (spacing: 2a):
 - 1. {1, 3, 5, 7}
 - 2. {2, 4, 6, 8}
 - ...
 - k. {k, (k + 1 · 2), (k + 2 · 2), (k + 3 · 2)}
 - (n_e - 5): {(n_e - 6), (n_e - 4), (n_e - 2), n_e}
- ...
- mth row (spacing $m \cdot a$):
 - k. {k, (k + 1 · m), (k + 2 · m), (k + 3 · m)}

This is repeated until the maximum spacing is reached.

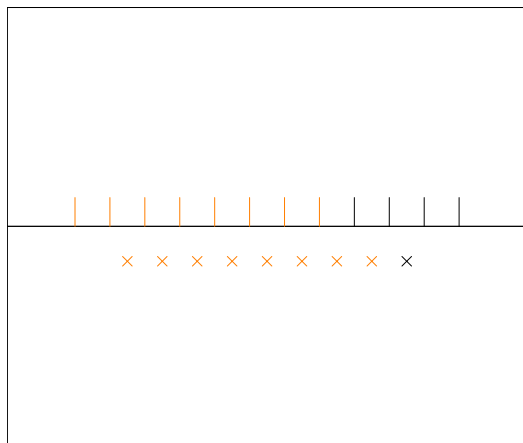
Figure 3.5 shows the switching process in an illustrative manner.



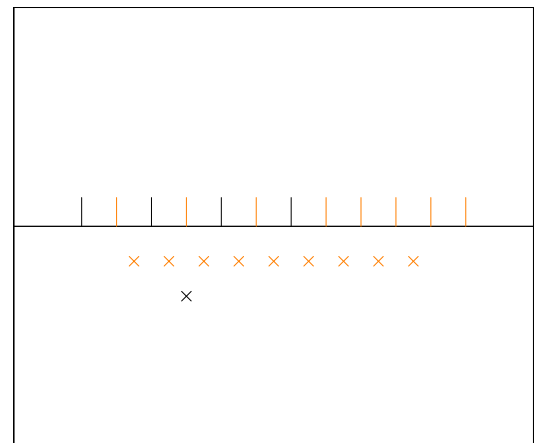
(a) 1st data point, in 1st row



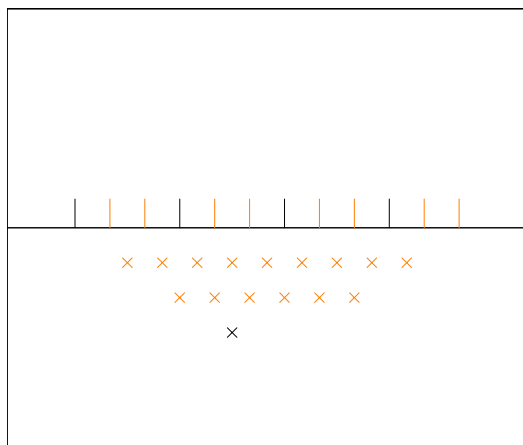
(b) 2nd data point, in 1st row



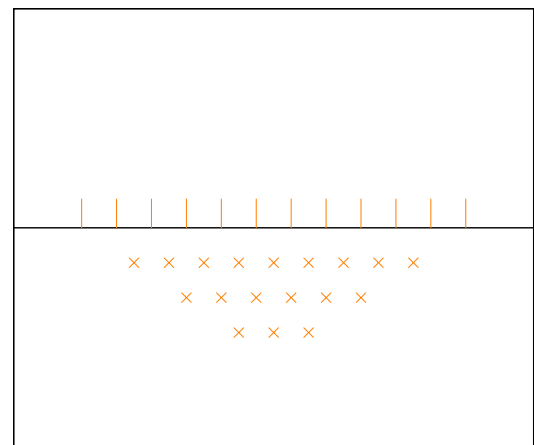
(c) nth data point, in 1st row



(d) 1st data point, in 2nd row



(e) 1st data point, in mth row



(f) all data points

Figure 3.5.: Selected electrodes with obtained data points (Wenner method)

The maximum number of the data points can be calculated by:

$$m = \lfloor \frac{n_e}{a} \rfloor \quad (3.20)$$

Where:

- m Maximum number of datapoint rows
- n_e Number of electrodes per line
- a Equidistant spacing of the electrodes in m

Let's assume homogeneous soil (as in figure 3.2a), then the apparent resistivity is equal to the resistivity of the soil, in this case its "real" resistivity. In reality the soil resistivity distribution will be arbitrary in shape (heterogeneous, as in figure 3.2d), and so the apparent resistivity is not equal to its true resistivity. Through an inversion process, it is possible to find an approximation, which will be called inversion model resistivity (the inversion process will be discussed in detail in chapter 4). So the apparent resistivity values are somehow pseudo values. To visualize them, they can be plotted in a scatter plot, for a first view of the ground, but they are not the resistivity of the soil.

Another fact in homogeneous soil is, that the spacing is representing the depth of the apparent resistivity (data point). For heterogeneous soil a common way to get stable estimation parameters, the median value of the sensitivity function is used - called "median depth". The median depth depends on the used array. [3]

3.1.6. 3D model

To provide the apparent resistivity data for the 3D inversion process, it is possible to measure in different ways. The methods can be categorized and provide different quality of the inversion process [3]:

- **Category 1**

In this category all necessary electrodes are placed in a rectangular grid on surface and the measurement unit evaluates all possible configurations (meaning every electrode is taken into account).

- **Category 2**

All electrodes are placed in a rectangular grid on surface and the measurement unit evaluates all orthogonal configuration and only a limited number of angled configuration (e.g. 45°).

- **Category 3**

Also all electrodes are placed in a rectangular grid on the surface, but only the orthogonal directed configurations are evaluated.

- **Category 4**

In this case the measurements are only taken in one direction (line survey). The third dimension is generated by making several line surveys.

From this point of view it is clear that Category 1 has the largest number of data points, where Category 4 has the least number of data points. For that reason the last category provides the worst quality for 3D inversion, but can be achieved with lowest amount of equipment.

3.2. Method

To get the apparent resistivity distribution, an ERT from an exemplary area is performed. To get data for a 3D resistivity distribution, several 2D line surveys are made. That means a 3D model, Category 4 (section [3.1.6](#)), is built.

3.2.1. General

The criteria for the exemplarily measured area are:

- no hilly ground
- no sewer
- no water pipeline
- no metal fences
- etc.

These criteria are set to minimize the influence on the soil resistivity measurement. The selected place is a flat field located in southern of Styria in the township "Tillmitsch" (around 30 – 40 km, southern of Graz). The GPS (Global Positioning System) coordinates of the first line are:

- N46°48,281' E15°31,595' for the starting point and
- N46°48,244' E15°31,605' for the ending point.

The survey line is nearly oriented in a north to south way (South-South-East), where the further lines are parallel to the first one and going into an East-North-East way.

Some information on the local site: A medium voltage line crossed the measured area, but the wooden-tar towers are not near the measurement, so no influence on the measurement is expected from this side. The main branch of the river "Laßnitz" is also far away. The survey lines are orthogonally oriented to the secondary channel of the river, the distribution network line and the stable.

The day of measurement: 28th December 2019.

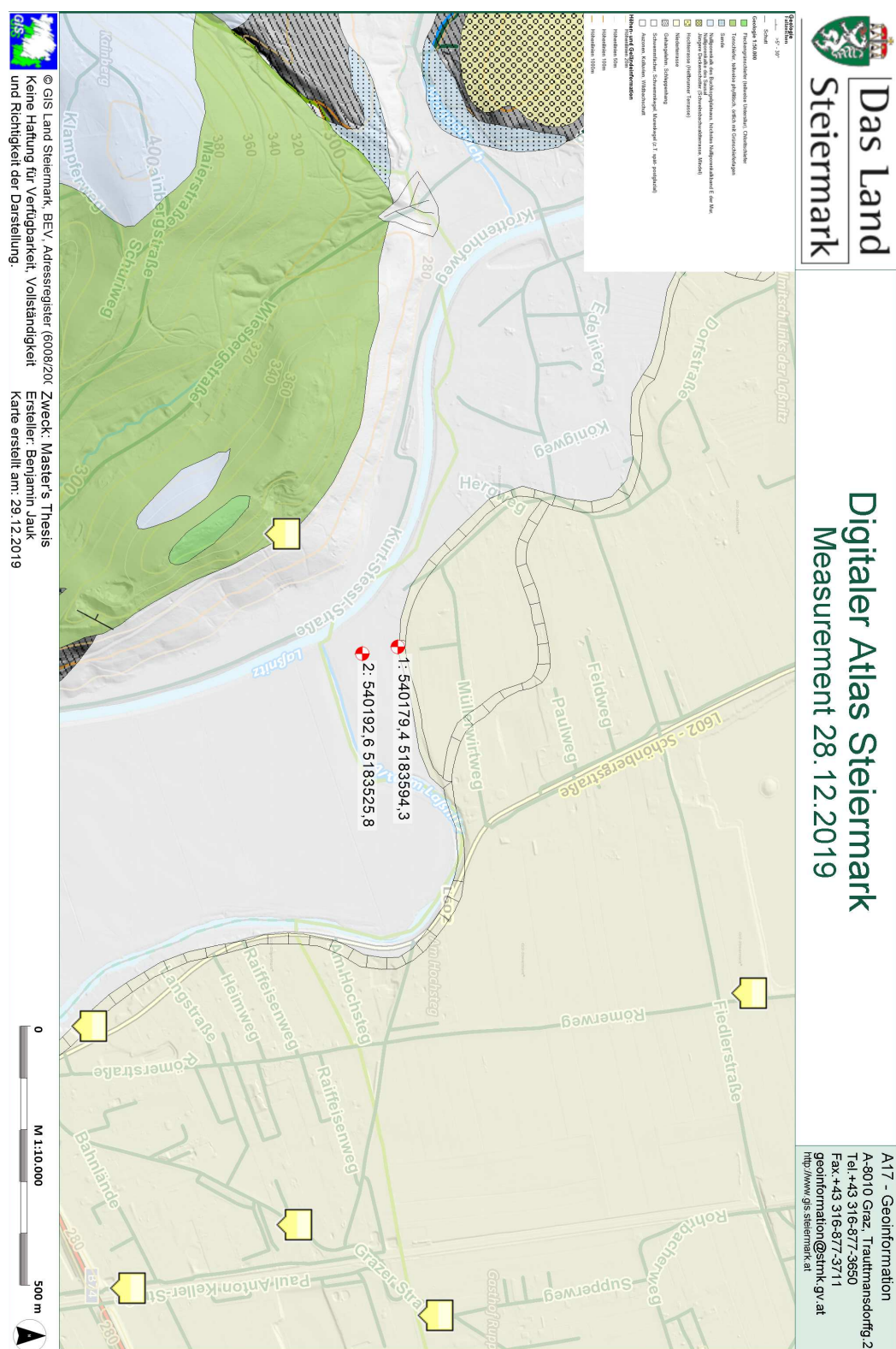


Figure 3.6.: Measured Site [6]



(a) View: North



(b) View: South

Figure 3.7.: Photos from site

3.2.2. Weather Condition

The soil resistivity is heavily dependent on the moistness of the soil. It can be seen in figure 3.8 that the last rain was on 23rd of December 2019 with $25 \frac{l}{m^2}$, followed by a neglectable amount on 27th of December 2019. The soil moisture was not identified on the day of measurement.

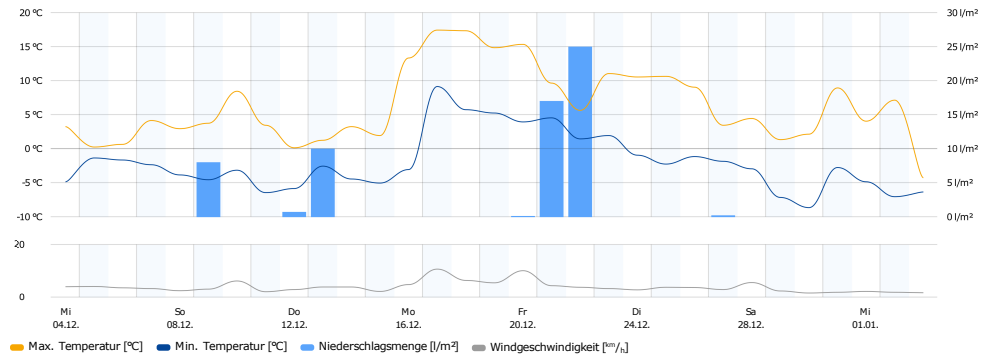


Figure 3.8.: Weather Archive for the site [7]

3.2.3. Measurement

As written before, the measurement is a pseudo-3D (Category 4). The measurement setup, illustrated in figure 3.9, contains six 2D line surveys, where each line has 24 electrodes. The spacing between each electrode and the distance between two lines is equal to 3 m respectively and the penetration depth of the electrodes is approximately 300 mm. The observed area is then: $69 \text{ m} \times 15 \text{ m}$ (x,y direction). The used array for the 3D inversion data is a Wenner array. Both, line 0 and line 5 are measured also using Dipole-Dipole method, to compare those two data sets.

To ensure a stable measurement, the measurement takes place during daytime on one day. The duration for one line measurement was: approximately 30 min for Wenner and 50 min for the Dipole-Dipole method (only measurement time, no set up time taken into account). So only six survey lines were possible to measure on that day.

In total:

- six survey lines
- 504 data points in Wenner method
- 306 data points in Dipole-Dipole method

were measured.

For the measurement a IRIS Instruments SYSCAL KID SWITCH-24 is used. The injected current is pulsed to compensate the self potential, which is caused by telluric currents or human caused stray currents.

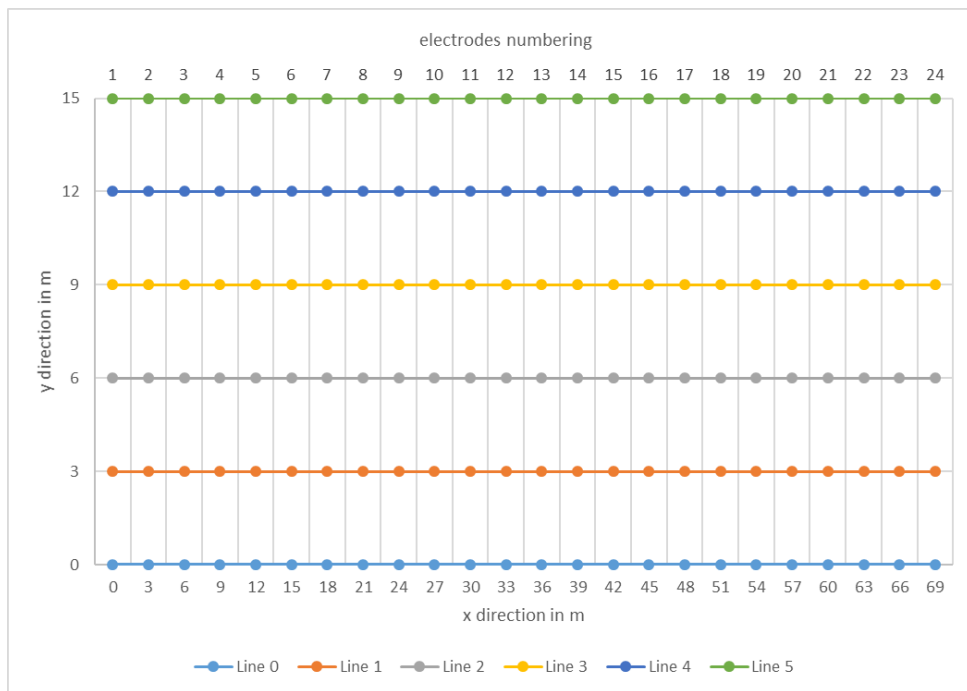


Figure 3.9.: Electrodes Arrangement

The parameters of the unit are:

- Time: *Standard*
The pulse duration is about 2 s, with an injection cycle of about 4 s.
- Number of measurements: 4-5
The minimum and maximum amount of measurements per quadrupole.
- Limit σ (Standard deviation in %): 9
The Standard deviation in % is calculated after each measurement. If the σ of the measured values, after the minimum number of measurements, is less than the limit, the measurement stops. If not, the measurement process is continued until σ is smaller than the limit or the maximum number is reached, whichever occurs first.
- Array: *Wenner* (line 0-5), *Dipole-Dipole* (line 0,5)
The used arrays for the measurement.
- #lvl: 7 (*Wenner*), 9 (*Dipole-Dipole*)
The Lvl (Depth Level) for the investigation.
- Nodes, spacing: 24, 3 m
Number of used electrodes with their distance between.

3.2.4. Apparent Resistivity Plot

As written in section 3.1.5, for the inversion process the median depth of the array is used. For calculation of the median depth values the program RES2DMOD¹ is used. The theoretical depths (in case for a Wenner array: depth equal a) of the arrays are corrected with the factors printed in table 3.2.

The measurement unit denotes the spacing (y direction) between two survey lines (e.g. line 0 and line 1) by 1 m. For further plotting and calculation the spacing in the data has been changed to 3 m to ensure the correct position of the data points.

3.3. Results

3.3.1. Median Depths

The median depths, shown in table 3.2, are the values per total array length L . All following plots are shown in corrected depth.

Table 3.2.: Calculated Median Depths of investigation

Array	$\frac{z_e}{L}$
Wenner- α	0,173
Dipole-Dipole	
n	
1	0,1386
2	0,1743
3	0,1386
4	0,2034
5	0,2108
6	0,2162
7	0,2204
8	0,2236
9	0,2262
10	0,2283

¹Software for 2D Forward Modelling from Geotomo Software <https://www.geotomosoft.com>

3.3.2. Measurement results

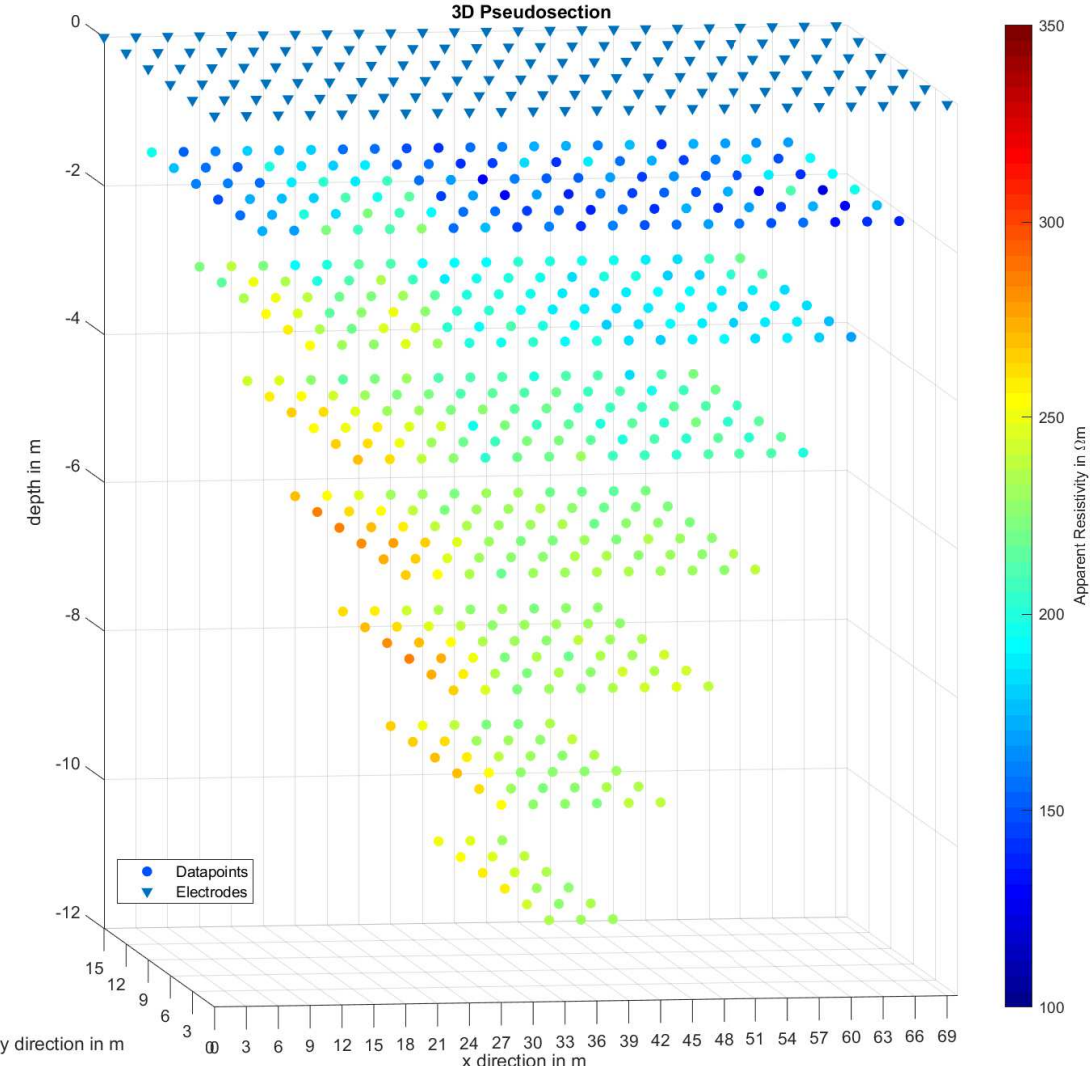


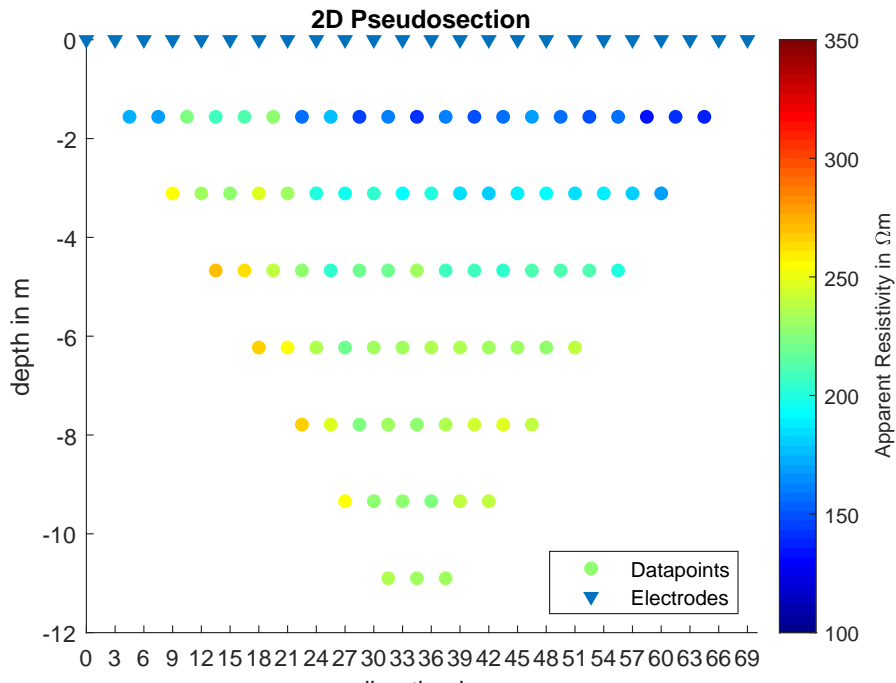
Figure 3.10.: 3D Pseudosection

In figure 3.10 all measured apparent resistivities of the Wenner measurement can be seen. All survey lines have a comparable resistivity distribution. For that reason, the further discussion is in a detailed view on Line 0 (figure 3.11) only.

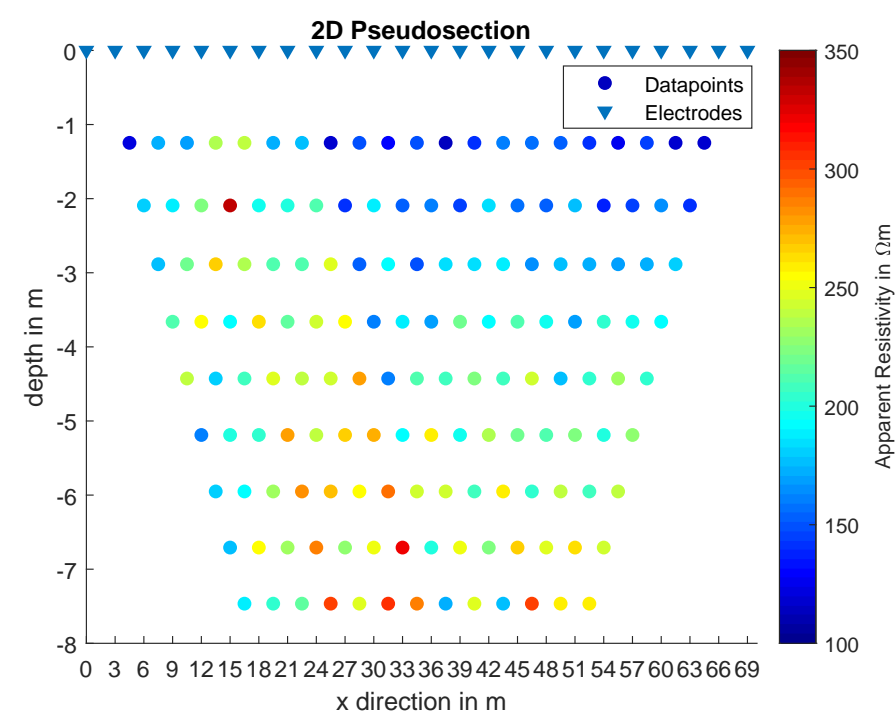
It can be seen that the topmost data points show the least resistivity values, where the deeper layers have higher values. The triangulated shape of the data points is given by the measurement setup (profiling).

The Wenner measurement (figure 3.11a) compared to the Dipole-Dipole measurement (figure 3.11b) has less data points, but is deeper in measurement (Wenner: -10.9 m , Dipole-Dipole: -7.5 m). That is the reason why the Dipole-Dipole measurement needs more measuring time.

The pseudosection plot provides a first overview of the measured data. For the Dipole-Dipole data points it is noticeable that there are some "bad data points" (e.g. fourth datapoint, in second row) meaning, resistivity values which differ with high deviation to their neighbouring values. For example the fourth value in the second row is around $100\Omega\text{m}$ higher than the left and right point. This can occur by a bad electrode-ground contact or measured artefacts. If only the standard deviation σ is taken into account these bad data points can't be found. In this case $\sigma = 0.13\%$ (table B.2, #29), which is even a good value, compared to some other measurements of this line.



(a) Wenner Array



(b) Dipole-Dipole Array

Figure 3.11.: Apparent resistivity Line 0 - Wenner vs. Dipole-Dipole Array

4. Inverse Modelling

4.1. Theory

For the inverse modelling process the start parameters are limited to measured (observed) data. The basic idea is to find model parameters, that describe the model, where the model response is causing the set of observed data. Solving this inverse models is done by a numerical approach. With estimated start parameters for the model, the discrepancy between the observed data and the model response is minimized. The minimization is done by least-square method with an optimized Gauss-Newton algorithm. [3]

Compared to that, forward modelling, would be the classical approach in engineering. One first defines model parameters, use physical laws to find the model response.

An illustrative example will be a resistor network:

- In case of forward modelling all resistor values will be predefined, the resistors soldered together and the total resistance or apparent resistance between two points can be obtained.
- In case of inverse modelling only the measured apparent resistance of the accessible points is available. With that values the resistor values have to be calculated. One big disadvantage in soil resistivity measurement is, that only the points on the ground surface can be connected and the distribution of the resistance values are not visible.

The mathematical approach for inverse modelling can be written as the following [3], [8]:

$$\vec{y} = \begin{pmatrix} y_1 \\ y_2 \\ \vdots \\ y_m \end{pmatrix}, \quad \vec{f} = \begin{pmatrix} f_1 \\ f_2 \\ \vdots \\ f_m \end{pmatrix}, \quad \vec{q} = \begin{pmatrix} q_1 \\ q_2 \\ \vdots \\ q_n \end{pmatrix} \quad (4.1)$$

Where:

- \vec{y} Measured data vector
 \vec{f} Model response vector
 \vec{q} Model parameter vector

The discrepancy is mapped to the Error function.

$$E = \vec{g}^T \vec{g} = \sum_{i=1}^n g_i^2, \text{ with } \vec{g} = \vec{y} - \vec{f} \quad (4.2)$$

Where:

E Error function

The Gauss-Newton equation is used for calculating the model parameter.

$$\mathbf{J}^T \mathbf{J} \Delta \vec{q}_k = \mathbf{J}^T \vec{g}, \text{ with } J_{ij} = \frac{\partial f_i}{\partial q_j} \quad (4.3)$$

Where:

\mathbf{J} Jacobian Matrix

Δ Finite change of the variable

When the change of the model vector $\Delta \vec{q}_k$ is calculated, a new model is obtained by:

$$\vec{q}_{k+1} = \vec{q}_k + \Delta \vec{q}_k \quad (4.4)$$

The software RES3DINV¹, which is used for inverse modelling of the apparent resistivity data, is using an optimized Gauss-Newton algorithm. This algorithm is based on the smoothness-constrained least-squares method:

$$(\mathbf{J}^T \mathbf{J} + \lambda \mathbf{F}) \Delta \vec{q}_k = \mathbf{J}^T \vec{g} - \lambda \mathbf{F} \vec{q}_k \quad (4.5)$$

With:

$$\mathbf{F} = \alpha_x \mathbf{C}_x^T \mathbf{C}_x + \alpha_y \mathbf{C}_y^T \mathbf{C}_y + \alpha_z \mathbf{C}_z^T \mathbf{C}_z \quad (4.6)$$

Where:

\mathbf{F} Filter Matrix

λ Damping factor

α_i Relative weighting factor in direction i

\mathbf{C}_i Roughness Filter Matrix in direction i

So the new model parameter can be calculated, using equations (4.4) and (4.5):

$$\vec{q}_{k+1} = \vec{q}_k + (\mathbf{J}^T \mathbf{J} + \lambda \mathbf{F})^{-1} (\mathbf{J}^T \vec{g} - \lambda \mathbf{F} \vec{q}_k) \quad (4.7)$$

The reason for this optimization is the fact, that the matrix product $\mathbf{J}^T \mathbf{J}$ can be singular. To avoid singularities several optimizations are used. [3]

¹Software for 3D Inversion from Geotomo Software <https://www.geotomosoft.com>

4.2. Method

The inversion was carried out by the software RES3DINV and RES2DINV². Most of the parameters were left Default, the changed ones are summarized and listed. The overall settings are printed in the appendix C.

Table 4.1.: Changed Forward modelling Parameters for 3D inversion

Forward Modelling	
Type of forward modelling	FEM
Horizontal Mesh Size	4nodes
Vertical Mesh Size	Ultra-Fine (4nodes)
Borehole Mesh Size	4nodes
Mesh Boundary	medium extended
Inversion Parameters	
Error Change convergence	2 %
Thickness of first layer	1.35

Table 4.2.: Changed Forward modelling Parameters for 2D inversion

Forward Modelling	
Horizontal Mesh Size	4nodes
Vertical Mesh Size	Finest
Forward Modelling Type	FEM
Convergence Limit	
Error Change convergence	2 %
Model Refinement	
Model cells	0.5 of unit spacing

²Software for 2D Inversion from Geotomo Software <https://www.geotomosoft.com>

4.3. Results

The result of the inversion process can be seen in figure 4.1, showing the inversion model resistivity. The topmost two layers show lower resistivities, where the deeper section have higher resistivities.

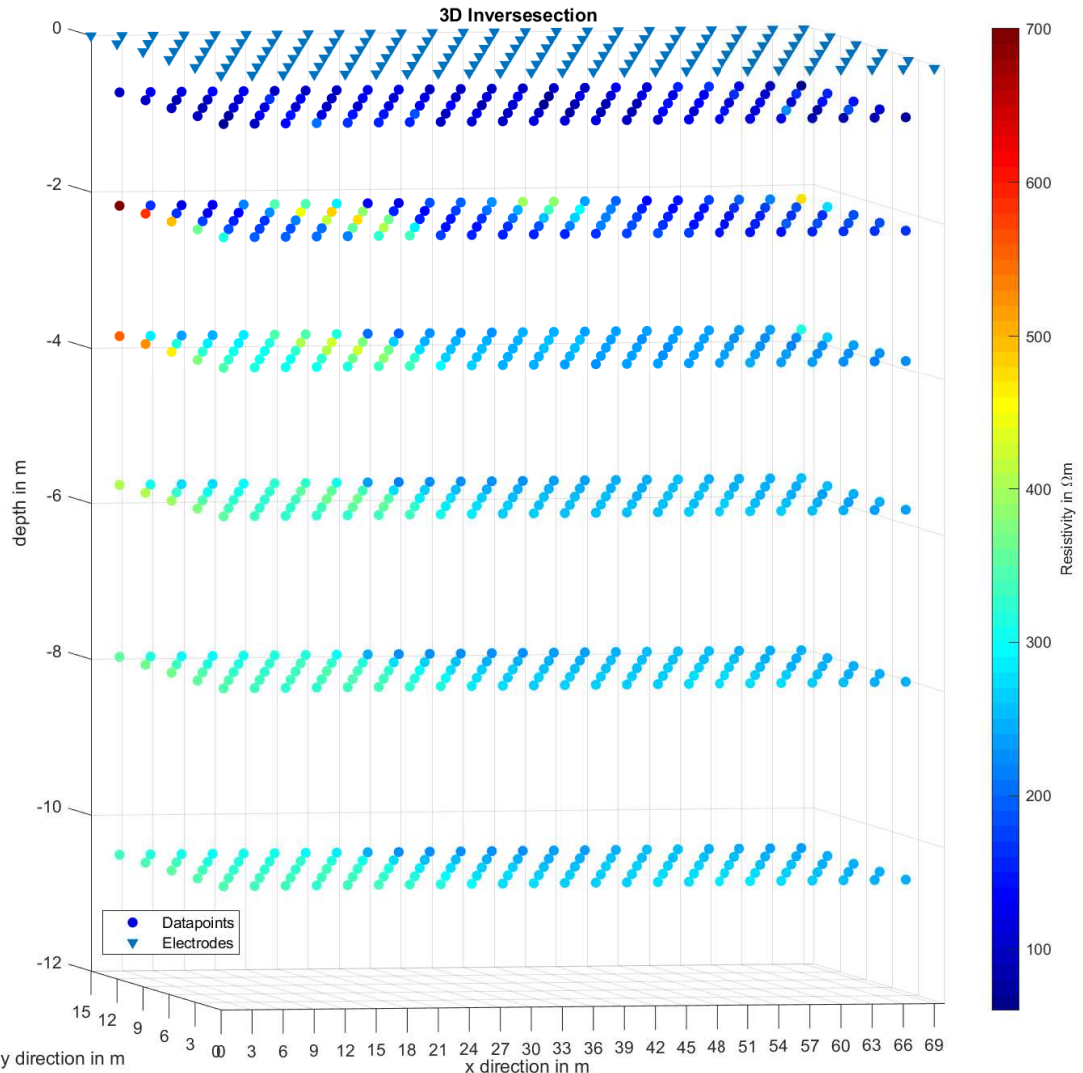
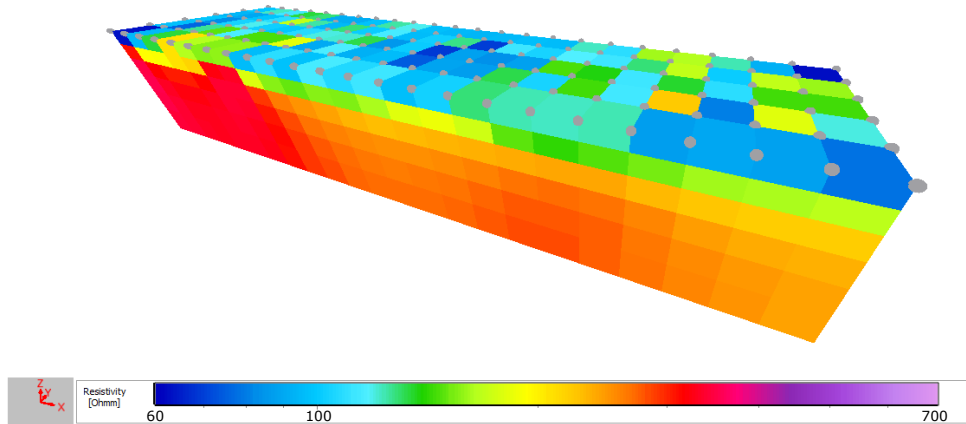


Figure 4.1.: 3D Inversesection

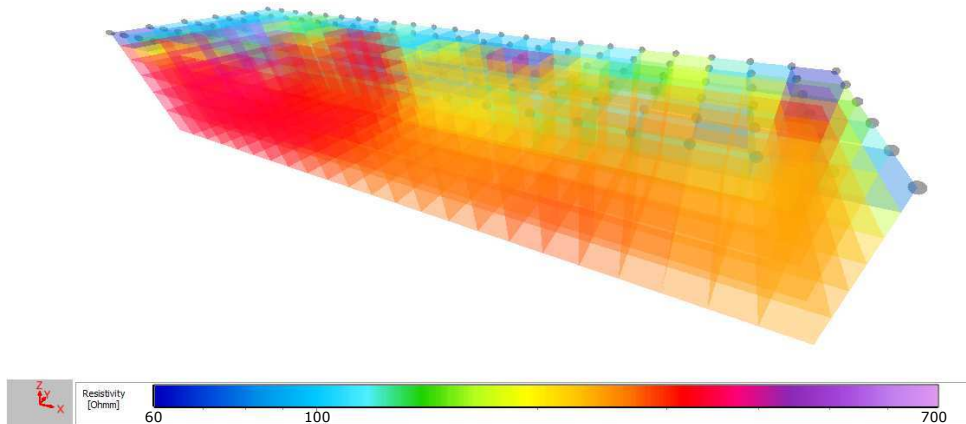
Figure 4.2 shows the discrete resistivity blocks for the following numerical simulation.

Resistivity model with data misfit 1.36%



(a) full view

Resistivity model with data misfit 1.36%



(b) transparent view

Figure 4.2.: 3D Inversion Model

A more detailed view on Line 0, figure 4.3 shows the 2D Pseudosection and 2D Inversesection. It can be seen, that the apparent resistivity is not equal the inversion model resistivity. The pseudosection is the model response of the inversesection. In general the inversion model resistivity distribution is in a smooth manner, only in the second layer, three blocks appear with higher values than the neighbouring ones. There is also a difference in the depths of the data points. The reason for this is, that in the pseudosection (figure 4.3a), the depths are given by the used array with its median depth, but in the inversesection (figure 4.3b) the depths can be adjusted with parameters of the inversion software. The thickness of the layers is increasing in depth as well, due to software parameters.

It is noticeable that the data points in the pseudosection is "V" shaped, so for the rectangular shaped inversesection there is data missing at the surroundings in deeper layers. So the inversion model resistivity is in this section not as trustable as in the middle of the measurement. There can be boundary effects during the inversion process, ending up with wrong inversion model resistivities.

In this work, there will be no further investigation of the resistivity values of the soil, meaning the interpretation of the values. That will be more in the field of geophysics than electrical engineering. The values will be directly used for the numerical simulation.

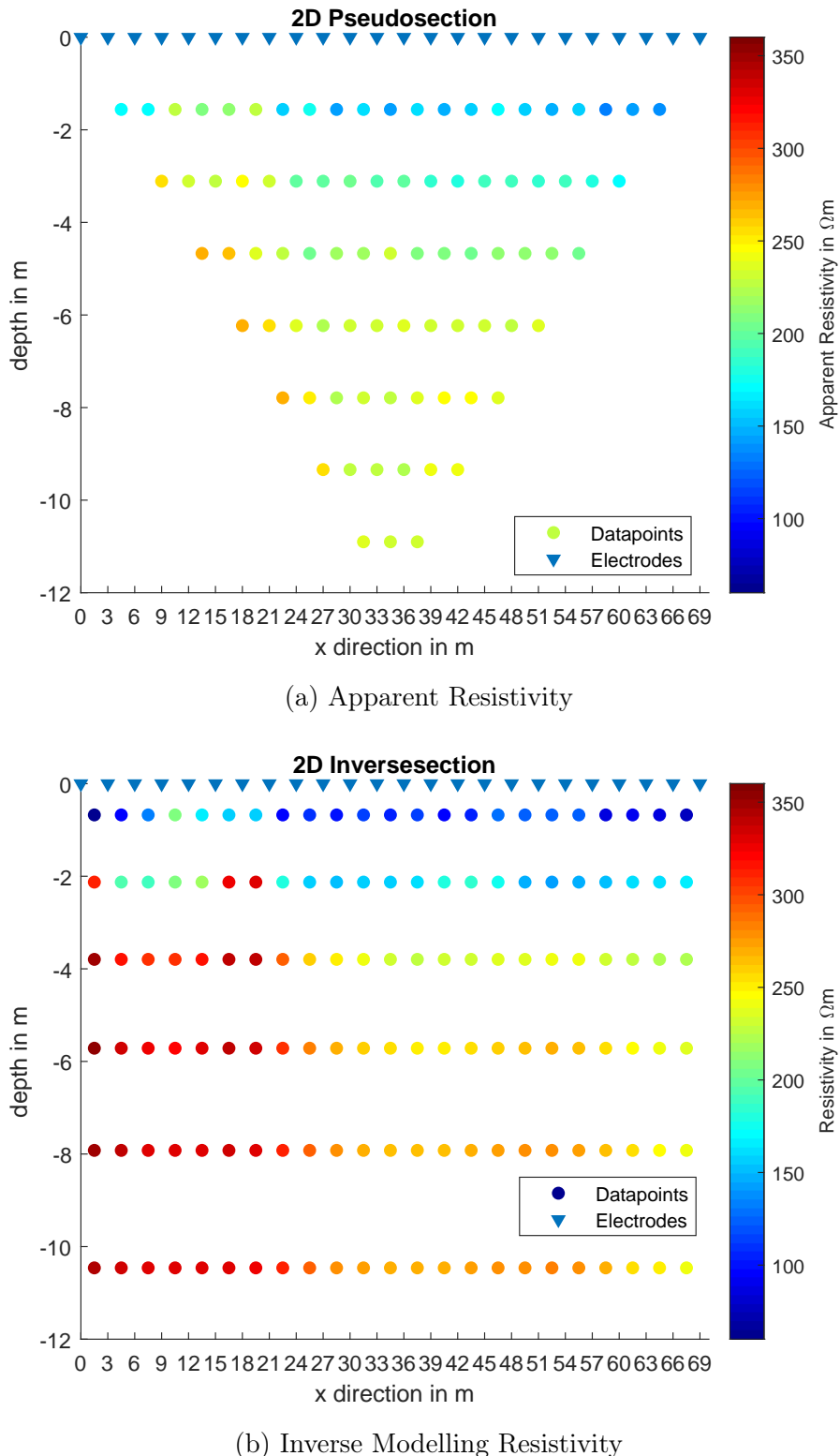


Figure 4.3.: Apparent vs. Inverse Modelling resistivity of Line 0

5. Simulation

5.1. Theory

When geometries are getting more complex or the materials are heterogeneous, analytical methods are getting difficult to solve the PDE of the problem. In this case numerical approaches are used for calculation. In the following sections FDM and FEM are discussed more in detail. The explanation of the basics is limited to 2D case.

The final simulation is performed with FEM due to possible complex geometries in earthing systems.

5.1.1. Finite Difference Method

FDM is an approximation where the differential equations are replaced by finite difference equations, the point of calculation has a relationship to the neighbouring points. The FDM is a simple approach and can be used universally in different applications. [9]

The FDM solution involves the following main three steps [9]:

1. dividing into grid of nodes
2. approximating the differential equation by its equivalent finite difference, depending on the values of the neighbouring points
3. solving the finite difference equations in subject to the predefined boundary/initial conditions

Common grid patterns for FDM are, as shown in figure 5.1:

- (a) rectangular grid
- (b) skew grid
- (c) triangular grid
- (d) circular grid

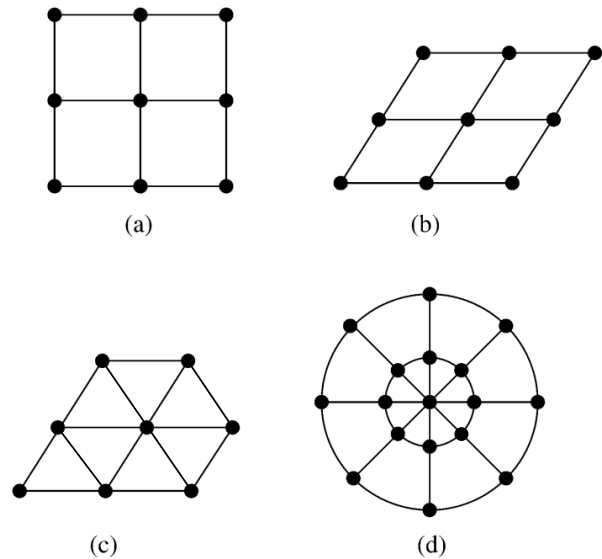


Figure 5.1.: Common FDM grid patterns [9]

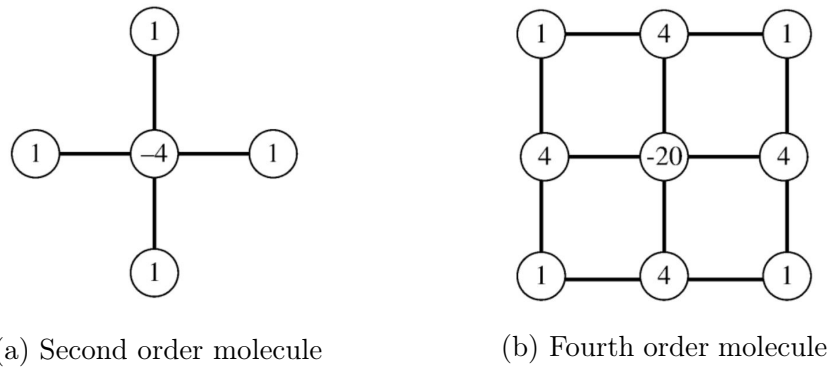


Figure 5.2.: FDM molecules [9]

The problem, introduced in section 3.1, leads to Laplace's equation (3.10). Second order linear PDEs (Partial Differential Equations) are categorized as either parabolic, hyperbolic or elliptic. Laplace's equation is a typical elliptic PDE. A numerical solution for the point i, j , as shown in figure 5.3, of a general Laplace equation [9]:

$$\vec{\nabla}^2 \Phi = \frac{\partial^2 \Phi}{\partial x^2} + \frac{\partial^2 \Phi}{\partial y^2} = 0 \quad (5.1)$$

Where:

Φ Potential

is found by [9]:

$$\Phi(i, j) = \frac{1}{4} [\Phi(i+1, j) + \Phi(i-1, j) + \Phi(i, j+1) + \Phi(i, j-1)] \quad (5.2)$$

This solution is depending on the four surrounding points, which is a second order approximation (shown in figure 5.2a).

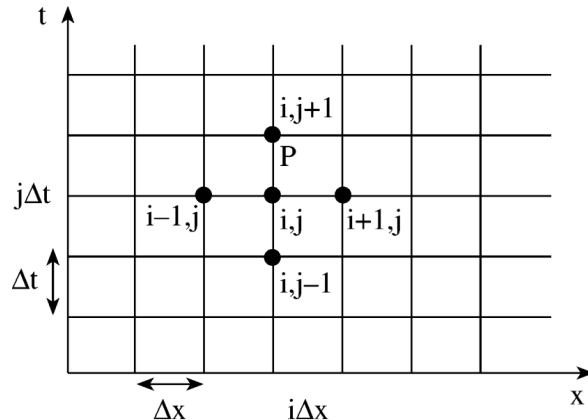


Figure 5.3.: FDM mesh in 2D [9]

If all surrounding points, not only the orthogonal points, but also the diagonal ones are used the solution is a four order approximation of the PDE. The molecule to indicate this approximation is shown in figure 5.2b.

5.1.2. Finite Element Method

FDM is basically easier in implementation than FEM, but FEM has some advantages in more complex geometries and inhomogeneous materials. [9]

The FEM approach takes advantage of the equivalent physical principle, that the system will minimize the total power loss. [10]

The following four steps are involved for finding the solution [9]:

1. discretizing the region into finite number of elements
2. deriving the equation for the elements
3. assembling of all elements
4. solving the system of equations

Common finite elements are shown in figure 5.4:

- (a) 1D space
 - Six-Node Triangle
- (b) 2D space
 - Three-Node Triangle
 - Six-Node Triangle
 - Five-Node Rectangle
 - Four-Node Quadrilateral
- (c) 3D space
 - Four-Node Tetrahedron
 - Eight-Node Hexahedron

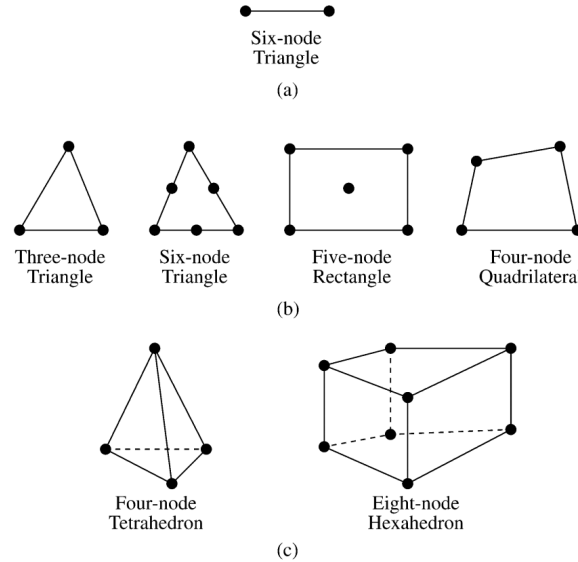


Figure 5.4.: Common finite elements [9]

The mathematical process can be written in an abstract way as the following [10]:
Lost energy expressed as function of the voltage distribution

$$W = W\{\varphi(x)\} \quad (5.3)$$

Where:

W Energy loss in J

Subdividing the interested domain into finite elements and approximating using a separate expression

$$\varphi(x) = \sum_{i=1}^M \varphi_i f_i(x) \quad (5.4)$$

Where:

φ_i Unknown coefficients on each element

$f_i(x)$ Convenient set of known functions

By expressing the energy by $f_i(x)$ and φ_i the energy becomes $W = W(\varphi_1, \varphi_2, \dots, \varphi_M)$ and introduction on the MK coefficients for continuity between the elements, the coefficients can be find by minimization of the energy.

$$\frac{\partial W}{\partial \varphi_i} = 0, \quad i = 1, 2, \dots, N \quad (5.5)$$

5.1.3. Earthing system

An earthing system is an *arrangement of connections and devices necessary to earth equipment or a system separately or jointly* [11] to ensure human safety. An occurring fault current can lead to a hazardous earth potential rise, due to finite earth resistivity. By accessing regions near the fault current, due touching or stepping of humans, unacceptable body currents can be attained. For better usability of the body current limits, they are converted to voltage limits. [11], [12]

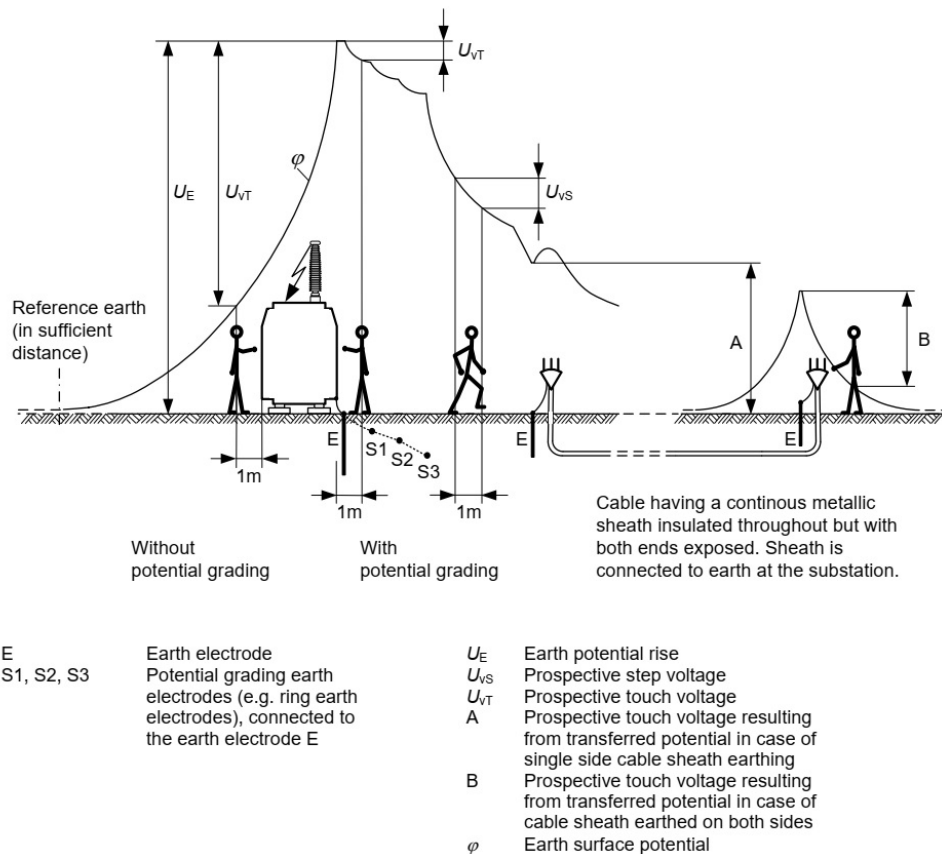


Figure 5.5.: Example surface potential profile (left: without potential grading, right: with potential grading) [11]

5.2. Method

To simulate the influence of the different resistivity distribution models on the voltage distribution of an earthing system, the FEM software Maxwell 3D¹ is used. The solution type for the simulation is DC Conduction. The inverse resistivity model from the previous section is exported to get the following data: coordinates of the blocks and their resistivity values. To do so, an IronPython script is generated with MATLAB² to draw the model in Maxwell 3D. Due to the different resistivity values, each block is represented by a dummy material with its resistivity. Every block by itself is homogeneous. Also the apparent resistivities are used in the same way for simulation.

In the soil model two half spherical shaped electrodes, with $r = 0.5$ m are inserted as a source and a sink. They are placed in the middle of the y direction and in one third and two third section of the x direction. The excitation current to simulate the fault current is 10 A.

For verification purposes of the FEM model, a simple model is chosen in which the calculation can also be performed analytically. This model is homogeneous with $\rho = 100 \Omega\text{m}$. The surface potential distribution can be calculated, using equation (3.15).

In total, eight different models with this electrodes configuration are simulated:

1. Apparent resistivity Minimum - $\rho = 122 \Omega\text{m}$
Homogeneous soil model representing the lower end of the apparent resistivity range.
2. Apparent resistivity Maximum $\rho = 287 \Omega\text{m}$
Homogeneous soil model representing the upper end of the apparent resistivity range.
3. Apparent resistivity Average $\rho = 287 \Omega\text{m}$
Homogeneous soil model with the average of all apparent resistivity values.
4. Apparent resistivity Layered
Layered soil model where each layer is the average value of the apparent resistivity of this layer (values see table 5.2).
5. Apparent resistivity Layered 1-2
Layered soil model which consists only of two layers. The first layer is the same as the previous, where the layers 2-7 are building the second layer, with the resistivity of the second from the previous model.
6. Inversion model resistivity
This soil model is actually representing the "real" soil resistivity distribution. Meaning it is kind of a reference model with the closest match to the investigated area.

¹Software for multiphysics FEM simulation by ANSYS, Inc. - Version: Electronics Desktop 2019 R3

²Software for numeric calculation by The MathWorks, Inc.

7. Inversion model resistivity Average - $\rho = 242 \Omega\text{m}$
Homogeneous soil model with the average of all inversion model resistivity values.
8. Inversion model resistivity Layered
Layered soil model where each layer is the average value of the inversion model resistivity of this layer (values see table 5.4).

The summarizing data for the models are printed in the following tables:

Table 5.1.: Minimum, Maximum, Average of all apparent resistivities

Parameter	ρ
	Ωm
Minimum	122
Maximum	287
Average	210

Table 5.2.: Layers with average of apparent resistivities

Depth	Thickness	Average ρ
m	m	Ωm
0	-1.56	166
-1.56	-1.55	205
-3.11	-1.56	222
-4.67	-1.56	238
-6.23	-1.56	241
-7.79	-1.55	239
-9.34	-1.56	240

Table 5.3.: Average of all inversion model resistivities

Parameter	ρ
	Ωm
Average	242

Table 5.4.: Layers with average of inversion model resistivities

Depth m	Thickness m	Average ρ Ωm
0	-1.350	115
-1.350	-1.552	222
-2.902	-1.786	275
-4.688	-2.053	281
-6.741	-2.361	281
-9.102	-2.716	281

The values of all inversion model resistivities with the center coordinates of the resistivity blocks can be found in table B.4.

Due to software parameter thresholds all conductivity values are multiplied by a factor of 1000 as well the excitation current to ensure the same voltage distribution according to the linear behaviour (Ohm's law). The whole model is placed in vacuum, so the excitation current can flow in the soil model only, from one electrode to the other. The mesh size is set to a maximum line length of 1 m inside the volume. Except the verification model $569 \text{ m} \times 519 \text{ m} \times 250 \text{ m}$, this is set to a length of 50 m inside, to minimize the needed working storage.

The solution set up for the software is:

- Maximum number of passes: 10
- Solution error: 1%

The results are showing the potential distribution on a line between the source and sink electrode. All plots are vertically shifted, so that the plot is showing the EPR.

For better illustration, the Error related on the EPR of the inversion model resistivity (which is equal to the occurring voltage at the source electrode). The related error is calculated as follows:

$$E_{U_S} = \frac{\Delta \varphi_{Surf}}{U_S} \quad (5.6)$$

Where:

E_{U_S} Error related on earthing voltage in p.u.

φ_{Surf} Electric Potential on the surface in V

U_S Step voltage

5.3. Results

The first simulation is the verification model. The result is shown in figure 5.6. It is observable that the analytical calculated potential differs significantly from the simulated line from the original resistivity block with $69 \text{ m} \times 15 \text{ m} \times 12 \text{ m}$. The reason for this deviation is, that the formula for the surface potential distribution is valid for infinite half space. If the block dimensions are getting bigger, the deviation is decreasing, as the line for the $569 \text{ m} \times 519 \text{ m} \times 250 \text{ m}$ block is showing. In this case it can be assumed, that the simulation model is leading to plausible results.

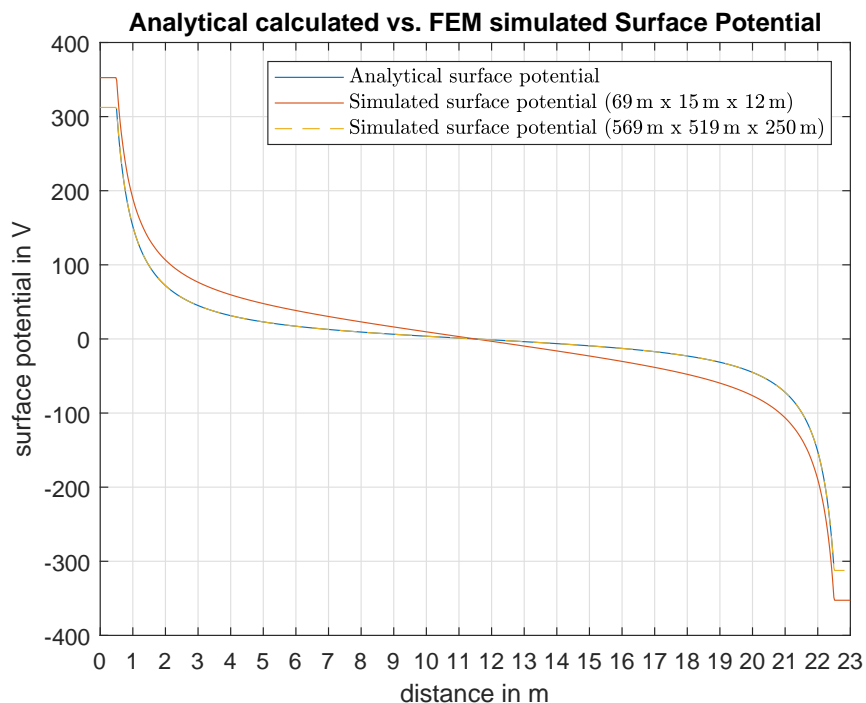


Figure 5.6.: Calculated vs. Simulated Line Surface Potential Distribution

Figure 5.7 shows the surface potential distribution between the two electrodes for the different simulation models. It is noticeable that the potential of the inversion model resistivity has its zero potential not in the middle of the two electrodes. Reason for this is probably the change of the resistivity values along the line, all other models don't have a change of the resistivity in this direction.

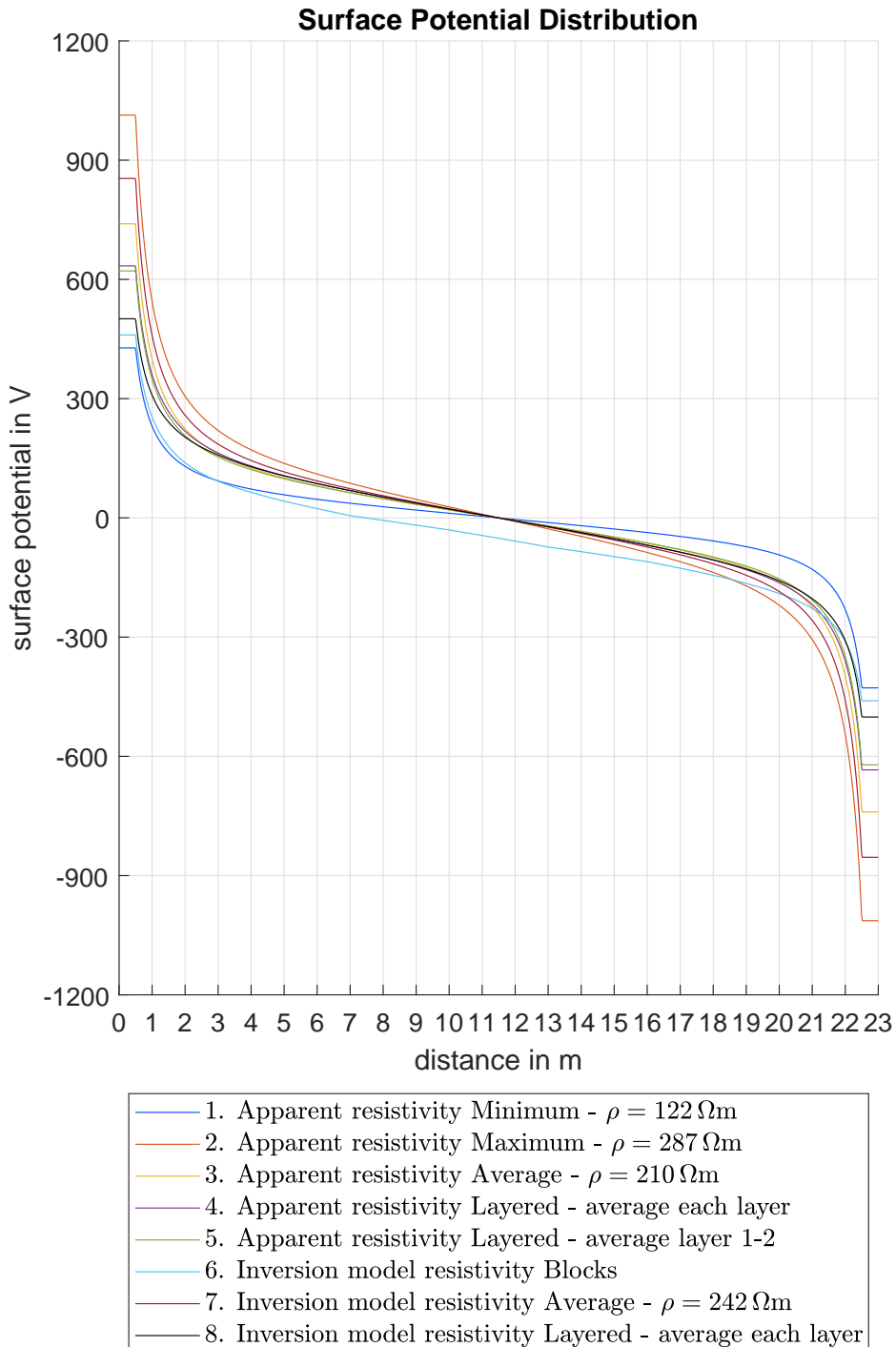


Figure 5.7.: Different Surface Potential Distributions on the line between the electrodes

Due to the linearity of Ohm's law, the simulation of all other homogeneous soil models would not be necessary. They could have been calculated out of the $100 \Omega\text{m}$ curve. If this calculation is done by this, figure 5.8 shows the relative error related to the calculated surface potential distribution.

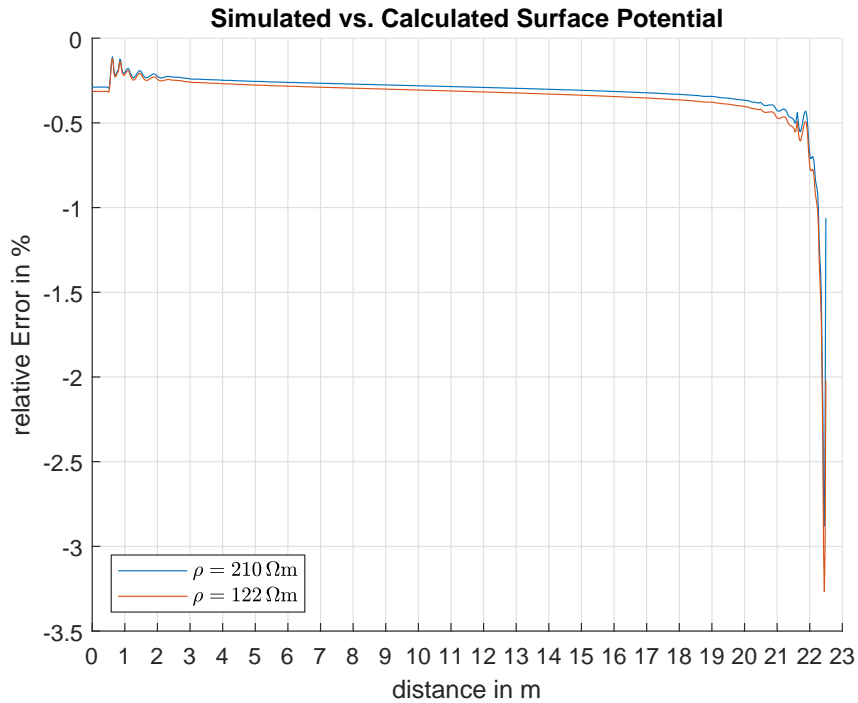


Figure 5.8.: Relative error between simulated and calculated surface potential distribution

In figure 5.9 the absolute error is related to the positive earthing voltage at the source electrode. In these two plots it is noticeable that the layered inversion model resistivity shows the best approximation.

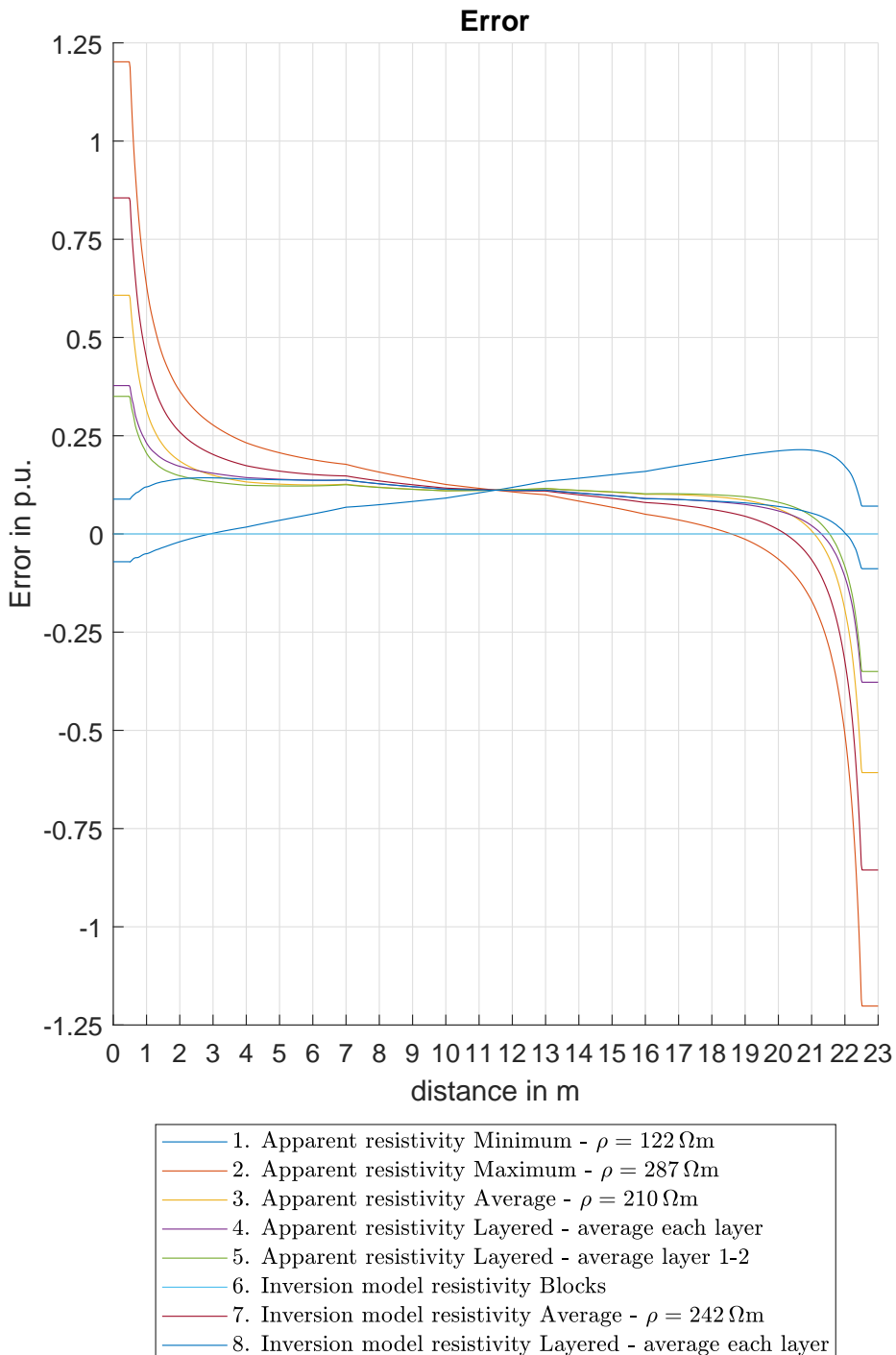


Figure 5.9.: Error of the models in comparison to the inversion model related to the EPR

Figure 5.10 shows the surface potential distribution from figure 5.11c as a 3D plot.

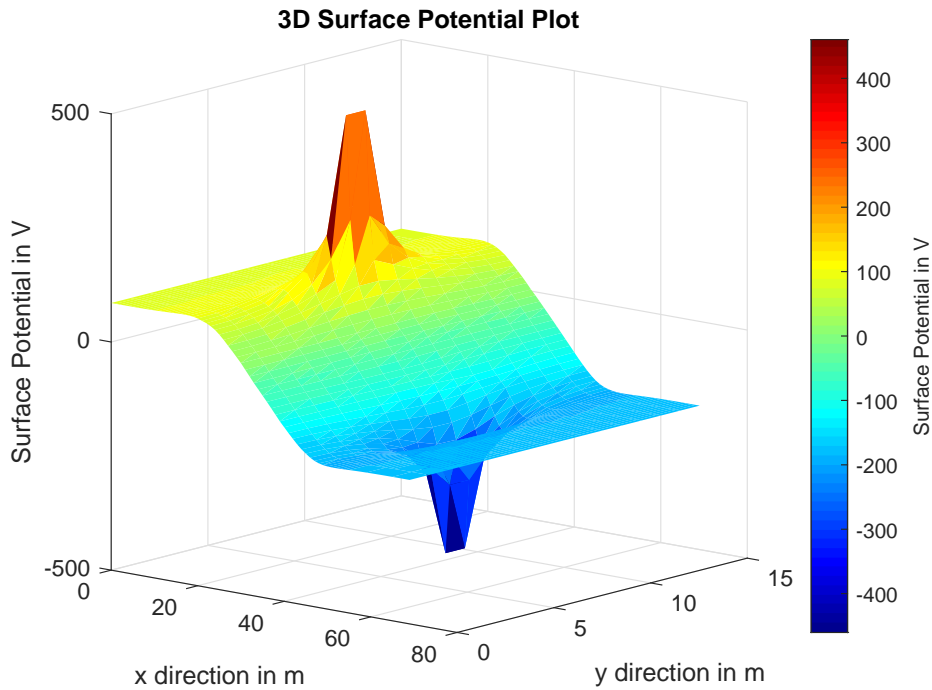


Figure 5.10.: 3D surface potential distribution of Resistivity blocks model

Figure 5.11 gives a view on the simulation process. Starting with the resistivity blocks (figure 5.11a), the software meshes the model (figure 5.11b) with the predefined maximum length of 1 m. After solving the model, the surface potential distribution can be plotted (figure 5.11c). It is also possible to plot other physical quantities, e.g. the current density vector (figure 5.11d).

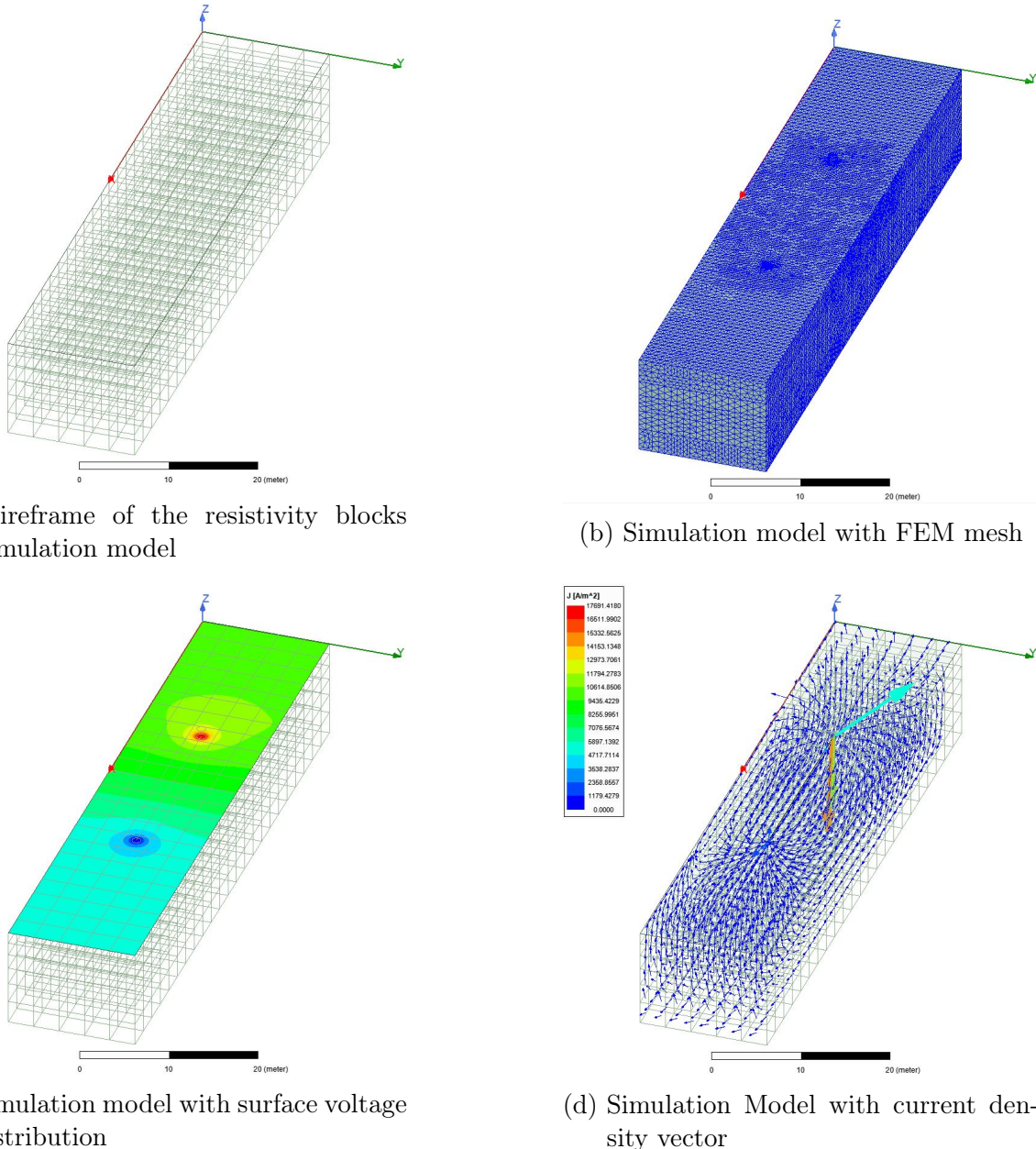


Figure 5.11.: FEM simulation model

6. Conclusion

6.1. Discussion

This work presented the measurement of soil resistivity, the inversion process to find the inversion model resistivity (which is a good approximation to the real resistivity of the soil) and the FEM simulation of the surface potential. Such a 3D survey is time-consuming, so it should be checked, whether this effort is needed or not. In my opinion in this case, one 2D survey would have been enough for the investigation, because the other survey lines are showing quite the same apparent resistivity values. The performed pseudo 3D measurement needs lots of electrodes movements, where in a true 3D resistivity measurement the electrodes would be set once, but more materials are needed. It is now clear that the relationship between apparent and true resistivity is a complex one. In this case the measurement was taken in a field with no disturbances, so if the measurement is performed near a earthing system, the influence of the earthing grid has to be taken into account. With the right boundary condition and some inversion tries, it should be possible to detect and locate the earthing system. For the inversion process lots of other software is available, also another, more complex one was available for the author. One gets a lot of free parameters to set, but with rising complexity the usability shrinks. With the used software it was possible to get fast and stable inversion results, thanks to the predefined parameters, which were set with lots of experience by the programmers.

The impact on the surface potential distribution has been shown. It can be seen, that the apparent resistivity values are ranging between $122\Omega\text{m}$ and $287\Omega\text{m}$ (figure 3.10). So in case, that homogeneous soil is assumed and only a few measurements are performed it is possible to detect and set values in between this range. In case the resistivity is then set to the upper end, the EPR would be much higher as the real one, leading to the need of a bigger earthing system. Where the opposite extreme (assuming the lower end of resistivity values), will cause only a little surface potential, needing only a small earthing system. Such a under designed earthing system causes unacceptable surface and step/touch voltages! Taking the average value of each inversion model resistivity layer and modelling it with these values, shows a good approximation to the surface potential distribution of the inversion model resistivity. But the need for the total measurement can not be omitted. For layered soil analytical solutions can be easier found than for arbitrary shaped resistivity, so the need for a FEM software will then not be given.

For verification of the simulation results it would be possible to make measurements at site again. But this measurement has to be taken quite after the resistivity measurement to make sure that the soil condition is the same and the electrodes have to be the same geometry as in the simulation. The idea for this verification measurement only occurred

at the end of the work, so it was by this time not possible anymore to find the same soil condition. The whole measurement series has to be made again.

Regarding to the problem and the questions introduced in chapter 2: For good dimensioning of the earthing grid it is necessary to have a good soil model. So the better the measurement is, the better is the inversion process, the better is the final soil model. If only a quick estimation is needed, the apparent resistivity is enough, but for the dimensioning, detailed ground investigations are recommended. As written in the chapters before the "real" resistivity can be found by solving the inverse problem. This solution can be imported, with its geometric data into the FEM software. It is also shown that the change of the resistivity in the inversion model along the line is influencing the surface potential in such a way that its zero potential is not in the middle of the electrodes, but slightly before. When simplifying the model, one accepts greater inaccuracies.

6.2. Outlook

For further investigations in this topic, a true 3D measurement, where also the IP (Induced Polarization) is taken into account can be made, to show the discrepancy between the measurement results of the pseudo 3D survey. As already mentioned in section 6.1, a true 3D measurement near a earthing system can be made to investigate the influence on the measurement and maybe there is a way to investigate the quality or the condition state of the system.

There are papers (e.g. [1]) showing that the effect of soil ionization lead to significant lower surface potential distributions, so for dimensioning it is not neglect able. To take this effect into account, some adjustments in the simulation model would be needed.

This work also shows the impact on the surface potential distribution between the two electrodes only. Really interesting would be the step voltage on the surface. The question is, in which direction the step voltages should be calculated, the calculation on a line can be easily done by subtracting the potential values of two neighbouring points, which are 1 m apart. But on earth surface (a 2D shape), each point representing the step voltage has to be the difference of the 1 m apart values in every direction. So maybe a way to show the step voltage on a surface is somehow to represent it by finding the maximum value of the different directions.

All calculations and assumptions were made with direct current (static current field), as shown in section 3.1. Electrical power systems are normally not dealing with direct current. So the next steps would be the simulation with alternating current, where the magnetic couplings and the permeability of the materials are taken into account. Working with alternating current, the resistivities change to impedances, where the influence of the frequency can be analysed.

With the exemplarily measured area, it is not possible to give a general statement on the behaviour. So there will be more modelling work by variing the soil resistivities and present a fast, easy and save method to find a good approximation for the real soil resistivity (instead of the inversion process).

In this work the behaviour of the surface potential was only analysed with two simple

grounding electrodes, but in electrical power systems, the earthing systems are bigger and more complex.

Bibliography

- [1] M. Trlep A. Habjanic. “The simulation of the soil ionization phenomenon around the grounding system by the finite element method”. In: *IEEE Transactions on Magnetics* vol. 42, no. 4, pp. 867-870 (Apr. 2006) (cit. on pp. 4, 52).
- [2] David J. Griffith. *Introduction to Electrodynamics*. 3rd ed. Prentice Hall, 1999 (cit. on p. 7).
- [3] M. H. Loke. *Tutorial : 2-D and 3-D electrical imaging surveys*. M. H. Loke, Oct. 2019 (cit. on pp. 9–13, 16, 27, 28).
- [4] Asger Eriksen John Milsom. *Field Geophysics, Fourth Edition*. John Wiley and Sons, Ltd., 2011. ISBN: 978-0-470-74984-5 (cit. on p. 11).
- [5] IRIS Instruments. *SYSCAL KID / SYSCAL KID SWITCH-24 Compact resistivity-meters Multi-Electrode switching system (Switch-24 model) User’s manual*. Feb. 2018 (cit. on p. 14).
- [6] *Digitaler Atlas der Steiermark*. Das Land Steiermark . URL: <http://www.landesentwicklung.steiermark.at/cms/ziel/141979637/DE/> (cit. on p. 18).
- [7] *wetter.com*. wetter.com GmbH. URL: https://at.wetter.com/wetter_aktuell/rueckblick/oesterreich/tillmitsch-links-der-lassnitz/ATAT20236020.html?sid=11296&timeframe=30d (cit. on p. 20).
- [8] M. H. Loke. *RES3DINVx64 ver. 3.16 Manual*. May 2019 (cit. on p. 27).
- [9] Matthew N. O. Sadiku. *Numerical Techniques in Electromagnetics*. Second Edition. CRC Press, 2000 (cit. on pp. 35–39).
- [10] Ronald L. Ferrari Peter P. Sylvester. *Finite elements for electrical engineers*. Third Edition. Cambridge University Press, 1996 (cit. on pp. 38, 39).
- [11] Austrian Standards Institute OVE Austrian Electrotechnical Association. *ÖVE/ÖNORM EN 50522 Earthing of power installations exceeding 1 kV a.c.* English. effects2.0. Dec. 2011 (cit. on p. 40).
- [12] International Electrotechnical Commission. *IEC/TR 60479-5 Effects of current on human beings and livestock – Part 5: Touch voltage threshold values for physiological effects*. Tech. rep. Nov. 2007 (cit. on p. 40).

A. Figures

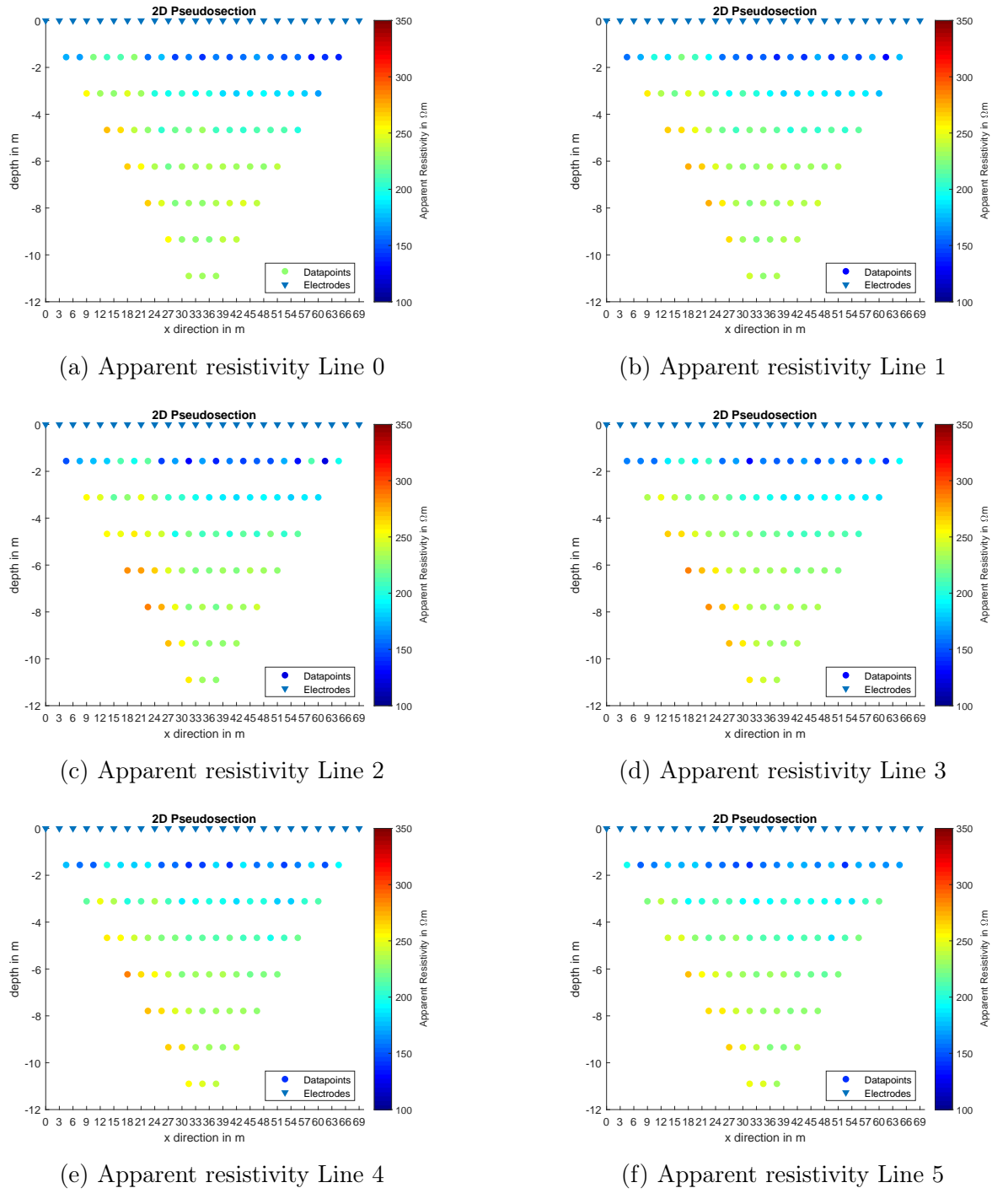
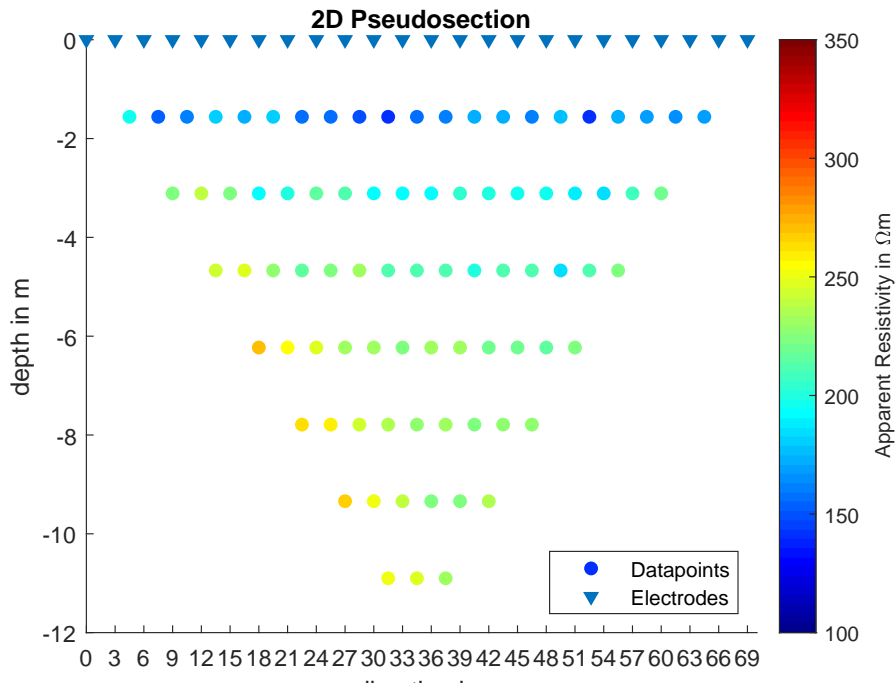
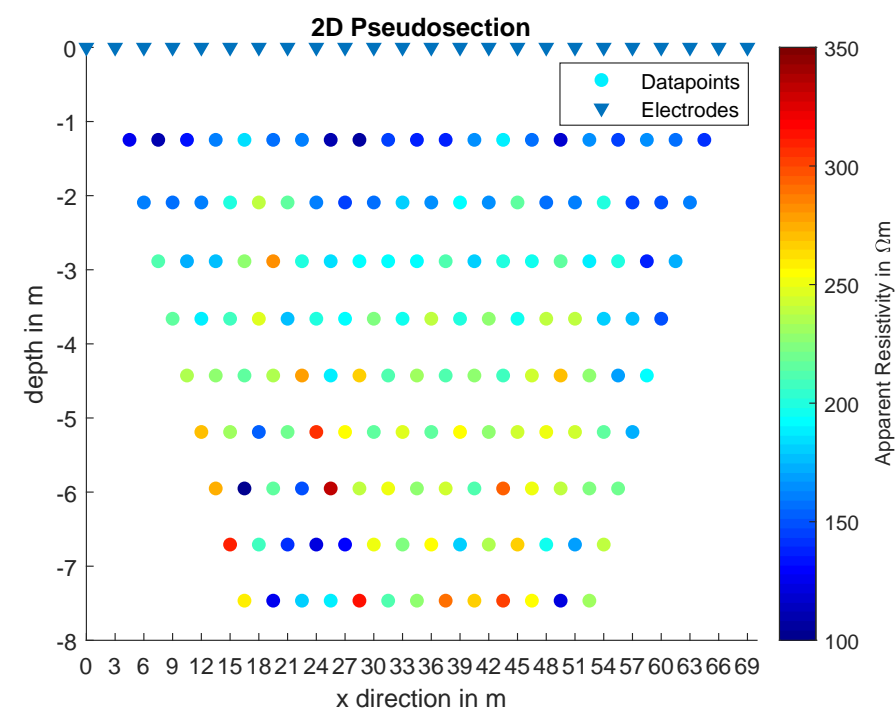


Figure A.1.: Apparent Resistivities Line 0-5



(a) Wenner Array



(b) Dipole-Dipole Array

Figure A.2.: Apparent resistivity Line 5 - Wenner vs. Dipole-Dipole Array

B. Tables

Table B.1.: Measured values Wenner Pseudo-3D

#	Line	location					measured values				
		x_{C1}	x_{C2}	x_{P1}	x_{P2}	z	U_P	I_C	ρ_a	σ	SP
		m	m	m	m	m	mV	mA	Ωm	%	mV
1	0	0	9	3	6	1,56	63,127	6,963	170,9	0,03	-136,93
2	0	0	18	6	12	3,11	224,504	33,178	255,1	0,04	-9,96
3	0	0	27	9	18	4,67	35,334	7,428	269,01	3,5	657,7
4	0	0	36	12	24	6,23	124,463	35,142	267,04	0,05	103,56
5	0	0	45	15	30	7,79	167,645	59,241	266,71	0,03	-46,83
6	0	0	54	18	36	9,34	125,39	56,162	252,51	0,1	67,78
7	0	0	63	21	42	10,90	158,428	89,263	234,19	0,06	-43,79
8	0	3	12	6	9	1,56	85,38	9,463	170,07	0,05	106,65
9	0	3	21	9	15	3,11	106,218	17,242	232,24	0,03	-73,18
10	0	3	30	12	21	4,67	42,819	9,206	263,01	2,62	518,87
11	0	3	39	15	27	6,23	195,875	58,109	254,15	0,04	41,39
12	0	3	48	18	33	7,79	22,629	8,59	248,3	0,16	-213,38
13	0	3	57	21	39	9,34	32,47	16,056	228,72	0,46	192,05
14	0	3	66	24	45	10,90	14,537	8,357	229,52	0,27	273,99
15	0	6	15	9	12	1,56	181,695	15,245	224,66	0,07	50,86
16	0	6	24	12	18	3,11	47,966	8,027	225,26	0,12	150,63
17	0	6	33	15	24	4,67	28,612	6,82	237,25	3,77	294,96
18	0	6	42	18	30	6,23	53,455	17,076	236,03	0,08	-149,35
19	0	6	51	21	36	7,79	228,261	96,443	223,07	0,09	9,98
20	0	6	60	24	42	9,34	86,697	42,96	228,24	0,09	132,13
21	0	6	69	27	48	10,90	115,382	66,135	230,2	0	85,39
22	0	9	18	12	15	1,56	82,069	7,462	207,31	0,21	130,57
23	0	9	27	15	21	3,11	118,709	18,131	246,82	0,09	-21,95
24	0	9	36	18	27	4,67	32,516	8,062	228,08	3,53	245,62
25	0	9	45	21	33	6,23	201,752	69,137	220,02	0,1	51,35
26	0	9	54	24	39	7,79	114,523	47,055	229,38	0,11	118,3
27	0	9	63	27	45	9,34	15,265	7,723	223,55	0,49	311,89
28	0	12	21	15	18	1,56	82,383	7,299	212,76	0,22	159,56
29	0	12	30	18	24	3,11	49,301	8,053	230,81	0,05	-156,24
30	0	12	39	21	30	4,67	26,835	7,433	204,17	3,62	208,06
31	0	12	48	24	36	6,23	117,103	38,54	229,1	0,03	120,31
32	0	12	57	27	42	7,79	158,125	65,309	228,19	0,15	61,58
33	0	12	66	30	48	9,34	32,726	15,402	240,31	0,09	181,03
34	0	15	24	18	21	1,56	190,921	15,779	228,08	0	33,89
35	0	15	33	21	27	3,11	33,947	6,449	198,44	0,05	-185,16
36	0	15	42	24	33	4,67	29,537	7,664	217,95	3,18	307,32
37	0	15	51	27	39	6,23	20,004	6,521	231,29	0,18	244,45
38	0	15	60	30	45	7,79	40,085	16,081	234,94	0,18	201,82
39	0	15	69	33	51	9,34	72,401	34,155	239,74	0,11	148,36
40	0	18	27	21	24	1,56	137,569	16,63	155,93	0,06	34,52
41	0	18	36	24	30	3,11	80,041	15,4	195,94	0,03	-123,94
42	0	18	45	27	36	4,67	26,207	6,783	218,48	3,62	411,03
43	0	18	54	30	42	6,23	102,647	33,018	234,4	0,15	122,63
44	0	18	63	33	48	7,79	167,863	65,129	242,91	0,19	-12,59
45	0	21	30	24	27	1,56	140,289	15,038	175,85	0,03	-12,45
46	0	21	39	27	33	3,11	247,228	46,011	202,57	0	3,27
47	0	21	48	30	39	4,67	27,961	6,884	229,69	4,12	540,43
48	0	21	57	33	45	6,23	40,721	13,164	233,24	0,19	179,68

continued on next page

Influence of arbitrary resistivity distribution of ground on the surface potential of earthing systems

#	Line	location					measured values				
		x_{C1}	x_{C2}	x_{P2}	x_{P2}	z	U_P	I_C	ρ_a	σ	SP
		m	m	m	m	m	mV	mA	Ωm	%	mV
49	0	21	66	36	51	7,79	163,679	62,63	246,31	0	-26,87
50	0	24	33	27	30	1,56	113,139	14,834	143,77	0,11	104,86
51	0	24	42	30	36	3,11	227,32	44,454	192,78	0,03	3,24
52	0	24	51	33	42	4,67	26,945	7,299	208,76	4,38	402,67
53	0	24	60	36	48	6,23	251,219	82,12	230,65	0,1	-4,79
54	0	24	69	39	54	7,79	173,02	68,659	237,5	0,19	-11,53
55	0	27	36	30	33	1,56	73,675	8,61	161,3	0,07	98,65
56	0	27	45	33	39	3,11	213,886	40,282	200,17	0,05	71,3
57	0	27	54	36	45	4,67	27,214	7,41	207,67	4,04	485,78
58	0	27	63	39	51	6,23	165,809	54,44	229,64	0,04	-60,87
59	0	30	39	33	36	1,56	115,41	15,294	142,24	0	64,17
60	0	30	48	36	42	3,11	185,334	38,041	183,67	0,05	-32,48
61	0	30	57	39	48	4,67	24,883	6,945	202,6	4,88	295,23
62	0	30	66	42	54	6,23	150,391	49,689	228,2	0,15	87,94
63	0	33	42	36	39	1,56	61,187	7,217	159,82	0,22	193,89
64	0	33	51	39	45	3,11	200,288	42,365	178,23	0,02	-63,8
65	0	33	60	42	51	4,67	27,494	7,333	212,03	4,49	471,96
66	0	33	69	45	57	6,23	187,376	59,565	237,18	0,04	-47,89
67	0	36	45	39	42	1,56	118,73	15,073	148,48	0,03	-82,57
68	0	36	54	42	48	3,11	233,554	46,404	189,74	0	0,83
69	0	36	63	45	54	4,67	28,062	7,48	212,15	4,46	423,93
70	0	39	48	42	45	1,56	57,229	6,874	156,92	0,15	173,43
71	0	39	57	45	51	3,11	166,618	32,874	191,07	0,03	-60,58
72	0	39	66	48	57	4,67	25,409	6,757	212,64	4,46	432,94
73	0	42	51	45	48	1,56	135,926	15,165	168,95	0,03	-18,06
74	0	42	60	48	54	3,11	222,304	45,543	184,02	0	50,05
75	0	42	69	51	60	4,67	26,936	7,567	201,29	4,35	416,68
76	0	45	54	48	51	1,56	109,801	13,174	157,1	0,05	111,04
77	0	45	63	51	57	3,11	231,002	46,199	188,5	0	-24,91
78	0	48	57	51	54	1,56	106,1	13,419	149,04	0,03	122,98
79	0	48	66	54	60	3,11	168,638	34,975	181,77	0	-68,04
80	0	51	60	54	57	1,56	127,627	15,192	158,35	0,1	50,41
81	0	51	69	57	63	3,11	193,461	42,901	170	0,08	-25,85
82	0	54	63	57	60	1,56	94,706	13,333	133,89	0,03	73,36
83	0	57	66	60	63	1,56	47,66	6,32	142,14	1,95	333,83
84	0	60	69	63	66	1,56	53,384	7,44	135,26	1,36	190
85	1	0	9	3	6	1,56	132,265	16,063	155,21	0,06	2,91
86	1	0	18	6	12	3,11	250,039	36,488	258,34	0,03	12,54
87	1	0	27	9	18	4,67	41,158	8,69	267,84	2,95	713,61
88	1	0	36	12	24	6,23	207,018	56,825	274,68	0,03	-15,65
89	1	0	45	15	30	7,79	191,372	65,488	275,42	0,05	-13,71
90	1	0	54	18	36	9,34	104,768	45,059	262,96	0,12	93,63
91	1	0	63	21	42	10,90	178,585	97,411	241,9	0,1	-54,53
92	1	3	12	6	9	1,56	149,586	16,388	172,06	0,08	49,91
93	1	3	21	9	15	3,11	97,326	15,702	233,67	0,04	-74,74
94	1	3	30	12	21	4,67	35,955	7,778	261,42	3,63	466,07
95	1	3	39	15	27	6,23	233,137	66,355	264,91	0,07	13,72
96	1	3	48	18	33	7,79	36,392	13,347	256,97	0,15	-196,63
97	1	3	57	21	39	9,34	12,762	6,205	232,61	0,24	300,3
98	1	3	66	24	45	10,90	11,448	6,651	227,11	0,22	247,57
99	1	6	15	9	12	1,56	208,526	19,551	201,05	0,06	25,53
100	1	6	24	12	18	3,11	105,949	18,269	218,63	0,04	107,87
101	1	6	33	15	24	4,67	27,426	6,225	249,13	4,56	382,68
102	1	6	42	18	30	6,23	55,228	16,97	245,38	0,11	-181,57
103	1	6	51	21	36	7,79	162,16	65,17	234,51	0,11	85,62
104	1	6	60	24	42	9,34	103,736	52,29	224,37	0,06	71,45
105	1	6	69	27	48	10,90	193,084	108,806	234,15	0,13	37,4
106	1	9	18	12	15	1,56	149,389	15,246	184,7	0,07	31,78
107	1	9	27	15	21	3,11	122,734	18,735	246,97	0	-16,58

continued on next page

Influence of arbitrary resistivity distribution of ground on the surface potential of earthing systems

#	Line	location					measured values				
		x_{C1}	x_{C2}	x_{P1}	x_{P2}	z	U_P	I_C	ρ_a	σ	SP
		m	m	m	m	m	mV	mA	Ωm	%	mV
108	1	9	36	18	27	4,67	34,647	8,486	230,87	3,67	250,6
109	1	9	45	21	33	6,23	207,573	68,11	229,78	0,09	-33,9
110	1	9	54	24	39	7,79	34,092	14,285	224,92	0,13	185,77
111	1	9	63	27	45	9,34	14,299	7,153	226,09	0,43	364,66
112	1	12	21	15	18	1,56	94,359	8,023	221,69	0,08	213,45
113	1	12	30	18	24	3,11	53,314	8,338	241,05	0,19	-242,27
114	1	12	39	21	30	4,67	28,204	7,33	217,58	5,59	258,22
115	1	12	48	24	36	6,23	105,351	34,842	227,98	0,05	133,05
116	1	12	57	27	42	7,79	154,821	62,501	233,46	0,08	-64,5
117	1	12	66	30	48	9,34	15,243	7,354	234,43	0,27	357,92
118	1	15	24	18	21	1,56	125,814	11,407	207,91	0,12	-97,94
119	1	15	33	21	27	3,11	214,965	40,008	202,56	0,04	-44,12
120	1	15	42	24	33	4,67	39,32	10,641	208,96	3,7	733,58
121	1	15	51	27	39	6,23	53,264	17,547	228,88	0,11	152,72
122	1	15	60	30	45	7,79	22,649	9,41	226,84	0,05	296,05
123	1	15	69	33	51	9,34	105,202	50,758	234,41	0,08	103,24
124	1	18	27	21	24	1,56	172,491	17,029	190,93	0,03	-23,47
125	1	18	36	24	30	3,11	208,207	40,666	193,02	0,03	-40,4
126	1	18	45	27	36	4,67	26,531	6,674	224,78	5,12	562,7
127	1	18	54	30	42	6,23	184,933	59,709	233,52	0,12	20,07
128	1	18	63	33	48	7,79	161,294	62,932	241,55	0,27	-23,28
129	1	21	30	24	27	1,56	66,137	8,047	154,92	0,05	141,53
130	1	21	39	27	33	3,11	208,464	37,398	210,14	0,04	55,39
131	1	21	48	30	39	4,67	26,247	6,691	221,82	5,24	704,49
132	1	21	57	33	45	6,23	188,178	60,896	232,99	0,05	66,75
133	1	21	66	36	51	7,79	166,219	66,387	235,98	0,06	-22,66
134	1	24	33	27	30	1,56	125,714	15,265	155,24	0,14	-63,3
135	1	24	42	30	36	3,11	51,798	9,837	198,5	0,13	215,96
136	1	24	51	33	42	4,67	30,23	7,936	215,42	4,91	210,18
137	1	24	60	36	48	6,23	142,248	46,979	228,3	0,08	-124,4
138	1	24	69	39	54	7,79	164,022	63,503	243,43	0	26,44
139	1	27	36	30	33	1,56	74,067	9,724	143,57	0,22	245,09
140	1	27	45	33	39	3,11	208,986	41,259	190,95	0,05	22,98
141	1	27	54	36	45	4,67	26,828	7,588	199,94	5,59	598,65
142	1	27	63	39	51	6,23	230,224	75,814	228,96	0,03	-18,48
143	1	30	39	33	36	1,56	127,407	15,554	154,4	0,04	51,05
144	1	30	48	36	42	3,11	32,028	6,764	178,52	0,12	-215,41
145	1	30	57	39	48	4,67	24,576	6,553	212,06	5,36	221,68
146	1	30	66	42	54	6,23	21,572	7,147	227,59	0,14	263,22
147	1	33	42	36	39	1,56	106,845	14,499	138,91	0,08	111,06
148	1	33	51	39	45	3,11	199,306	40,839	183,98	0,11	36,55
149	1	33	60	42	51	4,67	23,514	6,559	202,72	5,5	595,77
150	1	33	69	45	57	6,23	194,377	62,174	235,72	0,05	21,24
151	1	36	45	39	42	1,56	132,399	15,982	156,16	0,07	-81,47
152	1	36	54	42	48	3,11	190,65	37,582	191,24	0,05	-36,91
153	1	36	63	45	54	4,67	29,898	7,785	217,18	4,25	452,7
154	1	39	48	42	45	1,56	45,599	6,151	139,74	0,03	266,87
155	1	39	57	45	51	3,11	204,993	41,284	187,19	0	-38
156	1	39	66	48	57	4,67	23,772	6,644	202,34	5,34	595,19
157	1	42	51	45	48	1,56	144,302	15,815	171,99	0	-80,94
158	1	42	60	48	54	3,11	83,931	17,596	179,82	0,02	125,58
159	1	42	69	51	60	4,67	32,597	8,531	216,08	2,98	325,58
160	1	45	54	48	51	1,56	45,813	6,191	139,49	0,16	190,49
161	1	45	63	51	57	3,11	223,756	44,672	188,83	0,07	24,45
162	1	48	57	51	54	1,56	105,167	11,698	169,47	0,04	97,42
163	1	48	66	54	60	3,11	205,368	40,979	188,93	0	-46,17
164	1	51	60	54	57	1,56	113,862	14,649	146,51	0,09	121,81
165	1	51	69	57	63	3,11	171,775	36,725	176,33	0	-43,41
166	1	54	63	57	60	1,56	119,989	13,04	173,45	0,2	51,65

continued on next page

Influence of arbitrary resistivity distribution of ground on the surface potential of earthing systems

#	Line	location					measured values				
		x_{C1}	x_{C2}	x_{P1}	x_{P2}	z	U_P	I_C	ρ_a	σ	SP
		m	m	m	m	m	mV	mA	Ωm	%	mV
167	1	57	66	60	63	1,56	40,528	5,939	128,63	2,14	342,1
168	1	60	69	63	66	1,56	72,887	7,881	174,32	0,86	256,05
169	2	0	9	3	6	1,56	127,084	16,134	148,48	0,03	3,37
170	2	0	18	6	12	3,11	113,634	16,79	255,15	0	11,53
171	2	0	27	9	18	4,67	37,922	8,428	254,45	3,51	326,33
172	2	0	36	12	24	6,23	212,63	56,976	281,38	0,04	-6,65
173	2	0	45	15	30	7,79	168,702	55,897	284,45	0	-64,8
174	2	0	54	18	36	9,34	16,818	7,013	271,21	0,13	290,05
175	2	0	63	21	42	10,90	221,24	113,536	257,11	0,13	14,59
176	2	3	12	6	9	1,56	154,218	17,035	170,65	0,04	61,94
177	2	3	21	9	15	3,11	98,755	15,183	245,21	0	-68,08
178	2	3	30	12	21	4,67	36,082	8,103	251,82	3,49	355,93
179	2	3	39	15	27	6,23	252,855	69,024	276,21	0	-6,84
180	2	3	48	18	33	7,79	186,124	63,811	274,9	0,12	-30,14
181	2	3	57	21	39	9,34	16,162	7,193	254,12	0,22	337,37
182	2	3	66	24	45	10,90	12,955	7,373	231,85	0,22	231,2
183	2	6	15	9	12	1,56	185,783	19,84	176,51	0,04	39,76
184	2	6	24	12	18	3,11	95,157	16,628	215,74	0	-56,73
185	2	6	33	15	24	4,67	29,736	6,541	257,07	4,43	383,24
186	2	6	42	18	30	6,23	223,17	63,111	266,62	0	-30,76
187	2	6	51	21	36	7,79	102,638	38,559	250,87	0,04	119,68
188	2	6	60	24	42	9,34	15,262	7,578	227,78	1,27	265,03
189	2	6	69	27	48	10,90	11,395	6,582	228,43	0,1	271,65
190	2	9	18	12	15	1,56	191,9	20,285	178,32	0,08	33,19
191	2	9	27	15	21	3,11	127,362	21,146	227,07	0,07	-48,14
192	2	9	36	18	27	4,67	44,116	10,148	245,83	2,89	373,19
193	2	9	45	21	33	6,23	222,606	68,024	246,74	0,12	-13,91
194	2	9	54	24	39	7,79	38,892	16,332	224,44	0,06	165,31
195	2	9	63	27	45	9,34	15,828	7,879	227,19	0,27	297,73
196	2	12	21	15	18	1,56	90,539	8,11	210,44	0,08	86,71
197	2	12	30	18	24	3,11	124,463	18,753	250,21	0,02	-95,24
198	2	12	39	21	30	4,67	35,183	8,144	244,29	3,59	507,93
199	2	12	48	24	36	6,23	117,138	38,279	230,72	0,08	120,03
200	2	12	57	27	42	7,79	179,837	72,369	234,21	0,27	-9,83
201	2	12	66	30	48	9,34	16,565	8,299	225,75	0,3	234,31
202	2	15	24	18	21	1,56	118,65	11,442	195,46	0,11	-16,42
203	2	15	33	21	27	3,11	274,38	45,252	228,59	0	6,15
204	2	15	42	24	33	4,67	9,238	2,659	196,5	23,73	722,17
205	2	15	51	27	39	6,23	64,406	21,649	224,31	0,03	143,5
206	2	15	60	30	45	7,79	123,432	52,973	219,61	0,06	129,27
207	2	15	69	33	51	9,34	168,559	82,151	232,05	0,2	34,35
208	2	18	27	21	24	1,56	123,65	10,768	216,45	0,1	53,22
209	2	18	36	24	30	3,11	119,437	22,323	201,71	0,06	13,1
210	2	18	45	27	36	4,67	41,208	10,425	223,53	2,69	440,76
211	2	18	54	30	42	6,23	123,821	41,97	222,44	0	-98,65
212	2	18	63	33	48	7,79	190,831	77,001	233,57	0,03	38,06
213	2	21	30	24	27	1,56	128,37	16,616	145,62	0,08	87,75
214	2	21	39	27	33	3,11	200,703	37,408	202,27	0,05	67,08
215	2	21	48	30	39	4,67	25,278	6,883	207,68	5,26	499,66
216	2	21	57	33	45	6,23	198,949	65,094	230,44	0,09	33,71
217	2	21	66	36	51	7,79	166,141	67,772	231,04	0,05	-21,76
218	2	24	33	27	30	1,56	66,958	7,433	169,8	0,1	121,57
219	2	24	42	30	36	3,11	117,071	22,61	195,2	0,13	-10,15
220	2	24	51	33	42	4,67	32,603	8,621	213,85	9,55	739,11
221	2	24	60	36	48	6,23	236,761	80,46	221,87	0,08	-1,27
222	2	24	69	39	54	7,79	180,549	69,844	243,64	0	-41,57
223	2	27	36	30	33	1,56	161,22	23,527	129,17	0,05	43,62
224	2	27	45	33	39	3,11	114,878	22,834	189,67	0	83,37
225	2	27	54	36	45	4,67	29,708	8,489	197,89	3,95	390

continued on next page

Influence of arbitrary resistivity distribution of ground on the surface potential of earthing systems

#	Line	location					measured values				
		x_{C1}	x_{C2}	x_{P1}	x_{P2}	z	U_P	I_C	ρ_a	σ	SP
		m	m	m	m	m	mV	mA	Ωm	%	mV
226	2	27	63	39	51	6,23	135,525	43,769	233,46	0,1	-74,33
227	2	30	39	33	36	1,56	71,304	8,022	167,55	0	121,44
228	2	30	48	36	42	3,11	36,426	7,337	187,18	0,22	-202,43
229	2	30	57	39	48	4,67	28,918	7,581	215,71	3,62	266,92
230	2	30	66	42	54	6,23	24,159	7,9	230,58	0,28	199,67
231	2	33	42	36	39	1,56	1011,603	137,684	138,49	0	69,07
232	2	33	51	39	45	3,11	178,518	36,438	184,7	0,07	-47,65
233	2	33	60	42	51	4,67	25,697	7,11	204,39	4,7	360,73
234	2	33	69	45	57	6,23	96,442	32,007	227,18	0,06	138,08
235	2	36	45	39	42	1,56	93,457	10,909	161,48	0,04	116,42
236	2	36	54	42	48	3,11	87,403	17,52	188,07	0,06	-144,84
237	2	36	63	45	54	4,67	33,22	8,45	222,31	2,53	389,28
238	2	39	48	42	45	1,56	267,689	34,748	145,21	0,04	-20,63
239	2	39	57	45	51	3,11	183,304	35,788	193,09	0,09	26,54
240	2	39	66	48	57	4,67	26,591	7,397	203,29	4,51	446,66
241	2	42	51	45	48	1,56	77,106	9,414	154,39	0	154,33
242	2	42	60	48	54	3,11	235,555	47,668	186,29	0,14	-48,26
243	2	42	69	51	60	4,67	30,117	7,985	213,3	4,31	500,48
244	2	45	54	48	51	1,56	135,648	17,202	148,64	0,27	16,75
245	2	45	63	51	57	3,11	205,449	42,823	180,87	0,02	72,72
246	2	48	57	51	54	1,56	58,775	6,46	171,49	0,23	140,46
247	2	48	66	54	60	3,11	229,431	45,681	189,34	0,06	4,68
248	2	51	60	54	57	1,56	116,34	16,433	133,45	0,05	109,56
249	2	51	69	57	63	3,11	230,026	47,604	182,16	0,09	-23,03
250	2	54	63	57	60	1,56	76,162	6,839	209,9	0,06	89,52
251	2	57	66	60	63	1,56	44,689	6,923	121,68	1,62	256,24
252	2	60	69	63	66	1,56	72,021	6,937	195,69	1	241,72
253	3	0	9	3	6	1,56	72,691	8,533	160,57	0,06	317,23
254	3	0	18	6	12	3,11	56,156	8,983	235,66	0,08	-256,99
255	3	0	27	9	18	4,67	44,294	9,407	266,28	2,81	340,57
256	3	0	36	12	24	6,23	232,522	61,258	286,2	0,05	-8,63
257	3	0	45	15	30	7,79	165,891	55,6	281,2	0	-54,65
258	3	0	54	18	36	9,34	18,859	7,855	271,52	0,68	323,94
259	3	0	63	21	42	10,90	198,482	100,84	259,71	0	-60,5
260	3	3	12	6	9	1,56	88,132	10,277	161,64	0,22	-101,77
261	3	3	21	9	15	3,11	148,521	22,414	249,8	0,11	-49,13
262	3	3	30	12	21	4,67	44,912	9,755	260,34	2,97	532,64
263	3	3	39	15	27	6,23	216,738	60,261	271,18	0	26,51
264	3	3	48	18	33	7,79	218,333	76,763	268,06	0	-22,72
265	3	3	57	21	39	9,34	21,244	9,254	259,62	0,43	348,83
266	3	3	66	24	45	10,90	17,434	9,422	244,14	0,15	260,35
267	3	6	15	9	12	1,56	233,644	27,802	158,41	0,03	-28,84
268	3	6	24	12	18	3,11	186,172	29,418	238,58	0,11	28,84
269	3	6	33	15	24	4,67	18,406	4,214	247,01	6,37	328,01
270	3	6	42	18	30	6,23	166,596	49,017	256,26	0,05	-52,31
271	3	6	51	21	36	7,79	76,132	28,392	252,72	0,11	144,63
272	3	6	60	24	42	9,34	16,174	7,726	236,76	0,57	205,87
273	3	6	69	27	48	10,90	6,278	3,511	235,93	0,72	277,13
274	3	9	18	12	15	1,56	95,251	9,596	187,1	0,09	232,59
275	3	9	27	15	21	3,11	58,477	10,055	219,25	0,03	-190,55
276	3	9	36	18	27	4,67	39,509	9,687	230,63	3,45	423,98
277	3	9	45	21	33	6,23	190,096	59,623	240,39	0,12	-33,75
278	3	9	54	24	39	7,79	133,886	54,08	233,33	0,04	95,93
279	3	9	63	27	45	9,34	16,051	7,864	230,84	0,3	347,87
280	3	12	21	15	18	1,56	114,456	10,56	204,3	0	-96,81
281	3	12	30	18	24	3,11	115,455	19,611	221,94	0,14	48,12
282	3	12	39	21	30	4,67	35,8	8,717	232,25	3,37	471,07
283	3	12	48	24	36	6,23	169,637	54,764	233,56	0,04	77,59
284	3	12	57	27	42	7,79	108,611	44,498	230,04	0,11	148,36

continued on next page

Influence of arbitrary resistivity distribution of ground on the surface potential of earthing systems

#	Line	location					measured values				
		x_{C1}	x_{C2}	x_{P2}	x_{P2}	z	U_P	I_C	ρ_a	σ	SP
		m	m	m	m	m	mV	mA	Ωm	%	mV
285	3	12	66	30	48	9,34	18,672	9,345	225,98	0,1	340,45
286	3	15	24	18	21	1,56	206,291	20,699	187,86	0	-9,74
287	3	15	33	21	27	3,11	241,316	39,418	230,8	0,36	12,03
288	3	15	42	24	33	4,67	33,617	8,588	221,37	4,48	548,04
289	3	15	51	27	39	6,23	23,032	7,546	230,14	0,24	198,14
290	3	15	60	30	45	7,79	35,341	14,552	228,89	0,09	208,02
291	3	15	69	33	51	9,34	138,583	66,442	235,9	0,12	-38,68
292	3	18	27	21	24	1,56	117,276	10,727	206,08	0,03	165,23
293	3	18	36	24	30	3,11	58,482	10,321	213,62	0	-131,46
294	3	18	45	27	36	4,67	37,272	9,251	227,83	2,74	407,51
295	3	18	54	30	42	6,23	130,994	42,755	231,01	0,33	125,53
296	3	18	63	33	48	7,79	139,045	55,343	236,79	0,1	93,65
297	3	21	30	24	27	1,56	172,27	20,773	156,32	0,14	-14,36
298	3	21	39	27	33	3,11	99,706	18,954	198,32	0,08	76,04
299	3	21	48	30	39	4,67	32,588	8,529	216,05	3,31	474,97
300	3	21	57	33	45	6,23	145,989	46,844	234,98	0,05	78,36
301	3	21	66	36	51	7,79	159,67	65,064	231,29	0,04	-71,59
302	3	24	33	27	30	1,56	86,643	9,731	167,84	0,05	82,3
303	3	24	42	30	36	3,11	119,704	22,669	199,07	0,08	7,64
304	3	24	51	33	42	4,67	36,39	9,451	217,74	3,2	388,55
305	3	24	60	36	48	6,23	130,187	44,546	220,36	0,14	114,28
306	3	24	69	39	54	7,79	206,743	82,642	235,78	0,03	20,64
307	3	27	36	30	33	1,56	75,509	10,856	131,11	0,06	117,47
308	3	27	45	33	39	3,11	104,043	20,062	195,51	0,05	51,4
309	3	27	54	36	45	4,67	31,743	8,712	206,05	3,49	418,71
310	3	27	63	39	51	6,23	130,496	43,208	227,71	0,04	-86,77
311	3	30	39	33	36	1,56	149,825	17,381	162,48	0,1	69
312	3	30	48	36	42	3,11	197,143	39,826	186,61	0,09	-4,55
313	3	30	57	39	48	4,67	31,394	8,593	206,59	4,65	446,57
314	3	30	66	42	54	6,23	134,47	44,519	227,74	0	79,42
315	3	33	42	36	39	1,56	67,549	8,296	153,47	0,14	141,62
316	3	33	51	39	45	3,11	183,447	37,703	183,43	0,03	-53,73
317	3	33	60	42	51	4,67	26,058	7,063	208,62	4,76	455,27
318	3	33	69	45	57	6,23	195,285	65,745	223,96	0	3,4
319	3	36	45	39	42	1,56	156,18	19,445	151,4	0,09	-35,03
320	3	36	54	42	48	3,11	87,931	17,492	189,52	0,12	71,96
321	3	36	63	45	54	4,67	31,133	8,206	214,55	3,05	335,54
322	3	39	48	42	45	1,56	66,181	7,327	170,25	0	141,42
323	3	39	57	45	51	3,11	203,311	39,906	192,07	0,2	-50,7
324	3	39	66	48	57	4,67	30,559	8,2	210,75	3,8	423,23
325	3	42	51	45	48	1,56	128,48	16,77	144,41	0,12	53,19
326	3	42	60	48	54	3,11	196,739	38,602	192,14	0,19	1,69
327	3	42	69	51	60	4,67	28,912	7,855	208,15	4,43	500,73
328	3	45	54	48	51	1,56	139,997	16,106	163,84	0,1	58,89
329	3	45	63	51	57	3,11	190,395	38,518	186,35	0,23	17,41
330	3	48	57	51	54	1,56	60,335	7,36	154,53	0,09	137,51
331	3	48	66	54	60	3,11	191,75	38,396	188,27	0,19	-29,11
332	3	51	60	54	57	1,56	112,204	14,109	149,91	0,05	45,15
333	3	51	69	57	63	3,11	228,412	46,516	185,12	0,08	18,6
334	3	54	63	57	60	1,56	70,029	6,978	189,17	0,05	119,87
335	3	57	66	60	63	1,56	60,982	8,133	141,34	1,07	259,94
336	3	60	69	63	66	1,56	66,67	6,605	190,26	1,11	212,85
337	4	0	9	3	6	1,56	194,908	20,769	176,89	0,06	4,03
338	4	0	18	6	12	3,11	110,589	19,213	216,99	0,05	-70,41
339	4	0	27	9	18	4,67	51,964	11,465	256,31	2,44	419,02
340	4	0	36	12	24	6,23	178,561	46,842	287,41	0,04	23,33
341	4	0	45	15	30	7,79	166,444	58,088	270,06	0,18	-42,79
342	4	0	54	18	36	9,34	18,155	7,689	267,03	0,14	277,53
343	4	0	63	21	42	10,90	216,233	111,387	256,15	0,06	-31,36

continued on next page

Influence of arbitrary resistivity distribution of ground on the surface potential of earthing systems

#	Line	location					measured values				
		x_{C1}	x_{C2}	x_{P2}	x_{P2}	z	U_P	I_C	ρ_a	σ	SP
		m	m	m	m	m	mV	mA	Ωm	%	mV
344	4	3	12	6	9	1,56	133,397	16,179	155,41	0,05	29,09
345	4	3	21	9	15	3,11	107,306	16,27	248,64	0,03	-39,79
346	4	3	30	12	21	4,67	32,88	7,312	254,29	4,07	426,22
347	4	3	39	15	27	6,23	234,518	67,789	260,84	0,14	-3,01
348	4	3	48	18	33	7,79	170,748	61,642	261,07	0	-54,48
349	4	3	57	21	39	9,34	14,899	6,455	261,06	0,47	379,13
350	4	3	66	24	45	10,90	13,316	7,11	247,11	0,4	279,82
351	4	6	15	9	12	1,56	149,528	18,66	151,05	0,03	-13,75
352	4	6	24	12	18	3,11	135,977	21,886	234,23	0,14	34,46
353	4	6	33	15	24	4,67	43,053	10,043	242,42	2,66	362,76
354	4	6	42	18	30	6,23	175,998	52,505	252,74	0,09	-54,51
355	4	6	51	21	36	7,79	103,727	39,592	246,92	0,09	123,26
356	4	6	60	24	42	9,34	16,601	8,074	232,54	0,24	286,37
357	4	6	69	27	48	10,90	14,692	8,112	238,97	0,57	272,78
358	4	9	18	12	15	1,56	110,047	10,344	200,53	0,04	113,2
359	4	9	27	15	21	3,11	142,31	26,685	201,05	0,08	-62,56
360	4	9	36	18	27	4,67	41,677	10,271	229,46	2,74	439,81
361	4	9	45	21	33	6,23	202,584	64,122	238,21	0,05	-22,16
362	4	9	54	24	39	7,79	20,997	8,29	238,72	0,16	238,95
363	4	9	63	27	45	9,34	18,075	8,856	230,82	0,47	344,9
364	4	12	21	15	18	1,56	191,806	19,837	182,26	0,05	31,35
365	4	12	30	18	24	3,11	100,799	17,961	211,57	0,14	-71,85
366	4	12	39	21	30	4,67	34,556	8,727	223,91	3,9	342
367	4	12	48	24	36	6,23	117,054	39,653	222,57	0,11	139,63
368	4	12	57	27	42	7,79	116,525	48,615	225,9	0,06	115,04
369	4	12	66	30	48	9,34	17,299	8,572	228,25	0,46	349,36
370	4	15	24	18	21	1,56	168,818	17,667	180,11	0,12	64,34
371	4	15	33	21	27	3,11	103,785	16,76	233,45	0,08	-81,69
372	4	15	42	24	33	4,67	33,049	8,36	223,55	3,86	406,93
373	4	15	51	27	39	6,23	20,223	6,653	229,18	0,05	229,86
374	4	15	60	30	45	7,79	16,117	6,593	230,38	0,2	275,32
375	4	15	69	33	51	9,34	72,283	34,4	237,65	0,09	167,13
376	4	18	27	21	24	1,56	118,817	11,86	188,84	0	25,61
377	4	18	36	24	30	3,11	107,784	19,452	208,9	0,03	-84,99
378	4	18	45	27	36	4,67	32,971	8,831	211,13	3,57	525,64
379	4	18	54	30	42	6,23	47,646	15,555	230,94	0,17	148,89
380	4	18	63	33	48	7,79	20,422	8,291	232,15	0,04	212,09
381	4	21	30	24	27	1,56	147,226	18,108	153,25	0	2,42
382	4	21	39	27	33	3,11	221,849	44,927	186,16	0,03	-5,61
383	4	21	48	30	39	4,67	31,156	8,12	216,97	3,95	564,81
384	4	21	57	33	45	6,23	22,79	7,324	234,63	0,09	244,76
385	4	21	66	36	51	7,79	190,991	77,621	231,9	0,08	-59,09
386	4	24	33	27	30	1,56	78,885	9,473	156,97	0,08	103,84
387	4	24	42	30	36	3,11	103,444	19,886	196,1	0	52,15
388	4	24	51	33	42	4,67	28,316	7,513	213,12	3,8	494,92
389	4	24	60	36	48	6,23	207,675	69,122	226,53	0,06	33,07
390	4	24	69	39	54	7,79	38,223	15,876	226,91	0,11	-174,81
391	4	27	36	30	33	1,56	181,122	24,043	142	0	22,79
392	4	27	45	33	39	3,11	57,223	10,715	201,33	0	221,56
393	4	27	54	36	45	4,67	34,427	8,88	219,24	2,98	344,38
394	4	27	63	39	51	6,23	59,451	20,338	220,4	0	-122,54
395	4	30	39	33	36	1,56	62,772	8,087	146,32	0,37	193,87
396	4	30	48	36	42	3,11	190,296	36,848	194,69	0,06	-22,81
397	4	30	57	39	48	4,67	25,637	6,947	208,68	4,85	409,24
398	4	30	66	42	54	6,23	208,588	71,094	221,22	0,06	12,42
399	4	33	42	36	39	1,56	88,717	9,17	182,36	0,06	116,44
400	4	33	51	39	45	3,11	177,201	36,356	183,75	0,06	-51,56
401	4	33	60	42	51	4,67	27,317	7,299	211,65	4,74	485,89
402	4	33	69	45	57	6,23	145,989	49,488	222,42	0,05	-60,58

continued on next page

Influence of arbitrary resistivity distribution of ground on the surface potential of earthing systems

#	Line	location					measured values				
		x_{C1}	x_{C2}	x_{P2}	x_{P2}	z	U_P	I_C	ρ_a	σ	SP
		m	m	m	m	m	mV	mA	Ωm	%	mV
403	4	36	45	39	42	1,56	133,835	18,027	139,94	0,04	-21,57
404	4	36	54	42	48	3,11	202,986	38,12	200,75	0,04	73
405	4	36	63	45	54	4,67	29,062	8,39	195,87	4,19	392,04
406	4	39	48	42	45	1,56	72,886	7,347	187	0,11	180,71
407	4	39	57	45	51	3,11	183,315	34,398	200,91	0	-63,29
408	4	39	66	48	57	4,67	28,254	7,761	205,86	4,73	463,53
409	4	42	51	45	48	1,56	124,261	15,108	155,03	0	11,29
410	4	42	60	48	54	3,11	233,762	49,063	179,62	0,06	-13,06
411	4	42	69	51	60	4,67	29,715	7,722	217,62	4,52	514,64
412	4	45	54	48	51	1,56	133,689	14,661	171,88	0,03	74,31
413	4	45	63	51	57	3,11	186,274	39,288	178,74	0	-21,02
414	4	48	57	51	54	1,56	99,014	12,904	144,63	0	116,61
415	4	48	66	54	60	3,11	255,756	47,022	205,05	0,07	6,83
416	4	51	60	54	57	1,56	104,256	12,379	158,75	0,12	72,58
417	4	51	69	57	63	3,11	227,833	40,959	209,7	0	10,39
418	4	54	63	57	60	1,56	65,762	6,776	182,93	0,23	182,18
419	4	57	66	60	63	1,56	51,539	6,571	147,85	1,17	188,03
420	4	60	69	63	66	1,56	63,466	6,175	193,73	1,02	247,09
421	5	0	9	3	6	1,56	184,449	17,723	196,17	0,11	-31,6
422	5	0	18	6	12	3,11	51,187	8,628	223,65	0,19	179,11
423	5	0	27	9	18	4,67	17,113	3,972	243,63	7,26	340,18
424	5	0	36	12	24	6,23	29,255	8,158	270,39	0,18	-202,85
425	5	0	45	15	30	7,79	202,415	72,343	263,7	0,06	13,57
426	5	0	54	18	36	9,34	152,395	65,239	264,19	0,33	36,37
427	5	0	63	21	42	10,90	194,944	102,613	250,67	0,06	8,53
428	5	3	12	6	9	1,56	94,103	11,602	152,89	0,06	61,28
429	5	3	21	9	15	3,11	128,738	20,45	237,33	0,07	-37,23
430	5	3	30	12	21	4,67	43,215	9,99	244,63	2,53	281,8
431	5	3	39	15	27	6,23	181,216	53,519	255,3	0,16	58,85
432	5	3	48	18	33	7,79	170,719	62,759	256,38	0,1	-74,77
433	5	3	57	21	39	9,34	17,97	8,104	250,77	0,43	366,83
434	5	3	66	24	45	10,90	14,98	7,998	247,14	0,22	265,99
435	5	6	15	9	12	1,56	91,668	10,643	162,36	0,11	65,77
436	5	6	24	12	18	3,11	155,071	26,369	221,71	0,04	-65,39
437	5	6	33	15	24	4,67	49,918	12,486	226,08	2,43	460,89
438	5	6	42	18	30	6,23	220,877	67,668	246,11	0,1	1,37
439	5	6	51	21	36	7,79	201,644	78,318	242,66	0,04	7,15
440	5	6	60	24	42	9,34	16,098	7,676	237,18	0,34	335,92
441	5	6	69	27	48	10,90	91,494	52,173	231,39	0,07	139,19
442	5	9	18	12	15	1,56	175,763	18,208	181,96	0,1	-42,97
443	5	9	27	15	21	3,11	256,514	49,953	193,59	0,06	-25,64
444	5	9	36	18	27	4,67	31,801	8,425	213,45	11,39	1499,64
445	5	9	45	21	33	6,23	174,597	56,617	232,52	0	-45,38
446	5	9	54	24	39	7,79	105,819	42,75	233,29	0,13	147,91
447	5	9	63	27	45	9,34	77,701	39,127	224,6	0,04	139,06
448	5	12	21	15	18	1,56	94,076	10,305	172,08	0	147,15
449	5	12	30	18	24	3,11	54,72	10,262	201,02	0,05	-145,29
450	5	12	39	21	30	4,67	17,459	4,418	223,48	6,32	336,98
451	5	12	48	24	36	6,23	256,345	83,685	230,96	0,04	55,52
452	5	12	57	27	42	7,79	163,709	68,163	226,36	0,11	38,01
453	5	12	66	30	48	9,34	8,471	4,279	223,87	0,58	303,7
454	5	15	24	18	21	1,56	106,131	11,166	179,16	0,1	124,11
455	5	15	33	21	27	3,11	127,991	22,302	216,35	0	-63,52
456	5	15	42	24	33	4,67	36,472	8,973	229,85	3,69	393,68
457	5	15	51	27	39	6,23	212,184	71,653	223,28	0,14	23,86
458	5	15	60	30	45	7,79	153,583	63,199	229,03	0,06	86,21
459	5	15	69	33	51	9,34	15,165	7,361	233	0,53	443,83
460	5	18	27	21	24	1,56	152,228	18,247	157,26	0,1	-110,92
461	5	18	36	24	30	3,11	96,098	17,163	211,08	0,03	120,6

continued on next page

Influence of arbitrary resistivity distribution of ground on the surface potential of earthing systems

#	Line	location					measured values				
		x_{C1}	x_{C2}	x_{P2}	x_{P2}	z	U_P	I_C	ρ_a	σ	SP
		m	m	m	m	m	mV	mA	Ωm	%	mV
462	5	18	45	27	36	4,67	41,096	11,023	210,83	2,67	247,63
463	5	18	54	30	42	6,23	147,684	48,492	229,63	0,1	41,21
464	5	18	63	33	48	7,79	18,113	7,721	221,11	0,43	391,4
465	5	21	30	24	27	1,56	82,426	9,828	158,08	0,03	164,33
466	5	21	39	27	33	3,11	52,262	10,323	190,86	0,05	-169,33
467	5	21	48	30	39	4,67	33,917	9,11	210,52	3,24	379,83
468	5	21	57	33	45	6,23	23,495	7,665	231,13	0,41	279,07
469	5	21	66	36	51	7,79	95,644	39,613	227,55	0,07	171,73
470	5	24	33	27	30	1,56	102,696	13,113	147,63	0,07	81,85
471	5	24	42	30	36	3,11	110,263	21,57	192,71	0,06	-35,07
472	5	24	51	33	42	4,67	32,866	8,79	211,44	3,03	605,36
473	5	24	60	36	48	6,23	22,143	7,654	218,12	0,15	256,1
474	5	24	69	39	54	7,79	178,07	74,462	225,39	0,03	-83,46
475	5	27	36	30	33	1,56	252,43	33,721	141,1	0,05	-120,17
476	5	27	45	33	39	3,11	33,656	6,62	191,67	0,1	172,38
477	5	27	54	36	45	4,67	6,791	1,906	201,48	16,31	-41,91
478	5	27	63	39	51	6,23	146,638	50,565	218,65	0,06	131,37
479	5	30	39	33	36	1,56	86,481	10,416	156,5	0	516,37
480	5	30	48	36	42	3,11	49,27	9,131	203,42	0,04	-248,08
481	5	30	57	39	48	4,67	28,925	7,726	211,7	2,84	363,72
482	5	30	66	42	54	6,23	114,738	39,913	216,75	0,13	-136,75
483	5	33	42	36	39	1,56	88,084	10,236	162,21	0	-192,75
484	5	33	51	39	45	3,11	93,1	17,658	198,76	0	-110,97
485	5	33	60	42	51	4,67	28,18	7,496	212,59	3,25	400,91
486	5	33	69	45	57	6,23	23,267	7,874	222,79	0,1	250,65
487	5	36	45	39	42	1,56	95,43	10,39	173,12	0,05	60,19
488	5	36	54	42	48	3,11	199,576	38,104	197,46	0	57,06
489	5	36	63	45	54	4,67	24,348	7,413	185,72	12,24	885,27
490	5	39	48	42	45	1,56	89,116	9,663	173,84	0,11	79,93
491	5	39	57	45	51	3,11	211,599	41,084	194,17	0,03	45,71
492	5	39	66	48	57	4,67	30,643	8,241	210,26	4,35	492,61
493	5	42	51	45	48	1,56	63,19	7,462	159,62	0,09	134,88
494	5	42	60	48	54	3,11	33,197	6,621	189,02	0,05	-234,42
495	5	42	69	51	60	4,67	27,385	6,921	223,75	2,8	287,01
496	5	45	54	48	51	1,56	380,484	40,547	176,88	0,15	30,12
497	5	45	63	51	57	3,11	94,775	19,348	184,66	0,06	62,72
498	5	48	57	51	54	1,56	113,494	15,151	141,2	0,2	-14,29
499	5	48	66	54	60	3,11	83,798	15,312	206,31	0,04	133,09
500	5	51	60	54	57	1,56	54,184	5,939	171,98	0,17	349,16
501	5	51	69	57	63	3,11	178,461	30,928	217,53	0,1	62,96
502	5	54	63	57	60	1,56	274,033	30,614	168,73	0,18	19,66
503	5	57	66	60	63	1,56	56,71	6,489	164,73	2,69	853,78
504	5	60	69	63	66	1,56	50,645	5,641	169,24	1,42	-98,68

Table B.2.: Measured values Dipole-Dipole Line0

#	location					measured values				
	x_{C2}	x_{C1}	x_{P2}	x_{P2}	z	U_P	I_C	ρ_a	σ	SP
	m	m	m	m	m	mV	mA	Ωm	%	mV
1	0	3	6	9	1,247	162,108	76,414	119,96	0,13	48,79
2	0	3	9	12	2,092	111,299	138,862	181,3	0,03	-44,96
3	0	3	12	15	2,885	43,848	140,224	176,83	0,19	20,37
4	0	3	15	18	3,661	26,249	141,178	210,28	0,95	-16,85
5	0	3	18	21	4,427	17,071	141,813	238,25	1,17	9,58
6	0	3	21	24	5,189	7,263	141,886	162,1	0,36	-16,62

continued on next page

Influence of arbitrary resistivity distribution of ground on the surface potential of earthing systems

#	location					measured values				
	x_{C2}	x_{C1}	x_{P2}	x_{P2}	z	U_P	I_C	ρ_a	σ	SP
	m	m	m	m	m	mV	mA	Ωm	%	mV
7	0	3	24	27	5,951	5,345	142,189	178,57	1,86	-53,14
8	0	3	27	30	6,708	3,692	142,235	176,15	6,07	-11,58
9	0	3	30	33	7,465	2,888	142,282	189,38	0,67	34,44
10	3	6	9	12	1,247	201,065	65,821	172,74	0,09	-35,4
11	3	6	12	15	2,092	126,175	152,435	187,23	0,09	14,08
12	3	6	15	18	2,885	58,973	152,466	218,73	0,27	-11,06
13	3	6	18	21	3,661	34,29	152,484	254,33	0,4	5,12
14	3	6	21	24	4,427	13,909	152,618	180,38	1,17	-19,62
15	3	6	24	27	5,189	9,636	152,643	199,91	1,97	-43,59
16	3	6	27	30	5,951	6,132	152,642	190,81	3,16	-5,01
17	3	6	30	33	6,708	5,722	152,527	254,58	1,58	27,5
18	3	6	33	36	7,465	3,321	152,706	202,94	7,58	42,27
19	6	9	12	15	1,247	235,593	78,681	169,32	0	12,13
20	6	9	15	18	2,092	138,652	140,648	222,99	0,05	-7,72
21	6	9	18	21	2,885	65,961	140,982	264,57	0,19	3,18
22	6	9	21	24	3,661	23,95	140,758	192,44	0,87	-20,24
23	6	9	24	27	4,427	14,763	141,014	207,2	0,8	-38,71
24	6	9	27	30	5,189	9,126	141,006	204,95	1,29	-2,24
25	6	9	30	33	5,951	6,904	141,049	232,51	0,55	23,72
26	6	9	33	36	6,708	4,818	140,979	231,91	2,5	37,25
27	6	9	36	39	7,465	3,256	140,633	216,02	5,31	105,81
28	9	12	15	18	1,247	239,982	57,877	234,47	0	-5,62
29	9	12	18	21	2,092	207,429	141,815	330,85	0,13	1,97
30	9	12	21	24	2,885	58,482	141,796	233,23	0,32	-20,47
31	9	12	24	27	3,661	32,642	141,796	260,36	0,51	-35,86
32	9	12	27	30	4,427	17,632	141,814	246,08	0,49	-0,38
33	9	12	30	33	5,189	12,439	142,033	277,35	1,04	20,84
34	9	12	33	36	5,951	8,372	142,013	280,04	1,46	34,73
35	9	12	36	39	6,708	5,963	141,995	284,98	0,75	96,58
36	9	12	39	42	7,465	4,589	141,857	301,85	2,09	-119,67
37	12	15	18	21	1,247	309,883	73,398	238,75	0,04	1,18
38	12	15	21	24	2,092	115,052	134,002	194,21	0	-20,65
39	12	15	24	27	2,885	50,153	134,606	210,69	0,11	-33,82
40	12	15	27	30	3,661	25,597	134,925	214,56	0,53	0,89
41	12	15	30	33	4,427	16,36	135,07	239,72	0,51	18,27
42	12	15	33	36	5,189	10,158	135,575	237,27	1,19	33,2
43	12	15	36	39	5,951	7,695	135,757	269,25	3,13	89,04
44	12	15	39	42	6,708	4,555	136,052	227,18	1,12	-111,42
45	12	15	42	45	7,465	3,618	136,272	247,7	4,67	31,1
46	15	18	21	24	1,247	209,49	68,512	172,91	0,09	-20,88
47	15	18	24	27	2,092	111,155	124,84	201,4	0,17	-32,54
48	15	18	27	30	2,885	46,653	125,322	210,51	0,3	1,83
49	15	18	30	33	3,661	26,721	125,589	240,63	0,31	15,76
50	15	18	33	36	4,427	15,526	125,9	244,07	0,31	32,18
51	15	18	36	39	5,189	10,584	126,243	265,48	1,7	83,02
52	15	18	39	42	5,951	6,797	126,399	255,45	3,69	-104,81
53	15	18	42	45	6,708	4,653	126,66	249,31	7,07	33,16
54	15	18	45	48	7,465	4,152	127,062	304,88	4,32	-17,54
55	18	21	24	27	1,247	206,531	66,634	175,27	0,05	-31,65
56	18	21	27	30	2,092	113,449	121,245	211,65	0,13	2,68
57	18	21	30	33	2,885	53,266	121,884	247,13	0,18	13,17
58	18	21	33	36	3,661	27,471	122,317	254,01	0,19	31,84
59	18	21	36	39	4,427	17,345	122,8	279,55	1,02	77,99
60	18	21	39	42	5,189	10,651	123,165	273,85	1,06	-99,33
61	18	21	42	45	5,951	7,488	123,543	287,92	1,48	34,75
62	18	21	45	48	6,708	5,856	123,631	321,41	0,86	-17,9
63	18	21	48	51	7,465	3,794	123,938	285,66	1,93	22,91
64	21	24	27	30	1,247	279,277	134,281	117,61	0,08	3,5
65	21	24	30	33	2,092	84,731	134,756	142,23	0,21	11,08

continued on next page

Influence of arbitrary resistivity distribution of ground on the surface potential of earthing systems

#	location					measured values				
	x_{C2}	x_{C1}	x_{P2}	x_{P2}	z	U_P	I_C	ρ_a	σ	SP
	m	m	m	m	m	mV	mA	Ωm	%	mV
66	21	24	33	36	2,885	36,529	135,312	152,66	0,93	31,82
67	21	24	36	39	3,661	19,209	135,923	159,84	1,2	73,69
68	21	24	39	42	4,427	11,136	136,161	161,87	1,04	-94,76
69	21	24	42	45	5,189	8,286	136,283	192,53	2,26	36,52
70	21	24	45	48	5,951	6,918	136,541	240,65	13,15	-18,25
71	21	24	48	51	6,708	3,99	136,929	197,72	5,35	23,22
72	21	24	51	54	7,465	2,512	136,785	171,36	16,12	31,82
73	24	27	30	33	1,247	230,286	88,319	147,45	0	9,13
74	24	27	33	36	2,092	122,363	148,782	186,03	0,08	31,83
75	24	27	36	39	2,885	50,649	148,539	192,82	0,17	70,17
76	24	27	39	42	3,661	24,634	148,628	187,45	0,12	-90,58
77	24	27	42	45	4,427	15,98	148,893	212,42	0,64	37,45
78	24	27	45	48	5,189	12,12	149,001	257,58	0,56	-17,74
79	24	27	48	51	5,951	7,605	149,102	242,27	1,31	23,52
80	24	27	51	54	6,708	5,538	149,197	251,87	0,35	29,11
81	24	27	54	57	7,465	3,958	149,408	247,17	1,76	28,87
82	27	30	33	36	1,247	193,951	84,656	129,56	0,11	32,17
83	27	30	36	39	2,092	97,435	145,527	151,44	0,14	66,87
84	27	30	39	42	2,885	37,997	145,374	147,81	0,48	-87,24
85	27	30	42	45	3,661	21,907	145,606	170,16	0,33	38,54
86	27	30	45	48	4,427	15,319	145,863	207,86	1,2	-18,11
87	27	30	48	51	5,189	9,119	146,141	197,61	1,15	23,6
88	27	30	51	54	5,951	6,432	146,204	208,97	0,51	26,55
89	27	30	54	57	6,708	4,822	146,178	223,84	1,73	21,31
90	27	30	57	60	7,465	2,752	146,362	175,42	2,26	42,54
91	30	33	36	39	1,247	178,172	68,544	146,99	0,14	64,03
92	30	33	39	42	2,092	88,31	125,099	159,68	0,68	-84,01
93	30	33	42	45	2,885	40,671	125,786	182,84	0,36	39,41
94	30	33	45	48	3,661	24,694	126,349	221,04	0,47	-18,63
95	30	33	48	51	4,427	14,181	126,571	221,75	0,64	23,7
96	30	33	51	54	5,189	9,372	126,899	233,88	0,99	24,36
97	30	33	54	57	5,951	6,956	127,375	259,42	2,87	15,5
98	30	33	57	60	6,708	5,037	127,614	267,86	6,29	43,58
99	30	33	60	63	7,465	4,107	128,007	299,34	3,56	57,54
100	33	36	39	42	1,247	207,649	102,686	114,35	0,07	-81,27
101	33	36	42	45	2,092	79,922	126,24	143,2	0,09	40,44
102	33	36	45	48	2,885	41,026	126,78	182,99	0,14	-18,71
103	33	36	48	51	3,661	21,356	127,162	189,94	0,54	23,84
104	33	36	51	54	4,427	13,392	127,679	207,59	0,87	22,51
105	33	36	54	57	5,189	8,885	127,802	220,15	0,39	9,55
106	33	36	57	60	5,951	5,483	128,171	203,18	3,41	46,74
107	33	36	60	63	6,708	4,682	128,336	247,57	3,49	56,46
108	33	36	63	66	7,465	3,585	128,79	259,75	3,51	-35,8
109	36	39	42	45	1,247	180,294	71,593	142,41	0	41,24
110	36	39	45	48	2,092	105,585	130,826	182,55	0,12	-18,81
111	36	39	48	51	2,885	43,936	131,295	189,23	0,83	23,75
112	36	39	51	54	3,661	24,683	131,882	211,67	0,29	20,83
113	36	39	54	57	4,427	16,137	132,397	241,24	0,7	2,24
114	36	39	57	60	5,189	8,796	132,626	210,03	3,21	49,85
115	36	39	60	63	5,951	6,645	132,645	237,98	0,92	55,61
116	36	39	63	66	6,708	5,163	133,025	263,36	1,96	-35,53
117	36	39	66	69	7,465	3,689	133,501	257,82	5,8	-103,39
118	39	42	45	48	1,247	212,994	75,086	160,41	0	-19,07
119	39	42	48	51	2,092	95,024	136,664	157,28	0,17	23,83
120	39	42	51	54	2,885	39,727	136,944	164,05	0,43	19,23
121	39	42	54	57	3,661	23,768	136,986	196,23	0,35	-3,19
122	39	42	57	60	4,427	12,276	137,041	177,3	0,31	53,17
123	39	42	60	63	5,189	9,595	137,064	221,68	0,25	54,55
124	39	42	63	66	5,951	5,971	137,37	206,49	5,65	-35,57

continued on next page

#	location					measured values				
	x_{C2}	x_{C1}	x_{P2}	x_{P2}	z	U_P	I_C	ρ_a	σ	SP
	m	m	m	m	m	mV	mA	Ωm	%	mV
125	39	42	66	69	6,708	4,895	137,439	241,68	5,77	-99,03
126	42	45	48	51	1,247	202,434	73,455	155,84	0,03	23,65
127	42	45	51	54	2,092	89,799	133,61	152,03	0,4	17,84
128	42	45	54	57	2,885	42,238	134,252	177,91	0,29	-6,64
129	42	45	57	60	3,661	20,034	134,811	168,07	0,35	52,57
130	42	45	60	63	4,427	13,878	135,141	203,25	0,87	53,7
131	42	45	63	66	5,189	8,5	135,315	198,92	1,55	-35,72
132	42	45	66	69	5,951	6,841	135,722	239,43	4,01	-95,74
133	45	48	51	54	1,247	259,857	97,33	150,98	0,07	16,66
134	45	48	54	57	2,092	92,615	119,059	175,95	0,16	-0,65
135	45	48	57	60	2,885	36,265	119,364	171,8	0,56	50,05
136	45	48	60	63	3,661	21,435	119,772	202,4	0,41	52,87
137	45	48	63	66	4,427	13,894	119,984	229,18	1,22	-35,8
138	45	48	66	69	5,189	8,687	120,257	228,75	1,03	-92,89
139	48	51	54	57	1,247	234,324	92,725	142,9	0,04	-15,4
140	48	51	57	60	2,092	68,086	113,467	135,73	0,1	59,31
141	48	51	60	63	2,885	33,485	113,645	166,62	0,16	52,25
142	48	51	63	66	3,661	19,546	113,893	194,09	0,66	-35,97
143	48	51	66	69	4,427	11,663	114,115	202,28	1,63	-90,75
144	51	54	57	60	1,247	190,162	86,269	124,65	0,09	63,26
145	51	54	60	63	2,092	67,172	105,592	143,89	0,03	51,64
146	51	54	63	66	2,885	32,581	105,798	174,15	0,49	-36,22
147	51	54	66	69	3,661	18,041	105,92	192,63	1,09	-89,13
148	54	57	60	63	1,247	217,867	85,112	144,75	0,06	51,17
149	54	57	63	66	2,092	75,125	104,328	162,88	0,35	-36,37
150	54	57	66	69	2,885	33,135	104,558	179,21	0,64	-87,96
151	57	60	63	66	1,247	216,271	102,471	119,35	0,11	-36,34
152	57	60	66	69	2,092	78,013	125,617	140,48	0,68	-87,22
153	60	63	66	69	1,247	154,456	74,157	117,78	0,06	-86,77

Table B.3.: Measured values Dipole-Dipole Line5

#	location					measured values				
	x_{C2}	x_{C1}	x_{P2}	x_{P2}	z	U_P	I_C	ρ_a	σ	SP
	m	m	m	m	m	mV	mA	Ωm	%	mV
1	0	3	6	9	1,247	139,65	63,201	124,95	0,09	-94,48
2	0	3	9	12	2,092	92,497	129,043	162,13	0,07	157,84
3	0	3	12	15	2,885	55,279	148,751	210,15	0,23	39,85
4	0	3	15	18	3,661	28,168	148,671	214,28	0,46	11,15
5	0	3	18	21	4,427	17,685	148,663	235,45	2,01	-77
6	0	3	21	24	5,189	12,645	148,718	269,25	1,26	-157,95
7	0	3	24	27	5,951	8,522	148,677	272,28	2,9	35,87
8	0	3	27	30	6,708	0,444	9,8	307,75	8,92	250
9	0	3	30	33	7,465	4,116	148,557	258,49	7,75	-205,26
10	3	6	9	12	1,247	210,028	106,5	111,52	0,06	73,07
11	3	6	12	15	2,092	114,02	163,561	157,68	0,41	15,32
12	3	6	15	18	2,885	49,389	163,712	170,6	0,73	35,81
13	3	6	18	21	3,661	27,146	163,748	187,49	0,34	-70,85
14	3	6	21	24	4,427	18,914	163,76	228,59	0,14	-122,42
15	3	6	24	27	5,189	11,968	163,729	231,48	0,51	18,83
16	3	6	27	30	5,951	3,571	164,145	103,35	6,63	200,39
17	3	6	30	33	6,708	4,975	163,767	206,15	3,97	-162,66
18	3	6	33	36	7,465	2,173	163,866	123,7	8,85	220,25
19	6	9	12	15	1,247	227,307	97,823	131,4	0,06	1,08
20	6	9	15	18	2,092	111,155	155,671	161,51	0,23	44,29

continued on next page

Influence of arbitrary resistivity distribution of ground on the surface potential of earthing systems

#	location					measured values				
	x_{C2}	x_{C1}	x_{P2}	x_{P2}	z	U_P	I_C	ρ_a	σ	SP
	m	m	m	m	m	mV	mA	Ωm	%	mV
21	6	9	18	21	2,885	48,554	155,83	176,2	0,1	-66,67
22	6	9	21	24	3,661	28,559	155,932	207,14	0,14	-105,82
23	6	9	24	27	4,427	16,895	156,281	213,96	1,74	17,24
24	6	9	27	30	5,189	7,567	156,294	153,32	1,28	167,5
25	6	9	30	33	5,951	7,068	156,209	214,91	2,57	-138,29
26	6	9	33	36	6,708	3,221	156,609	139,56	1,69	203,98
27	6	9	36	39	7,465	3,041	155,951	181,95	7,66	-168
28	9	12	15	18	1,247	205,77	71,697	162,3	0	48,38
29	9	12	18	21	2,092	67,084	76,439	198,51	0,31	-63,48
30	9	12	21	24	2,885	30,444	76,296	225,65	0,34	-95,41
31	9	12	24	27	3,661	16,182	74,199	246,65	0,68	18,63
32	9	12	27	30	4,427	8,481	71,392	235,12	1,67	144,17
33	9	12	30	33	5,189	4,81	69,275	219,87	3,57	-122,23
34	9	12	33	36	5,951	2,019	64,996	147,53	5,03	192,34
35	9	12	36	39	6,708	1,085	60,611	121,44	45,08	-158,34
36	9	12	39	42	7,465	1,144	56,971	187,33	5,39	87,32
37	12	15	18	21	1,247	166,878	51,671	182,63	0,12	-60,72
38	12	15	21	24	2,092	47,709	45,025	239,68	0,2	-88,21
39	12	15	24	27	2,885	20,877	41,693	283,15	0,4	21,45
40	12	15	27	30	3,661	5,086	32,545	176,76	3,4	125,85
41	12	15	30	33	4,427	3,82	27,313	276,8	2,27	-110,78
42	12	15	33	36	5,189	1,946	20,247	304,29	7,16	183,28
43	12	15	36	39	5,951	1,346	19,164	333,63	6,48	-151,04
44	12	15	39	42	6,708	0,271	14,308	128,46	44,77	80,52
45	12	15	42	45	7,465	0,35	10,436	312,66	7,31	-58,74
46	15	18	21	24	1,247	174,878	63,547	155,62	0	-82,67
47	15	18	24	27	2,092	140,607	147,806	215,18	0,08	23,49
48	15	18	27	30	2,885	51,906	148,157	198,11	0,14	111,67
49	15	18	30	33	3,661	25,91	148,218	197,71	0,31	-102,25
50	15	18	33	36	4,427	14,149	148,516	188,55	0,73	175,79
51	15	18	36	39	5,189	11,893	147,94	254,57	1,03	-144,87
52	15	18	39	42	5,951	7,475	148,415	239,24	6,84	74,69
53	15	18	42	45	6,708	5,442	148,132	249,29	0,56	-53,71
54	15	18	45	48	7,465	3,379	148,258	212,67	1,37	-0,08
55	18	21	24	27	1,247	256,892	90,445	160,62	0,03	25,22
56	18	21	27	30	2,092	106,159	149,198	160,94	0,07	100,14
57	18	21	30	33	2,885	48,62	149,252	184,21	0,46	-95,46
58	18	21	33	36	3,661	25,483	149,515	192,76	0,28	169,5
59	18	21	36	39	4,427	20,149	148,891	267,83	1,77	-139,39
60	18	21	39	42	5,189	10,168	148,996	216,12	0,6	69,81
61	18	21	42	45	5,951	7,835	149,147	249,53	0,91	-49,75
62	18	21	45	48	6,708	4,91	149,375	223,04	3,34	1,82
63	18	21	48	51	7,465	3,657	149,486	228,27	2,12	11,8
64	21	24	27	30	1,247	156,919	80,682	109,98	0,1	90,26
65	21	24	30	33	2,092	106,166	165,022	145,52	0,17	-89,84
66	21	24	33	36	2,885	55,486	165,266	189,85	0,24	164,27
67	21	24	36	39	3,661	32,664	164,869	224,07	0,52	-134,73
68	21	24	39	42	4,427	17,481	164,982	209,71	0,44	65,78
69	21	24	42	45	5,189	12,815	165,003	245,95	0,88	-46,26
70	21	24	45	48	5,951	7,942	165,216	228,35	1,88	3,47
71	21	24	48	51	6,708	6,197	165,08	254,72	1,89	11,2
72	21	24	51	54	7,465	5,14	165,076	290,52	7,15	-173,18
73	24	27	30	33	1,247	309,868	164,983	106,21	0,16	-85,41
74	24	27	33	36	2,092	81,057	118,412	154,84	0,25	159,56
75	24	27	36	39	2,885	57,413	169,32	191,75	0,6	-130,56
76	24	27	39	42	3,661	29,598	169,697	197,26	0,16	62,4
77	24	27	42	45	4,427	19,932	169,959	232,12	0,81	-43,45
78	24	27	45	48	5,189	11,479	169,876	213,98	2,14	4,74
79	24	27	48	51	5,951	8,688	169,755	243,11	1,54	10,87

continued on next page

Influence of arbitrary resistivity distribution of ground on the surface potential of earthing systems

#	location					measured values				
	x_{C2}	x_{C1}	x_{P2}	x_{P2}	z	U_P	I_C	ρ_a	σ	SP
	m	m	m	m	m	mV	mA	Ωm	%	mV
80	24	27	51	54	6,708	4,525	169,972	180,65	10,37	-168,44
81	24	27	54	57	7,465	0,36	12,636	266,19	19,11	287,22
82	27	30	33	36	1,247	55,825	21,678	145,62	0,1	155,78
83	27	30	36	39	2,092	118,767	149,027	180,27	0,22	-126,78
84	27	30	39	42	2,885	53,137	155,964	192,66	0,33	59,31
85	27	30	42	45	3,661	32,738	156,015	237,32	0,99	-40,98
86	27	30	45	48	4,427	16,77	156,123	212,6	1,06	5,93
87	27	30	48	51	5,189	12,58	156,147	255,13	0,43	10,34
88	27	30	51	54	5,951	6,94	156,366	210,82	0,75	-164,29
89	27	30	54	57	6,708	0,371	10,736	234,3	32,8	274,5
90	27	30	57	60	7,465	5,073	156,503	302,45	1,57	-51,44
91	30	33	36	39	1,247	141,242	58,354	136,87	0,06	-123,8
92	30	33	39	42	2,092	115,992	160,835	163,13	0,14	56,55
93	30	33	42	45	2,885	60,394	160,851	212,32	0,24	-39,08
94	30	33	45	48	3,661	28,139	160,829	197,88	0,3	6,76
95	30	33	48	51	4,427	18,626	161,081	228,86	0,3	10,03
96	30	33	51	54	5,189	11,546	161,155	226,87	2,29	-160,64
97	30	33	54	57	5,951	0,705	11,386	294,16	1,66	263,2
98	30	33	57	60	6,708	6,361	161,227	267,73	1,49	-47,84
99	30	33	60	63	7,465	0,313	11,424	256	11,54	338,45
100	33	36	39	42	1,247	221,555	91,943	136,27	0,03	54,42
101	33	36	42	45	2,092	126,897	149,248	192,32	0,18	-37,18
102	33	36	45	48	2,885	48,049	149,452	181,8	0,11	7,72
103	33	36	48	51	3,661	29,863	149,699	225,61	0,34	10,02
104	33	36	51	54	4,427	15,589	149,924	205,79	0,27	-157,11
105	33	36	54	57	5,189	0,762	9,953	242,34	1,53	253,13
106	33	36	57	60	5,951	7,842	149,93	248,45	1,17	-44,29
107	33	36	60	63	6,708	0,286	9,954	195,05	7,28	336,54
108	33	36	63	66	7,465	0,13	9,815	123,3	20,17	-350,51
109	36	39	42	45	1,247	253,358	87,992	162,82	0,05	-35,11
110	36	39	45	48	2,092	105,541	145,824	163,71	0,04	8,23
111	36	39	48	51	2,885	51,174	146,074	198,11	0,3	9,89
112	36	39	51	54	3,661	25,31	146,152	195,86	0,96	-153,74
113	36	39	54	57	4,427	2,41	19,602	243,37	3,27	243,87
114	36	39	57	60	5,189	11,518	146,398	249,15	1,29	-41,03
115	36	39	60	63	5,951	0,474	9,501	236,81	8,58	334,7
116	36	39	63	66	6,708	0,233	9,437	167,32	2,62	-349,32
117	36	39	66	69	7,465	3,631	146,545	231,19	6,91	-42,01
118	39	42	45	48	1,247	220,129	66,392	187,49	0,03	8,71
119	39	42	48	51	2,092	142,677	148,9	216,74	0,14	9,87
120	39	42	51	54	2,885	51,945	149,114	196,99	0,49	-150,86
121	39	42	54	57	3,661	14,188	66,769	240,32	0,26	235,18
122	39	42	57	60	4,427	20,266	148,96	269,26	1,1	-38,22
123	39	42	60	63	5,189	0,763	9,889	244,33	3,22	332,52
124	39	42	63	66	5,951	0,45	9,653	221,52	1,88	-348,1
125	39	42	66	69	6,708	5,293	149,429	240,37	6,83	-39
126	42	45	48	51	1,247	292,773	104,526	158,39	0	9,46
127	42	45	51	54	2,092	73,32	104,734	158,35	0,17	-148,61
128	42	45	54	57	2,885	21,596	57,187	213,55	1,34	228,14
129	42	45	57	60	3,661	33,498	159,491	237,54	0,49	-36,27
130	42	45	60	63	4,427	1,277	11,203	225,54	1,15	330,95
131	42	45	63	66	5,189	0,753	11,005	216,61	1,8	-347
132	42	45	66	69	5,951	7,41	159,554	220,59	0,2	-36,51
133	45	48	51	54	1,247	118,076	57,353	116,42	0,08	-146,68
134	45	48	54	57	2,092	16,147	22,8	160,19	0,19	222,59
135	45	48	57	60	2,885	53,046	160,296	187,13	0,25	-34,26
136	45	48	60	63	3,661	1,794	11,318	179,29	1,81	329,45
137	45	48	63	66	4,427	0,947	11,023	170,09	5,26	-345,99
138	45	48	66	69	5,189	8,775	160,597	173,04	0,57	-34,59

continued on next page

#	location					measured values				
	x_{C2}	x_{C1}	x_{P2}	x_{P1}	z	U_P	I_C	ρ_a	σ	SP
	m	m	m	m	m	mV	mA	Ωm	%	mV
139	48	51	54	57	1,247	21,485	7,34	165,53	0,13	218,09
140	48	51	57	60	2,092	111,628	126,314	199,9	0,09	-32,73
141	48	51	60	63	2,885	2,686	7,621	199,29	0,36	328,14
142	48	51	63	66	3,661	1,173	7,468	177,64	2,78	-345,06
143	48	51	66	69	4,427	12,302	126,403	192,62	0,62	-33,07
144	51	54	57	60	1,247	212,238	83,811	143,2	0,04	-31,89
145	51	54	60	63	2,092	3,977	6,196	145,18	0,23	327,04
146	51	54	63	66	2,885	1,475	6,129	136,1	1,67	-344,4
147	51	54	66	69	3,661	13,598	102,377	150,22	0,58	-32,07
148	54	57	60	63	1,247	17,301	5,957	164,24	0,19	326,15
149	54	57	63	66	2,092	3,956	5,948	150,45	0,45	-343,92
150	54	57	66	69	2,885	30,604	101,336	170,78	0,1	-31,26
151	57	60	63	66	1,247	15,773	5,744	155,27	0,18	-343,69
152	57	60	66	69	2,092	69,786	97,885	161,26	0,1	-30,72
153	60	63	66	69	1,247	206,039	83,107	140,2	0	-30,54

Table B.4.: Center coordinates of inversion model resistivity

x	y	z	inversion model ρ
m	m	m	Ωm
4.5	0	1.56	170.9
9	0	3.11	255.1
13.5	0	4.67	269.01
18	0	6.23	267.04
22.5	0	7.79	266.71
27	0	9.34	252.51
31.5	0	10.90	234.19
7.5	0	1.56	170.07
12	0	3.11	232.24
16.5	0	4.67	263.01
21	0	6.23	254.15
25.5	0	7.79	248.3
30	0	9.34	228.72
34.5	0	10.90	229.52
10.5	0	1.56	224.66
15	0	3.11	225.26
19.5	0	4.67	237.25
24	0	6.23	236.03
28.5	0	7.79	223.07
33	0	9.34	228.24
37.5	0	10.90	230.2
13.5	0	1.56	207.31
18	0	3.11	246.82
22.5	0	4.67	228.08
27	0	6.23	220.02
31.5	0	7.79	229.38
36	0	9.34	223.55
16.5	0	1.56	212.76
21	0	3.11	230.81
25.5	0	4.67	204.17
30	0	6.23	229.1
34.5	0	7.79	228.19
39	0	9.34	240.31
19.5	0	1.56	228.08
24	0	3.11	198.44

continued on next page

x m	y m	z m	inversion model ρ Ωm
28.5	0	4.67	217.95
33	0	6.23	231.29
37.5	0	7.79	234.94
42	0	9.34	239.74
22.5	0	1.56	155.93
27	0	3.11	195.94
31.5	0	4.67	218.48
36	0	6.23	234.4
40.5	0	7.79	242.91
25.5	0	1.56	175.85
30	0	3.11	202.57
34.5	0	4.67	229.69
39	0	6.23	233.24
43.5	0	7.79	246.31
28.5	0	1.56	143.77
33	0	3.11	192.78
37.5	0	4.67	208.76
42	0	6.23	230.65
46.5	0	7.79	237.5
31.5	0	1.56	161.3
36	0	3.11	200.17
40.5	0	4.67	207.67
45	0	6.23	229.64
34.5	0	1.56	142.24
39	0	3.11	183.67
43.5	0	4.67	202.6
48	0	6.23	228.2
37.5	0	1.56	159.82
42	0	3.11	178.23
46.5	0	4.67	212.03
51	0	6.23	237.18
40.5	0	1.56	148.48
45	0	3.11	189.74
49.5	0	4.67	212.15
43.5	0	1.56	156.92
48	0	3.11	191.07
52.5	0	4.67	212.64
46.5	0	1.56	168.95
51	0	3.11	184.02
55.5	0	4.67	201.29
49.5	0	1.56	157.1
54	0	3.11	188.5
52.5	0	1.56	149.04
57	0	3.11	181.77
55.5	0	1.56	158.35
60	0	3.11	170
58.5	0	1.56	133.89
61.5	0	1.56	142.14
64.5	0	1.56	135.26
4.5	3	1.56	155.21
9	3	3.11	258.34
13.5	3	4.67	267.84
18	3	6.23	274.68
22.5	3	7.79	275.42
27	3	9.34	262.96
31.5	3	10.90	241.9
7.5	3	1.56	172.06
12	3	3.11	233.67
16.5	3	4.67	261.42
21	3	6.23	264.91

continued on next page

x m	y m	z m	inversion model ρ Ωm
25.5	3	7.79	256.97
30	3	9.34	232.61
34.5	3	10.90	227.11
10.5	3	1.56	201.05
15	3	3.11	218.63
19.5	3	4.67	249.13
24	3	6.23	245.38
28.5	3	7.79	234.51
33	3	9.34	224.37
37.5	3	10.90	234.15
13.5	3	1.56	184.7
18	3	3.11	246.97
22.5	3	4.67	230.87
27	3	6.23	229.78
31.5	3	7.79	224.92
36	3	9.34	226.09
16.5	3	1.56	221.69
21	3	3.11	241.05
25.5	3	4.67	217.58
30	3	6.23	227.98
34.5	3	7.79	233.46
39	3	9.34	234.43
19.5	3	1.56	207.91
24	3	3.11	202.56
28.5	3	4.67	208.96
33	3	6.23	228.88
37.5	3	7.79	226.84
42	3	9.34	234.41
22.5	3	1.56	190.93
27	3	3.11	193.02
31.5	3	4.67	224.78
36	3	6.23	233.52
40.5	3	7.79	241.55
25.5	3	1.56	154.92
30	3	3.11	210.14
34.5	3	4.67	221.82
39	3	6.23	232.99
43.5	3	7.79	235.98
28.5	3	1.56	155.24
33	3	3.11	198.5
37.5	3	4.67	215.42
42	3	6.23	228.3
46.5	3	7.79	243.43
31.5	3	1.56	143.57
36	3	3.11	190.95
40.5	3	4.67	199.94
45	3	6.23	228.96
34.5	3	1.56	154.4
39	3	3.11	178.52
43.5	3	4.67	212.06
48	3	6.23	227.59
37.5	3	1.56	138.91
42	3	3.11	183.98
46.5	3	4.67	202.72
51	3	6.23	235.72
40.5	3	1.56	156.16
45	3	3.11	191.24
49.5	3	4.67	217.18
43.5	3	1.56	139.74
48	3	3.11	187.19

continued on next page

x m	y m	z m	inversion model ρ Ωm
52.5	3	4.67	202.34
46.5	3	1.56	171.99
51	3	3.11	179.82
55.5	3	4.67	216.08
49.5	3	1.56	139.49
54	3	3.11	188.83
52.5	3	1.56	169.47
57	3	3.11	188.93
55.5	3	1.56	146.51
60	3	3.11	176.33
58.5	3	1.56	173.45
61.5	3	1.56	128.63
64.5	3	1.56	174.32
4.5	6	1.56	148.48
9	6	3.11	255.15
13.5	6	4.67	254.45
18	6	6.23	281.38
22.5	6	7.79	284.45
27	6	9.34	271.21
31.5	6	10.90	257.11
7.5	6	1.56	170.65
12	6	3.11	245.21
16.5	6	4.67	251.82
21	6	6.23	276.21
25.5	6	7.79	274.9
30	6	9.34	254.12
34.5	6	10.90	231.85
10.5	6	1.56	176.51
15	6	3.11	215.74
19.5	6	4.67	257.07
24	6	6.23	266.62
28.5	6	7.79	250.87
33	6	9.34	227.78
37.5	6	10.90	228.43
13.5	6	1.56	178.32
18	6	3.11	227.07
22.5	6	4.67	245.83
27	6	6.23	246.74
31.5	6	7.79	224.44
36	6	9.34	227.19
16.5	6	1.56	210.44
21	6	3.11	250.21
25.5	6	4.67	244.29
30	6	6.23	230.72
34.5	6	7.79	234.21
39	6	9.34	225.75
19.5	6	1.56	195.46
24	6	3.11	228.59
28.5	6	4.67	196.5
33	6	6.23	224.31
37.5	6	7.79	219.61
42	6	9.34	232.05
22.5	6	1.56	216.45
27	6	3.11	201.71
31.5	6	4.67	223.53
36	6	6.23	222.44
40.5	6	7.79	233.57
25.5	6	1.56	145.62
30	6	3.11	202.27
34.5	6	4.67	207.68

continued on next page

x m	y m	z m	inversion model ρ Ωm
39	6	6.23	230.44
43.5	6	7.79	231.04
28.5	6	1.56	169.8
33	6	3.11	195.2
37.5	6	4.67	213.85
42	6	6.23	221.87
46.5	6	7.79	243.64
31.5	6	1.56	129.17
36	6	3.11	189.67
40.5	6	4.67	197.89
45	6	6.23	233.46
34.5	6	1.56	167.55
39	6	3.11	187.18
43.5	6	4.67	215.71
48	6	6.23	230.58
37.5	6	1.56	138.49
42	6	3.11	184.7
46.5	6	4.67	204.39
51	6	6.23	227.18
40.5	6	1.56	161.48
45	6	3.11	188.07
49.5	6	4.67	222.31
43.5	6	1.56	145.21
48	6	3.11	193.09
52.5	6	4.67	203.29
46.5	6	1.56	154.39
51	6	3.11	186.29
55.5	6	4.67	213.3
49.5	6	1.56	148.64
54	6	3.11	180.87
52.5	6	1.56	171.49
57	6	3.11	189.34
55.5	6	1.56	133.45
60	6	3.11	182.16
58.5	6	1.56	209.9
61.5	6	1.56	121.68
64.5	6	1.56	195.69
4.5	9	1.56	160.57
9	9	3.11	235.66
13.5	9	4.67	266.28
18	9	6.23	286.2
22.5	9	7.79	281.2
27	9	9.34	271.52
31.5	9	10.90	259.71
7.5	9	1.56	161.64
12	9	3.11	249.8
16.5	9	4.67	260.34
21	9	6.23	271.18
25.5	9	7.79	268.06
30	9	9.34	259.62
34.5	9	10.90	244.14
10.5	9	1.56	158.41
15	9	3.11	238.58
19.5	9	4.67	247.01
24	9	6.23	256.26
28.5	9	7.79	252.72
33	9	9.34	236.76
37.5	9	10.90	235.93
13.5	9	1.56	187.1
18	9	3.11	219.25

continued on next page

x m	y m	z m	inversion model ρ Ωm
22.5	9	4.67	230.63
27	9	6.23	240.39
31.5	9	7.79	233.33
36	9	9.34	230.84
16.5	9	1.56	204.3
21	9	3.11	221.94
25.5	9	4.67	232.25
30	9	6.23	233.56
34.5	9	7.79	230.04
39	9	9.34	225.98
19.5	9	1.56	187.86
24	9	3.11	230.8
28.5	9	4.67	221.37
33	9	6.23	230.14
37.5	9	7.79	228.89
42	9	9.34	235.9
22.5	9	1.56	206.08
27	9	3.11	213.62
31.5	9	4.67	227.83
36	9	6.23	231.01
40.5	9	7.79	236.79
25.5	9	1.56	156.32
30	9	3.11	198.32
34.5	9	4.67	216.05
39	9	6.23	234.98
43.5	9	7.79	231.29
28.5	9	1.56	167.84
33	9	3.11	199.07
37.5	9	4.67	217.74
42	9	6.23	220.36
46.5	9	7.79	235.78
31.5	9	1.56	131.11
36	9	3.11	195.51
40.5	9	4.67	206.05
45	9	6.23	227.71
34.5	9	1.56	162.48
39	9	3.11	186.61
43.5	9	4.67	206.59
48	9	6.23	227.74
37.5	9	1.56	153.47
42	9	3.11	183.43
46.5	9	4.67	208.62
51	9	6.23	223.96
40.5	9	1.56	151.4
45	9	3.11	189.52
49.5	9	4.67	214.55
43.5	9	1.56	170.25
48	9	3.11	192.07
52.5	9	4.67	210.75
46.5	9	1.56	144.41
51	9	3.11	192.14
55.5	9	4.67	208.15
49.5	9	1.56	163.84
54	9	3.11	186.35
52.5	9	1.56	154.53
57	9	3.11	188.27
55.5	9	1.56	149.91
60	9	3.11	185.12
58.5	9	1.56	189.17
61.5	9	1.56	141.34

continued on next page

x m	y m	z m	inversion model ρ Ωm
64.5	9	1.56	190.26
4.5	12	1.56	176.89
9	12	3.11	216.99
13.5	12	4.67	256.31
18	12	6.23	287.41
22.5	12	7.79	270.06
27	12	9.34	267.03
31.5	12	10.90	256.15
7.5	12	1.56	155.41
12	12	3.11	248.64
16.5	12	4.67	254.29
21	12	6.23	260.84
25.5	12	7.79	261.07
30	12	9.34	261.06
34.5	12	10.90	247.11
10.5	12	1.56	151.05
15	12	3.11	234.23
19.5	12	4.67	242.42
24	12	6.23	252.74
28.5	12	7.79	246.92
33	12	9.34	232.54
37.5	12	10.90	238.97
13.5	12	1.56	200.53
18	12	3.11	201.05
22.5	12	4.67	229.46
27	12	6.23	238.21
31.5	12	7.79	238.72
36	12	9.34	230.82
16.5	12	1.56	182.26
21	12	3.11	211.57
25.5	12	4.67	223.91
30	12	6.23	222.57
34.5	12	7.79	225.9
39	12	9.34	228.25
19.5	12	1.56	180.11
24	12	3.11	233.45
28.5	12	4.67	223.55
33	12	6.23	229.18
37.5	12	7.79	230.38
42	12	9.34	237.65
22.5	12	1.56	188.84
27	12	3.11	208.9
31.5	12	4.67	211.13
36	12	6.23	230.94
40.5	12	7.79	232.15
25.5	12	1.56	153.25
30	12	3.11	186.16
34.5	12	4.67	216.97
39	12	6.23	234.63
43.5	12	7.79	231.9
28.5	12	1.56	156.97
33	12	3.11	196.1
37.5	12	4.67	213.12
42	12	6.23	226.53
46.5	12	7.79	226.91
31.5	12	1.56	142
36	12	3.11	201.33
40.5	12	4.67	219.24
45	12	6.23	220.4
34.5	12	1.56	146.32

continued on next page

x m	y m	z m	inversion model ρ Ωm
39	12	3.11	194.69
43.5	12	4.67	208.68
48	12	6.23	221.22
37.5	12	1.56	182.36
42	12	3.11	183.75
46.5	12	4.67	211.65
51	12	6.23	222.42
40.5	12	1.56	139.94
45	12	3.11	200.75
49.5	12	4.67	195.87
43.5	12	1.56	187
48	12	3.11	200.91
52.5	12	4.67	205.86
46.5	12	1.56	155.03
51	12	3.11	179.62
55.5	12	4.67	217.62
49.5	12	1.56	171.88
54	12	3.11	178.74
52.5	12	1.56	144.63
57	12	3.11	205.05
55.5	12	1.56	158.75
60	12	3.11	209.7
58.5	12	1.56	182.93
61.5	12	1.56	147.85
64.5	12	1.56	193.73
4.5	15	1.56	196.17
9	15	3.11	223.65
13.5	15	4.67	243.63
18	15	6.23	270.39
22.5	15	7.79	263.7
27	15	9.34	264.19
31.5	15	10.90	250.67
7.5	15	1.56	152.89
12	15	3.11	237.33
16.5	15	4.67	244.63
21	15	6.23	255.3
25.5	15	7.79	256.38
30	15	9.34	250.77
34.5	15	10.90	247.14
10.5	15	1.56	162.36
15	15	3.11	221.71
19.5	15	4.67	226.08
24	15	6.23	246.11
28.5	15	7.79	242.66
33	15	9.34	237.18
37.5	15	10.90	231.39
13.5	15	1.56	181.96
18	15	3.11	193.59
22.5	15	4.67	213.45
27	15	6.23	232.52
31.5	15	7.79	233.29
36	15	9.34	224.6
16.5	15	1.56	172.08
21	15	3.11	201.02
25.5	15	4.67	223.48
30	15	6.23	230.96
34.5	15	7.79	226.36
39	15	9.34	223.87
19.5	15	1.56	179.16
24	15	3.11	216.35

continued on next page

x m	y m	z m	inversion model ρ Ωm
28.5	15	4.67	229.85
33	15	6.23	223.28
37.5	15	7.79	229.03
42	15	9.34	233
22.5	15	1.56	157.26
27	15	3.11	211.08
31.5	15	4.67	210.83
36	15	6.23	229.63
40.5	15	7.79	221.11
25.5	15	1.56	158.08
30	15	3.11	190.86
34.5	15	4.67	210.52
39	15	6.23	231.13
43.5	15	7.79	227.55
28.5	15	1.56	147.63
33	15	3.11	192.71
37.5	15	4.67	211.44
42	15	6.23	218.12
46.5	15	7.79	225.39
31.5	15	1.56	141.1
36	15	3.11	191.67
40.5	15	4.67	201.48
45	15	6.23	218.65
34.5	15	1.56	156.5
39	15	3.11	203.42
43.5	15	4.67	211.7
48	15	6.23	216.75
37.5	15	1.56	162.21
42	15	3.11	198.76
46.5	15	4.67	212.59
51	15	6.23	222.79
40.5	15	1.56	173.12
45	15	3.11	197.46
49.5	15	4.67	185.72
43.5	15	1.56	173.84
48	15	3.11	194.17
52.5	15	4.67	210.26
46.5	15	1.56	159.62
51	15	3.11	189.02
55.5	15	4.67	223.75
49.5	15	1.56	176.88
54	15	3.11	184.66
52.5	15	1.56	141.2
57	15	3.11	206.31
55.5	15	1.56	171.98
60	15	3.11	217.53
58.5	15	1.56	168.73
61.5	15	1.56	164.73
64.5	15	1.56	169.24

C. Parameters

3D Inversion Parameters

```
Inversion parameters used
Inversion settings
Initial damping factor
0.1000
Minimum damping factor
0.0100
Line search option
0
Convergence limit
2.0000
Minimum change in RMS error
0.2000
Number of iterations
5
Number of iterations to recalculate Jacobian matrix
100
Vertical to horizontal flatness filter ratio
1.0000
X horizontal flatness filter weight
1.0000
Y horizontal flatness filter weight
1.0000
Flatness filter weight for half-size layers
1.0
Number of nodes between adjacent electrodes
4
Normalise potentials
0
Flatness filter type, Include smoothing of model resistivity
1
Increase of damping factor with depth
1.0100
Type of topographical modeling
0
Factor for damped topography model
0.50
Type of topography trend removal
0
Robust data constrain?
1
Cutoff factor for data constrain
0.1000
Robust model constrain?
1
Cutoff factor for model constrain
0.1000
Reduce effect of side blocks?
1
Optimise damping factor?
0
Thickness of first layer
0.4500
Factor to increase thickness layer with depth
1.1500
```

Number of half-size layers
0
Divide half-size layers vertically (1=YES,0=NO)
0
Factor to increase model depth range
1.0000
USE FINITE ELEMENT METHOD (YES=1,NO=0)
1
RMS CONVERGENCE LIMIT (IN PERCENT)
5.000
USE LOGARITHM OF APPARENT RESISTIVITY (0=LOG OF APP. RESIS., 1=RESISTANCE, 2=APP. RESIS.)
0
TYPE OF IP INVERSION METHOD (0=CONCURRENT,1=SEQUENTIAL)
1
PROCEED AUTOMATICALLY FOR SEQUENTIAL METHOD (1=YES,0=NO)
1
IP DAMPING FACTOR
0.2500
USE AUTOMATIC IP DAMPING FACTOR (YES=1,NO=0)
0
CUTOFF FACTOR FOR LOW POTENTIALS (0.0005 to 0.02)
0.00010
LIMIT RESISTIVITY VALUES(0=No,1=Yes)
1
Upper limit factor (10–50)
50.000
Lower limit factor (0.02 to 0.1)
0.020
Type of reference resistivity (0=average,1=first iteration)
0
Type of optimisation method (0=Gauss–Newton,2=Incomplete GN)
2
Convergence limit for Incomplete Gauss–Newton method
0.01000
Use data compression with Incomplete Gauss–Newton (0=No,1=Yes)
0
Use reference model in inversion (0=No,1=Yes)
0
Damping factor for reference model
0.07000
Type of initial model (0=Homogeneous,1=approx.inverse)
0
Time-lapse inversion constrain
1
Type of time-lapse inversion method
0
Type of time reference model,0=first ,1=preceding
0
Reduce effect of side blocks? (0=No,1=Yes)
1
Use higher damping for first layer? (0=No,1=Yes)
0
Extra damping factor for first layer
5.00000
Automatically re-sort data points (0=No, 1=Yes)
1
Automatically switch electrodes for negative geometric factor (0=No, 1=Yes)
1
Automatically force apparent resistivity values to be positive (0=No, 1=Yes)
0
Scale Incomplete Gauss–Newton method (0=No, 1=Yes)
1
Type of scaling for Incomplete Gauss–Newton method (1=First , 1=Second 3=Third order)
1
Use uniform filter weights (0=No, 1=Yes)
1

Type of data compression (0=Simple, 1=Aggressive)
1
Type of IP constraints (0=always smooth, 1=same as resistivity)
1
Type of IP transform (0=none, 1=square-root, 3=range)
1
Lower limit for IP model value (-50 to +10 mV/V)
0.0
Upper limit for IP model value (650 to 900 mV/V)
800.0
Optimize use of CPU cache (0=No, 1=Yes)
1
Precision of cache optimization routines (0=Standard, 1=High)
1
Use parallel SSE computations (0=No, 1=Yes)
1
Use multi-core support (0=No, 1=Yes)
1
Reference model resistivity multiplication factor (0.1 to 10)
1.00
Disable convergence checking (0=No, 1=Yes)
0
Try to optimise model at each iteration (0=No, 1=Yes)
0
Use approximate IP inversion (0=No, 1=Yes)
0
Use horizontal diagonal filter (0=No, 1=Yes)
0
Use vertical diagonal filter (0=No, 1=Yes)
0
Use vertical cross-diagonal filter (0=No, 1=Yes)
0
Long electrode inversion mesh settings (0=Use same size, 1=Use smaller mesh)
0
Point electrode inversion settings (0=Use nearest nodes, 1=Use distorted grid)
0
Use more than 8GB RAM for finite-difference and finite-element methods (0=No, 1=Yes)
1
Type of time lapse inversion constraint (0=None, 1=Smooth, 2=Blocky)
1
Cross time model damping factor
0.2000
Use complex resistivity model for IP inversion (0=No, 1=Yes)
0
Number of nodes between adjacent borehole electrodes
4
Use active constraints (0=No, 1=Yes)
0
Type of active constraints
0
Parameters used for active constraints
0
Minimum damping for active constraints
0.000
Maximum damping for active constraints
0.000
Weight for diagonal components
1.000
Use optimized forward modeling routines for sparse electrodes (0=No, 1=Yes)
1
Use optimized routines for Intels CPUs (0=No, 1=Yes)
1
Use fast Jacobian calculation for dense data sets (0=No, 1=Yes)
0
Use assembly language subroutines? (0=No, 1=Yes)
1

```
Calculate model resolution? (0=No, 1=Yes)
0
Type of method to estimate topography. (0=Nearest 4 points, 1=All points)
1
Use apparent IP data in resistivity inversion. (0=No, 1=Yes)
0
Use direct calculation of IP Jacobian matrices. (0=No, 1=Yes)
1
Use geometric factor relative error to remove unstable arrays? (0=No, 1=Yes)
1
Geometric factor relative error cutoff values. (3 to 15)
5.00
Use extended boundary nodes for mesh? (0=Standard, 1=Medium, 2=Highly)
1
Use SSE registers in multi-CPU workstations? (0=No, 1=Yes)
1
Refine topography for model grid? (0=No, 1=Yes)
0
Vertical mesh size (0=Default,1=Finer,2=Finest)
3
Reduce time-lapse damping factor after each iteration (0=No, maintain constant value,1=Yes
, reduce)
1
Precision of calculations to solve least-squares equation using direct Gauss-Newton
method (0=Double,1=Single)
0
Type of reference model constraint (0=uniform,1=adaptive)
0
Try to load all potentials into RAM for Jacobian calculation (0=No, 1=Yes)
1
Use AVX instructions (0=SSE, 1=AVX, 2=FMA/AVX2)
0
Use combined Marquardt and Occam inversion (0=No, 1=Yes)
0
Weight for Marquardt method
0.100
Value of data compression cut-off factor (0.001 to 0.01)
0.00200
Automatically remove negative calculated apparent resistivity when using logarithm? (0 or
1)
0
Extend range of horizontal filter? (0,1,2)
0
Use the same reference damping factor for the I.P. model? (0=No,1=Yes)
1
I.P. damping factor value (0.01 to 1.00)
0.0700
Use zero reference I.P. model value? (0=No, 1=Yes)
0
Default number of extra iterations to add (0 to 10)
10
Use amplitude of potentials in non-linear complex resistivity forward model to calculate
apparent resistivity and IP values. (0 or 1)
0
Automatically continue inversion when number of iterations reached for models with large
meshes if program has not converged? (0 or 1)
1
Use L curve method to estimate damping factor? (0 or 1)
0
Type of scaling used for data errors (0=average weights 1.0, 1=minimum weight 1.0)
0
Automatically reset settings for pole-pole data? (0 or 1)
1

End of file
```

2D Inversion Parameters

```
Inversion settings
Initial damping factor (0.01 to 1.00)
0.1500
Minimum damping factor (0.001 to 0.75)
0.0200
Local optimization option (0=No, 1=Yes)
1
Convergence limit for relative change in RMS error in percent (0.1 to 20)
2.0000
Minimum change in RMS error for line search in percent (0.5 to 100)
0.5000
Number of iterations (1 to 30)
7
Vertical to horizontal flatness filter ratio (0.25 to 4.0)
1.0000
Model for increase in thickness of layers(0=default 10%, 1=default 25%, 2=user defined)
2
Number of nodes between adjacent electrodes (1, 2 or 4)
4
Flatness filter type, Include smoothing of model resistivity (0=model changes only,1=
directly on model)
1
Reduce number of topographical data points? (0=No,1=Yes. Recommend leave at 0)
0
Carry out topography modeling? (0=No,1=Yes)
1
Type of topography trend removal (0=Average,1=Least-squares,2=End to end)
2
Type of Jacobian matrix calculation (0=Quasi-Newton, 1=Gauss-Newton, 2=Mixed)
1
Increase of damping factor with depth (1.0 to 2.0)
1.0500
Type of topographical modeling (0=None, 1=No longer supported so do not use, 2=uniform
distorted FEM, 3=underwater, 4=damped FEM, 5=FEM with inverse Swartz-Christoffel)
4
Robust data constrain? (0=No, 1=Yes)
1
Cutoff factor for data constrain (0.0001 to 0.1))
0.0500
Robust model constrain? (0=No, 1=Yes)
1
Cutoff factor for model constrain (0.0001 to 1.0)
0.0050
Allow number of model parameters to exceed data points? (0=No, 1=Yes)
1
Use extended model? (0=No, 1=Yes)
1
Reduce effect of side blocks? (0=No, 1=Slight, 2=Severe, 3=Very Severe)
1
Type of mesh (0=Normal,1=Fine,2=Finest)
2
Optimise damping factor? (0=No, 1=Yes)
1
Time-lapse inversion constrain (0=None,1&2=Smooth,3=Robust)
3
Type of time-lapse inversion method (0=Simultaneous,1=Sequential)
0
Thickness of first layer (0.25 to 1.0)
0.5000
Factor to increase thickness layer with depth (1.0 to 1.25)
1.1000
USE FINITE ELEMENT METHOD (YES=1,NO=0)
1
```

WIDTH OF BLOCKS (1=NORMAL WIDTH, 2=DOUBLE, 3=TRIPLE, 4=QUADRUPLE, 5=QUINTUPLE)
1
MAKE SURE BLOCKS HAVE THE SAME WIDTH (YES=1,NO=0)
1
RMS CONVERGENCE LIMIT (IN PERCENT)
0.100
USE LOGARITHM OF APPARENT RESISTIVITY (0=USE LOG OF APPARENT RESISTIVITY, 1=USE
RESISTANCE VALUES, 2=USE APPARENT RESISTIVITY)
0
TYPE OF IP INVERSION METHOD (0=CONCURRENT,1=SEQUENTIAL)
0
PROCEED AUTOMATICALLY FOR SEQUENTIAL METHOD (1=YES,0=NO)
0
IP DAMPING FACTOR (0.01 to 1.0)
0.250
USE AUTOMATIC IP DAMPING FACTOR (YES=1,NO=0)
0
CUTOFF FACTOR FOR BOREHOLE DATA (0.0005 to 0.02)
0.00010
TYPE OF CROSS-BOREHOLE MODEL (0=normal,1=halfsize)
0
LIMIT RESISTIVITY VALUES(0=No,1=Yes)
0
Upper limit factor (10–50)
50.000
Lower limit factor (0.02 to 0.1)
0.020
Type of reference resistivity (0=average,1=first iteration)
0
Model refinement (1.0=Normal,0.5=Half-width cells)
0.50
Combined Combined Marquardt and Occam inversion (0=Not used,1=used)
0
Type of optimisation method (0=Gauss–Newton,2=Incomplete GN)
2
Convergence limit for Incomplete Gauss–Newton method (0.005 to 0.05)
0.005
Use data compression with Incomplete Gauss–Newton (0=No,1=Yes)
0
Use reference model in inversion (0=No,1=Yes)
1
Damping factor for reference model (0.0 to 1.0)
0.01000
Use fast method to calculate Jacobian matrix. (0=No,1=Yes)
1
Use higher damping for first layer? (0=No,1=Yes)
0
Extra damping factor for first layer (1.0 to 100.0)
5.00000
Type of finite-element method (0=Triangular,1=Trapezoidal elements)
1
Factor to increase model depth range (1.0 to 5.0)
1.050
Reduce model variations near borehole (0=No, 1=Yes)
0
Factor to control the degree variations near the boreholes are reduced (2 to 100)
5.0
Factor to control variation of borehole damping factor with distance (0.5 to 5.0)
1.0
Floating electrodes survey inversion method (0=use fixed water layer, 1=Incorporate water
layer into the model)
1
Resistivity variation within water layer (0=allow resistivity to vary freely,1=minimise
variation)
1
Use sparse inversion method for very long survey lines (0=No, 1=Yes)

```
0
Optimize Jacobian matrix calculation (0=No, 1=Yes)
0
Automatically switch electrodes for negative geometric factor (0=No, 1=Yes)
1
Force resistance value to be consistant with the geometric factor (0=No, 1=Yes)
0
Shift the electrodes to round up positions of electrodes (0=No, 1=Yes)
0
Use difference of measurements in time-lapse inversion (0=No, 1=Yes)
0
Use active constraint balancing (0=No, 1=Yes)
0
Type of active constraints (0=Normal, 1=Reverse)
0
Lower damping factor limit for active constraints
0.4000
Upper damping factor limit for active constraints
2.5000
Water resistivity variation damping factor
8.0000
Use automatic calculation for change of damping factor with depth (0=No, 1=Yes)
0
Type of I.P. model transformation (0=None, 1=square root, 3=range)
3
Model Chargeability Lower Limit (mV/V) for range
0.00
Model Chargeability Upper Limit (mV/V) for range
900.00
Use I.P. model refinement (0=No, 1=Yes)
1
Weight for I.P. data (0.1 to 10)
1.0000
I.P. model damping factor (0.05 to 1.0)
0.2500
Use program estimate for I.P. model damping factor (0=No, 1=Yes)
0
Type of I.P. smoothness constraint (1=Same as resistivity, 0=Different)
1
Joint or separate I.P. inversion method (1=Separate, 0=Joint)
1
Apparent I.P. cutoff value (300 to 899 mV/V)
899.00
Use diagonal filter (0=No, 1=Yes)
0
Diagonal filter weight (0.2 to 5.0)
1.00
Limit range of data weights from error estimates? (0=No, 1=Yes)
0
Lower limit of data weights (0.2 to 0.5)
0.30
Upper limit of data weights (2.0 to 5.0)
3.00
Use same data weights from error estimates for different time series? (0=No, 1=Yes)
0
Calculate model resolution? (0=No, 1=Yes)
0
Use L curve method? (0=No, 1=Yes)
0
Use same norms in L curve method? (0=No, 1=Yes)
0
Allow damping factor in increase in L curve method? (0=No, 1=Yes)
1
Type of borehole damping method (0=Horizontal distance from nearest borehole, 1=Distance
from nearest active electrode)
0
```

Use fast Jacobian calculation for dense data sets? (0=No,1=Yes)
0
Use higher damping factors at sides of model? (0=No,1=Yes)
1
Adjust damping factors for distances between the blocks in the model? (0=No,1=Yes)
1
Number of electrodes in segment for sparse inversion method for very long survey lines.
250
Time-lapse damping factor.
0.25
Reduce time-lapse damping with each iteration? (0=No,1=Yes)
1
Filter input data using geometric factor? (0=No,1=Yes)
0
Automatically remove negative apparent resistivity values? (0=No,1=Yes)
0
Automatically remove Gamma type arrays? (0=No,1=Yes)
0
Topography distortion damping factor (0.1 to 2.0)
0.750
Use zero reference I.P. model value? (0=No, 1=Yes)
0
Use apparent IP data in resistivity inversion. (0=No, 1=Yes)
0